May 17, 2017

Ms. Donna Jerry
Health Policy Analyst
Green Mountain Care Board
89 Main Street
Montpelier, VT 05620-3101

Re: RRMC CoN Application - Nuclear Medicine Camera Replacement
        Docket No. GMCB-012-16con

Dear Donna:

Please find enclosed Rutland Regional Medical Center's CoN application for
the replacement nuclear medicine camera.

Sincerely,

Thomas W. Huebner
President and CEO

TWH/jsb

Enclosure

Cc: Judi Fox, CFO
        Jim Greenough, Sr. Director

Rutland Regional Medical Center
An Affiliate of Rutland Regional Health Services

160 Allen Street
Rutland, VT 05701
802.775.7111

Form A - Verification Form

STATE OF VERMONT
DEPARTMENT OF BANKING, INSURANCE,
SECURITIES AND HEALTH CARE ADMINISTRATION

In re: Rutland Regional Medical Center   )
)   Docket No. GMCB-012-16con
)   Nuclear Medicine Camera Replacement
)

Exhibit A – Form of Verification Under Oath when filing a Certificate of Need Application.

Thomas W. Huebner, being duly sworn, states on oath as follows:

1. My name is Thomas W. Huebner. I am President and Chief Executive Officer of Rutland Regional Medical Center. I have reviewed the attached letter and Nuclear Medicine Camera Replacement Certificate of Need application dated May 17, 2017 from myself to Donna Jerry, Health Policy Analyst.

2. Based on my personal knowledge, after diligent inquiry, the information contained in this Certificate of Need application is true, accurate and complete, does not contain any untrue statement of a material fact, and does not omit to state a material fact necessary to make the statement made therein not misleading, except as specifically noted herein.

3. My personal knowledge of the truth, accuracy and completeness of the information contained in the Certificate of Need application is based upon either my actual knowledge of the subject information or, where identified below, upon information reasonably believed by me to be reliable and provided to me by the individuals identified below who have certified that the information they have provided is true, accurate and complete, does not contain any untrue statement of a material fact, and does not omit to state a material fact necessary to make the statement made therein not misleading.

4. I have evaluated, within the 12 months preceding the date of this affidavit, the policies and procedures by which information has been provided by the certifying individuals identified below, and I have determined that such policies and procedures are effective in ensuring that all

information submitted or used by Rutland Regional Medical Center in connection with the Certificate of Need program is true, accurate, and complete. I have disclosed to the RRHS-RRMC Board of Directors all significant deficiencies, of which I have personal knowledge after diligent inquiry, in such policies and procedures, and I have disclosed to the RRHS-RRMC Board of Directors any misrepresentation of facts, whether or not material, that involves management or any other employee participating in providing information submitted or used by Rutland Regional Medical Center in connection with the Certificate of Need program.

5. The following certifying individuals have provided information or documents to me in connection with the letter, and each such individual has certified, based on his or her actual knowledge of the subject information or, where specifically identified in such certification, based on information reasonably believed by the certifying individual to be reliable, that the information or documents they have provided are true, accurate and complete, do not contain any untrue statement of a material fact, and do not omit to state a material fact necessary to make the statement made therein not misleading:

(a) Judi Fox, Director of Finance
The information or documents provided by the certifying individual.
All financial related information.

Subject information of which the certifying individual has actual knowledge.
As stated above.

The individuals and the information reasonably relied on by the certifying individual.

In the case of documents identify the custodian of the documents.
Judi Fox

(b) James Greenough, Senior Director Corporate Services
The information or documents provided by the certifying individual.
All scope related information.

Subject information of which the certifying individual has actual knowledge.
As stated above.

The individuals and the information reasonably relied on by the certifying individual.

In the case of documents identify the custodian of the documents.
James Greenough

6. In the event that the information contained in the Certificate of Need application becomes untrue, inaccurate or incomplete in any material respect, I acknowledge my obligation to notify the Department of Banking, Insurance, Securities and Health Care Administration, and to supplement the Interim Report as soon as I know, or reasonably should know, that the information or document has become untrue, inaccurate or incomplete in any material respect.

_____
Thomas W. Huebner, President and CEO

On May 17, 2017, Thomas W. Huebner appeared before me and swore to the truth, accuracy and completeness of the foregoing.

_____   [seal]
Notary public
My commission expires February 10, 2019

_____
Judi Fox, VP Fiscal Services, CFO

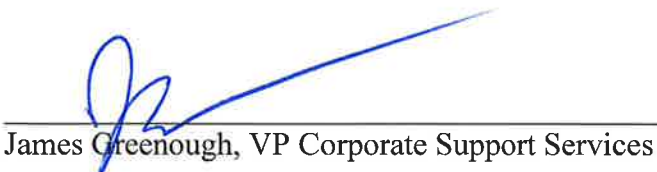On May 17, 2017 Judi Fox appeared before me and swore to the truth, accuracy and completeness of the foregoing.

_____   [seal]
Notary public
My commission expires February 10, 2019

_____
James Greenough, VP Corporate Support Services

On May 17, 2017, James Greenough appeared before me and swore to the truth, accuracy and completeness of the foregoing.

_____   [seal]
Notary public
My commission expires February 10, 2019

Rutland Regional Medical Center

Nuclear Medicine Camera Replacement
Docket No. GMCB-012-16con

Certificate of Need Application

May 17, 2017

Project Description

Rutland Regional Medical Center is requesting the replacement of the existing Infinia Hawkeye Nuclear Medicine camera with the new Discovery NM/CT 670 Pro nuclear medicine imaging system at a cost of $2,840,596.00. This new equipment replaces existing fully depreciated 12-year-old equipment with newer technology that provides safer and more efficient scans to our community of patients. The Discovery NM/CT 670 Pro allows for radiation does reductions by decreasing scan times and reducing radiopharmaceuticals exposure. The benefit of quicker scan times helps patients to be more compliant while lying on the scanner bed, therefore increasing image quality and patient comfort. Radiation dose reductions are paramount in patient safety and the Discovery NM/CT 670 Pro is able to reduce dose without compromising image quality through new software technologies; ASIR® and the Evolution® family of advanced reconstruction algorithms. In order to accommodate this equipment, facility renovations are necessary and a small 779 gross square foot addition is required.

The nuclear medicine camera is a core imaging modality used by our cardiologists, primary care physicians, physician specialists, ED physicians, and Hospitalists. The new equipment will continue to offer existing services for our patients. These primary services include cardiac imaging and general nuclear medicine exams, which are standard testing for a community hospital environment. Nuclear Medicine imaging is also essential in supporting our community cancer center physicians and their patients for diagnostic imaging through the course of the patient's treatment with tumor localization scans, bone scans, and lymph node localization scans. Nuclear Medicine is also vital for ED patients with chest pain, pulmonary emboli, and/or GI bleeds. The volume of services is not expected to be impacted by the purchase of this equipment. A review of the applicable CoN standards is found below.

Criteria Discussion

CON STANDARD 1.3: To the extent neighboring health care facilities provide the services proposed by a new health care project, an applicant shall demonstrate that a collaborative approach to delivering the service has been taken or is not feasible or appropriate.

Nuclear medicine cameras are standard technology in virtually all hospitals. They provide basic cardiac and oncology imaging. The replacement of the camera at Rutland should have no impact on other organizations.

CON STANDARD 1.4: If an application proposes services for which a higher volume of such service is positively correlated to better quality, the applicant shall show that it will be able to maintain appropriate volume for the service and that the addition of the service at the facility will not erode volume at any other Vermont facility in such a way that quality at that facility could be compromised.

No new volume or services are identified with this new technology. Discovery NM/CT 670 Pro would replace existing 12-year-old equipment, the Infinia Hawkeye, with newer technology that provides safer and more efficient scans to patients. The Discovery NM/CT 670 Pro allows for radiation dose reductions by decreasing scan times and reducing radiopharmaceuticals that patients are exposed to. The benefit of quicker scan times helps patients to be more compliant while lying on the scanner bed, therefore increasing image quality and patient comfort.

2

Radiation dose reductions are paramount in patient safety and the Discovery NM/CT 670 Pro is able to reduce dose without compromising image quality through new software technologies. The new equipment will continue to offer existing services for our patients in Cardiac Services, Foley Cancer Center, General Surgery and other general nuclear medicine exams.

CON Standard 1.9: Applicants proposing construction projects shall show that the costs and methods of the proposed construction are necessary and reasonable. Applicants shall show that the project is cost-effective and that reasonable energy conservation measures have been taken.

This project includes the renovation of 1,391 sq. ft. of existing space and the addition of 519 sq. ft. of new space adjoining the Diagnostic Imaging Department, for a total of 779 sq. ft. of new space. In order to create space for the expansion of the Diagnostic Imaging Department, the existing Decontamination Shed (260 sq. ft.) needs to be moved and reconstructed at the end of the Ambulance Garage. The addition of new space is required, because the new equipment is larger and cannot be accommodated in the existing space. Renovation of the interior space is required to properly position the control room relative to the new camera, create efficient work flow, provide sufficient space for support areas, and relocate the Hot Lab within the Nuclear Medicine Suite. To minimize construction costs, and ensure that construction is both cost-effective and reasonable, RRMC employed a strategy to maximize renovation of existing space to take advantage of existing infrastructure and minimize new construction to reduce overall construction costs.

The existing Nuclear Medicine Suite is located in the Diagnostic Imaging Department and the proposed project keeps the Nuclear Medicine Suite in the same location, with easy access to the Emergency Department, other related Departments, equipment and facilities.

Following is a summary of the existing and proposed spaces:

Existing Space		Proposed Space	
Waiting room,	122 nsf	Waiting room,	127 nsf
Injection	136 nsf	Injection	145 nsf
Stress Testing	264 nsf	Stress Testing	264 nsf
Control	194 nsf	Control	196 nsf
Nuc. Med.	387 nsf	Nuc. Med.	534 nsf
Corridor & Vest.	186 nsf	Corridor	194 nsf
Vestibule	0 nsf	Vestibule	98 nsf
Patient Toilet	0 nsf	Patient Toilet	45 nsf
Hot Lab	0 nsf*	Hot Lab	128 nsf*

*(existing 133 nsf located outside of suite, and new is located within suite)

Walls/Structure	102 nsf	Walls Structure	179 nsf
SUBTOTAL	1391 gsf	SUBTOTAL	1910 gsf
Decon Shed	260 gsf	Decon Shed	260 gsf
TOTAL	1651 gsf	TOTAL	2170 gsf

As can be seen from the above table, new construction in this project is solely focused on providing the appropriate space for the equipment and observation of the patient.

To ensure that construction costs are competitive and cost effective, RRMC will obtain multiple competitive bids from all trades providing services, and RRMC has worked with Efficiency Vermont to ensure reasonable energy conservation has occurred.

CON STANDARD 1.10: Applicants proposing new health care projects requiring construction shall show such projects are energy efficient. As appropriate, applicants shall show that Efficiency Vermont, or an organization with similar expertise, has been consulted on the proposal.

Efficiency VT collaborates with RRMC on all projects, and Efficiency VT has been involved in this project as well. LN Consulting, the project engineers on this project, has designed energy efficient systems to provide heating, ventilation, air conditioning and lighting in the space. The facilities staff and Efficiency VT have also been a part of the design process and together we have designed systems that will be energy efficient, reliable and easy to maintain. A letter from Efficiency Vermont is attached following this narrative.

CON STANDARD 1.11: Applicants proposing new health care projects requiring new construction shall demonstrate that the new construction is the more appropriate alternative when compared to renovation.

This project primarily consists of the renovation of 1391 sq. ft. of existing space, with new construction being limited to 519 sq. ft., the minimal amount necessary to accommodate the new Nuclear Camera. The project also includes the relocation and reconstruction of the 260 sq. ft. Decontamination Shed. The addition of new space is required, because the new equipment is larger and cannot be accommodated in the existing space, and the camera cannot be positioned properly in the existing space to properly position the control room relative to the camera. Location of the control room relative to the camera is critical to the care provider's observation of the patient. With the Nuclear Camera located in the new addition, the existing space can be renovated to provide proper observation of the patient, create efficient work flow, provide sufficient space for support areas, and relocate the Hot Lab within the Nuclear Medicine Suite. Relocation and reconstruction of the Decontamination Shed is required to create space for the expansion of the Nuclear Medicine room. Without relocation of the Decontamination Shed, and without taking advantage of existing space, facilities and services currently used for Nuclear Medicine, the entire Nuclear Medicine Suite would have to be relocated to a new location causing the entire project to have new construction.

CON STANADARD 1.12: New Construction of health care projects shall comply with the Guidelines for Construction and Equipment of Hospital and Medical Facilities as issued by the American Institute of Architects (AIA).

All new construction and renovation areas will comply with the Guidelines for Construction and Equipment of Hospital and Medical Facilities as issued by the American Institute of Architects (AIA). Lavallee Brensinger are the architects on the project, LN Consulting is serving as the engineer and Krebs & Lansing are the civil engineers.

CON STANDARD 3.4: Applicants subject to budget review shall demonstrate that a proposed project has been included in hospital budget submissions or explain why inclusion was not feasible.

Rutland Regional Medical Center has included the Replacement of the Nuclear Medicine Camera in the hospital budget submission. In the budget 2016 submission, the Nuclear Medicine Camera was included as an anticipated non-CoN project for $950,000. In the budget 2017 submission, it was included as a CoN project for $2.2 million as planning had resulted in the need to renovate and reconfigure rooms, in part adding new square footage.

CON STANDARD 3.7: Applicants proposing to replace diagnostic or therapeutic equipment shall demonstrate that existing equipment is fully depreciated, or the cost of the early replacement, including the cost of remaining depreciation on existing equipment, is less costly than keeping the existing equipment.

The Nuclear Medicine Camera that is being replaced was purchased for $555,342.50, and placed in service in fiscal year 2005. There was also a power injector purchased with this project in FY 2005. These items had a useful life of 5 years, and therefore is fully depreciated.

CON STANDARD 3.20: Applications to purchase diagnostic or therapeutic equipment, or to expand facilities to accommodate major medical equipment purchases, shall address the appropriateness of such distribution as compared to population, the availability of appropriately trained personnel, an evaluation of patient need versus convenience, urgent versus non-urgent use, and appropriate protocol to reduce the risk of repetitive testing (both within the facility purchasing the equipment and within the health care system).

Nuclear Medicine imaging is essential in supporting our aging community for cardiac testing, cancer center diagnostic imaging, ED patients with chest pain, pulmonary emboli, and/or GI bleeds. This is the replacement of standard technology found in most hospitals.

Protocols are utilized to reduce the risk of repetitive testing includes staff reviewing patient information in the Nuclear Medicine Information System located in the RRMC Nuclear Medicine department. The Nuclear Regulatory Commission, NRC, requires that all radiopharmaceuticals doses are tracked by patient in the Nuclear Medicine Information System. Per department policy, staff validate each patient prior to doing their exam that the patient has not had a recent prior exam.

CON STANDARD 3.22: For applications involving the purchase of diagnostic or therapeutic equipment, applicants shall establish, through the submission of evidence in the form of peer-reviewed or similar articles, the clinical efficacy of the diagnoses or procedures to be performed.

Please see attached articles.

CON STANDARD 3.23: In addition to proving need, applicants seeking to add or expand diagnostic or therapeutic equipment shall show that the equipment reduces costs and/or improves quality.

The Discovery NM/CT 670 Pro allows for radiation dose reductions by decreasing scan times and reducing radiopharmaceutical dosages. The benefit of quicker scan times helps patients to be more compliant while lying on the scanner bed, therefore increasing image quality and patient comfort. Initially 10% of patients that are scanned could see a reduction in the radiopharmaceutical costs due to utilizing less dosage.

CON STANDARD 3.24: An applicant shall disclose potential financial conflicts of interest between hospitals and physicians and an equipment purchase.

There are no conflicts of interest.

Statutory Criteria

CON Criteria (2) the cost of the project is reasonable, because:
    A. the applicant's financial condition will sustain any financial burden likely to result from completion of the project;

This equipment is necessary for routine patient care. RRMC included this project in the annual capital planning process and will fund the project with internal equity and cash reserves. The current Infinia Hawkeye Nuclear Medicine camera is over 10 years old and in need of replacement. This project has been fully reviewed by our Capital Planning Committee, and given the age of the equipment, it has been prioritized by our Capital Budget Committee as a high priority project. Additional operating expenses include $103,233.00 for an annual equipment support and maintenance agreement offset in part by $33,081.00 of annual savings related to radiologic pharmaceuticals. The net annual additional expense will be absorbed in RRMC's projected financial plan and will not mandate any change in our original projections. The costs of this project will be supported within the State mandated net revenue cap each year.

    B. the project will not result in an undue increase in the costs of medical care. In making a finding under this subdivision, the board shall consider and with relevant factors, including:
        i. the financial implications of the project on hospitals and other clinical settings, including the impact on their services, expenditures and charges;
        ii. whether the impact on services, expenditures and charges is outweighed by the benefit of the project to the public, and

RRMC's rate will not be impacted as a result of the project.

This equipment is necessary for routine patient care. We feel that the value the project brings to RRMC far outweighs the capital costs. The project will allow for replacement of equipment that exceeds its useful life. As well, the new camera will provide improved quality imaging, reduction of radiopharmaceutical dose (less patient radiation dose), and reduction of scanning times for patient comfort.

This project will be financed using the internal funds generated by the facility. No borrowing is anticipated.

C. Less expensive alternatives do not exist, would be unsatisfactory, or are not feasible or appropriate;

This is replacement of equipment needed to core testing at an institution the size of Rutland Regional Medical Center.

CON Criteria (3) there is an identifiable, existing, or reasonably anticipated need for the proposed project which is appropriate for the applicant to provide;

The Discovery NM/CT 670 Pro new equipment replaces existing 12-year-old equipment with newer technology that provides safer and more efficient scans to our community of patients. Enhanced image quality, radiation dose reduction, less radiopharmaceuticals injected, and faster scan times are benefits for our patients.

CON Criteria (4) the project will improve the quality of health care in the state or provide greater access to health care for Vermont's residents, or both;

The Discovery NM/CT 670 Pro allows for radiation dose reductions by decreasing scan times and reducing radiopharmaceuticals that patients are exposed to.

CON Criteria (5) the project will not have an undue adverse impact on any other existing services provided by the applicant;

The project will have no impact on other services.

CON Criteria (6) the project will serve the public good;

The project will serve the public good by letting RRMC continue to provide these core testing services.

PLEASE PROVIDE ASSUMPTIONS
Rutland Regional Medical Center
Nuclear Medicine

Table 1

* Capital costs include the Nuclear Medicine camera, other furnishings, and construction costs to expand the space for the new, larger camera.
* The trade in discount included in the quote is assumed to be the Fair Market Value of the existing Nuclear Medicine camera that will be traded in for the new camera. This fair market value was included in the costs in Table 1.

Table 2

* This project will not be financed, so there are no debt related expenses.

INCOME STATEMENT

* This project has been included in our Strategic Financial Plan and will not have an impact on rates.
* Assumes 3.4% annual growth in net patient revenue.
* Net to gross for FY 2017 and FY 2018 is based on information used to build the 2018 budget that will be submitted to the State at the end of June.
* The growth in Other Operating Income for FY 2018 - 2020 is related to Retail Pharmacy.
* Projection 2017 and 2018 are based on detailed information prepared during the development of our 2018 budget
* Projection 2019 and 2020 assumes merit/market for non-physician salaries of 3.5% per year and inflation of 3% per year for all other expenses

* Project expenses include $15,000 of asbestos abatement in 2018, depreciation of $155,160, Physicist annual equipment inspection of $2,200, training costs of $43,000 and Radiologic Pharmaceutical savings of $9,730 in 2019, and depreciation of $310,321, Physicist equipment inspection of $2,200, Equipment support & maintenance agreements of $40,833 and Radiologic Pharmaceutical savings of $23,351 in 2020.

BALANCE SHEET

* Additional debt will be incurred in FY 2019 for $21.7 million to support the Medical Office Building project.
* 60% of project expenditures will occur in FY 2018, and 40% in FY 2019.

CASH FLOW

* Per the State, we are not required to submit this since the formulas are not correct in the State's cash flow statement file.

REVENUE SOURCE-PAYER

* Payer mix is based on FYTD 3/31/17 actual.

UTILIZATION

* FY 2017 and FY 2018 projected utilization is based on information used to build the 2018 budget that will be submitted to the State at the end of June.
* FY 2019 and 2020 utilization is anticipated to remain consistent with budget 2018.

STAFFING

* FY 2017 and FY 2018 projected staffing is based on information used to build the 2018 budget that will be submitted to the State at the end of June.
* FY 2019 and 2020 staffing is anticipated to remain consistent with budget 2018.

STATISTICS

* Statistics will be calculated by the state after the CoN financial tables are e-mailed to and uploaded by the State to their Adaptive Planning software

Rutland Regional Medical Center
Nuclear Medicine
TABLE 1
PROJECT COSTS

Construction Costs		
1. New Construction	$	390,984
2. Renovation		$698,149
3. Site Work		32,440
4. Fixed Equipment		
5. Design/Bidding Contingency		
6. Construction Contingency		$112,157
7. Construction Manager Fee		41,800
8. Other (please specify)		-
Subtotal	$	1,275,530
Related Project Costs		
1. Major Moveable Equipment	$	826,307
2. Furnishings, Fixtures & Other Equip.		$398,625
3. Architectural/Engineering Fees		$156,064
4. Land Acquisition		
5. Purchase of Buildings		
6. Administrative Expenses & Permits		$56,517
7. Debt Financing Expenses (see below)		-
8. Debt Service Reserve Fund		-
9. Working Capital		-
10. Other (please specify)		-
Owners Contingency		127,553
		-
Subtotal	$	1,565,066
Total Project Costs	$	**2,840,596**

Debt Financing Expenses		
1. Capital Interest	$	-
2. Bond Discount or Placement Fee		-
3. Misc. Financing Fees & Exp. (issuance costs)		-
4. Other		-
Subtotal	$	-
Less Interest Earnings on Funds		
1. Debt Service Reserve Funds	$	-
2. Capitalized Interest Account		-
3. Construction Fund		-
4. Other		-
Subtotal	$	-
Total Debt Financing Expenses	$	-
feeds to line 7 above		

Rutland Regional Medical Center
Nuclear Medicine
TABLE 2
DEBT FINANCING ARRANGEMENT, SOURCES & USES OF FUNDS

Sources of Funds

1. Financing Instrument	Bond		
a. Interest Rate	0.0%		
b. Loan Period		To:	
c. Amount Financed			$ -
2. Equity Contribution			2,840,596
3. Other Sources			
a. Working Capital			-
b. Fundraising			-
c. Grants			-
d. Other			-
Total Required Funds			**$ 2,840,596**

Uses of Funds

Project Costs (feeds from Table 1)

1. New Construction	$ 390,984
2. Renovation	698,149
3. Site Work	32,440
4. Fixed Equipment	-
5. Design/Bidding Contingency	-
6. Construction Contingency	112,157
7. Construction Manager Fee	41,800
8. Major Moveable Equipment	826,307
9. Furnishings, Fixtures & Other Equip.	398,625
10. Architectural/Engineering Fees	156,064
11. Land Acquisition	-
12. Purchase of Buildings	-
13. Administrative Expenses & Permits	56,517
14. Debt Financing Expenses	-
15. Debt Service Reserve Fund	-
16. Working Capital	-
17. Other (Owner's Contingency)	127,553
Total Uses of Funds	**$ 2,840,596**

Total sources should equal total uses of funds.

RUTLAND REGIONAL MEDICAL CENTER

Nuclear Medicine

INCOME STATEMENT
Table 3A
WITHOUT PROJECT

	2015 Actual	2016 Budget	% change	2016 Actuals	% change	2017 Budget	% change	Projected 2017	% change	Proposed Yr 1 2018	% change	Proposed Yr 2 2019	% change	Proposed Yr 3 2020	% change
REVENUES															
INPATIENT CARE REVENUE	170,343,832	176,547,476	3.6%	191,888,077	8.7%	180,666,477	-5.8%	205,322,090	7.0%	214,308,929	18.6%	228,018,452	6.4%	243,100,927	6.6%
OUTPATIENT CARE REVENUE	281,110,791	274,404,944	-2.4%	274,399,840	0.0%	257,142,036	-6.3%	255,704,927	-6.8%	264,354,189	2.8%	281,265,149	6.4%	299,869,672	6.6%
OUTPATIENT CARE REVENUE - PHYSICI	40,880,965	58,686,415	43.6%	62,566,398	6.6%	63,107,825	0.9%	49,400,399	-21.0%	52,275,189	-17.2%	55,619,277	6.4%	59,298,261	6.6%
CHRONIC/SNF PT CARE REVENUE	-	-	#DIV/0!	-	#DIV/0!	-	#DIV/0!		#DIV/0!		#DIV/0!		#DIV/0!		#DIV/0!
SWING BEDS PT CARE REVENUE	1,058,924	793,290	-25.1%	-	-100.0%	-	#DIV/0!		#DIV/0!		#DIV/0!		#DIV/0!		#DIV/0!
GROSS PATIENT CARE REVENUE	493,394,512	510,432,125	3.5%	528,854,315	3.6%	500,916,338	-5.3%	510,427,416	-3.5%	530,938,307	6.0%	564,902,878	6.4%	602,268,860	6.6%
DISPROPORTIONATE SHARE PAYMENTS	4,576,163	4,169,146	-8.9%	4,573,554	9.7%	5,724,870	25.2%	5,724,870	25.2%	4,579,237	-20.0%	4,837,858	5.6%	5,002,345	3.4%
BAD DEBT FREE CARE	(9,687,417)	(13,964,808)	44.2%	(10,022,419)	-28.2%	(10,196,810)	1.7%	(10,989,502)	9.6%	(11,431,102)	12.1%	(12,162,359)	6.4%	(12,966,849)	6.6%
DEDUCTIONS FROM REVENUE	(259,954,621)	(267,388,301)	2.9%	(277,582,498)	3.8%	(253,028,950)	-8.8%	(259,915,041)	-6.4%	(272,539,164)	7.7%	(297,478,492)	9.2%	(325,361,075)	9.4%
NET PATIENT CARE REVENUE	228,328,637	233,248,162	2.2%	245,822,952	5.4%	243,415,448	-1.0%	245,247,743	-0.2%	251,547,278	3.3%	260,099,685	3.4%	268,943,281	3.4%
OTHER OPERATING REVENUE	9,275,938	9,938,846	7.1%	8,598,283	-13.5%	11,017,731	28.1%	11,959,805	39.1%	12,290,310	11.6%	12,490,310	1.6%	12,690,310	1.6%
TOTAL OPERATING REVENUE	237,604,575	243,187,008	2.3%	254,421,235	4.6%	254,433,179	0.0%	257,207,548	1.1%	263,837,588	3.7%	272,590,195	3.3%	281,633,591	3.3%
OPERATING EXPENSE															
SALARIES NON MD	70,594,783	73,162,616	3.6%	78,446,783	7.2%	82,628,937	5.3%	79,468,595	1.3%	82,525,214	-0.1%	85,413,596	3.5%	88,403,072	3.5%
FRINGE BENEFITS NON MD	27,728,540	25,651,715	-7.5%	25,172,851	-1.9%	27,673,380	9.9%	25,223,283	0.2%	26,994,266	-2.5%	27,804,094	3.0%	28,638,217	3.0%
FRINGE BENEFITS MD	2,101,246	2,008,606	-4.4%	1,375,451	-31.5%	1,529,901	11.2%	1,380,112	0.3%	1,439,639	-5.9%	1,482,828	3.0%	1,527,313	3.0%
PHYSICIAN FEES SALARIES CONTRACT:	30,053,013	30,114,342	0.2%	30,000,115	-0.4%	29,969,647	-0.1%	33,858,442	12.9%	35,060,044	17.0%	36,111,845	3.0%	37,195,201	3.0%
HEALTH CARE PROVIDER TAX	13,002,474	13,519,505	4.0%	14,052,304	3.9%	14,352,823	2.1%	14,740,749	4.9%	14,810,108	3.2%	15,254,411	3.0%	15,712,044	3.0%
DEPRECIATION AMORTIZATION	12,433,769	13,374,000	7.6%	13,596,263	1.7%	13,161,688	-3.2%	12,996,477	-4.4%	12,728,164	-3.3%	14,062,142	10.5%	16,539,642	17.6%
INTEREST - LONG/SHORT TERM	1,897,138	1,873,113	-1.3%	1,803,469	-3.7%	1,749,035	-3.0%	1,517,751	-15.8%	1,688,565	-3.5%	1,739,222	3.0%	1,791,399	3.0%
OTHER OPERATING EXPENSE	75,385,579	77,623,157	3.0%	79,195,624	2.0%	77,262,881	-2.4%	81,111,075	2.4%	82,303,323	6.5%	84,219,559	2.3%	85,111,858	1.1%
TOTAL OPERATING EXPENSE	233,196,542	237,327,054	1.8%	243,642,660	2.7%	248,328,292	1.9%	250,296,484	2.7%	257,549,323	3.7%	266,087,698	3.3%	274,918,745	3.3%
NET OPERATING INCOME (LOSS)	4,408,033	5,859,954	32.9%	10,778,375	83.9%	6,104,887	-43.4%	6,911,064	-35.9%	6,288,265	3.0%	6,502,497	3.4%	6,714,846	3.3%
NON-OPERATING REVENUE	(492,377)	5,973,111	-1313.1%	11,380,794	90.5%	7,136,913	-37.3%	9,727,331	-14.5%	8,905,374	24.8%	8,905,374	0.0%	8,905,374	0.0%
EXCESS (DEFICIT) OF REVENUE OVER E:	3,915,656	11,833,065	202.2%	22,159,169	87.3%	13,241,800	-40.2%	16,638,395	-24.9%	15,193,639	14.7%	15,407,871	1.4%	15,620,220	1.4%
Operating Margin %	1.9%	2.4%		4.2%		2.4%		2.7%		2.4%		2.4%		2.4%	
Bad Debt & Free Care%	2.0%	2.7%		1.9%		2.0%		2.2%		2.2%		2.2%		2.2%	
Compensation Ratio	56.0%	55.2%		55.4%		57.1%		55.9%		56.7%		56.7%		56.7%	
Capital Cost % of Total Expenses	6.1%	6.4%		6.3%		6.0%		5.8%		5.6%		5.9%		6.7%	

PROJECT NAME

INCOME STATEMENT

Table 3B

PROJECT ONLY

	2015	2016		2016		2017		Projected		Proposed Yr 2		Proposed Yr 2		Proposed Yr 3	
	Actual	Budget	% change	Actuals	% change	Budget	% change	2017	% change	2018	% change	2019	% change	2020	% change
REVENUES															
INPATIENT CARE REVENUE			#DIV/0!		#DIV/0!		#DIV/0!		#DIV/0!		#DIV/0!		#DIV/0!		#DIV/0!
OUTPATIENT CARE REVENUE			#DIV/0!		#DIV/0!		#DIV/0!		#DIV/0!		#DIV/0!		#DIV/0!		#DIV/0!
OUTPATIENT CARE REVENUE - PHYSICIAN			#DIV/0!		#DIV/0!		#DIV/0!		#DIV/0!		#DIV/0!		#DIV/0!		#DIV/0!
CHRONIC/SNF PT CARE REVENUE			#DIV/0!		#DIV/0!		#DIV/0!		#DIV/0!		#DIV/0!		#DIV/0!		#DIV/0!
SWING BEDS PT CARE REVENUE			#DIV/0!		#DIV/0!		#DIV/0!		#DIV/0!		#DIV/0!		#DIV/0!		#DIV/0!
GROSS PATIENT CARE REVENUE	-	-	#DIV/0!	-	#DIV/0!	-	#DIV/0!	-	#DIV/0!	-	#DIV/0!	-	#DIV/0!	-	#DIV/0!
DISPROPORTIONATE SHARE PAYMENTS			#DIV/0!		#DIV/0!		#DIV/0!		#DIV/0!		#DIV/0!		#DIV/0!		#DIV/0!
BAD DEBT FREE CARE			#DIV/0!		#DIV/0!		#DIV/0!		#DIV/0!		#DIV/0!		#DIV/0!		#DIV/0!
DEDUCTIONS FROM REVENUE			#DIV/0!		#DIV/0!		#DIV/0!		#DIV/0!		#DIV/0!		#DIV/0!		#DIV/0!
NET PATIENT CARE REVENUE	-	-	#DIV/0!	-	#DIV/0!	-	#DIV/0!	-	#DIV/0!	-	#DIV/0!	-	#DIV/0!	-	#DIV/0!
OTHER OPERATING REVENUE			#DIV/0!		#DIV/0!		#DIV/0!		#DIV/0!		#DIV/0!		#DIV/0!		#DIV/0!
TOTAL OPERATING REVENUE	-	-	#DIV/0!	-	#DIV/0!	-	#DIV/0!	-	#DIV/0!	-	#DIV/0!	-	#DIV/0!	-	#DIV/0!
OPERATING EXPENSE															
SALARIES NON MD			#DIV/0!		#DIV/0!		#DIV/0!		#DIV/0!		#DIV/0!		#DIV/0!		#DIV/0!
FRINGE BENEFITS NON MD			#DIV/0!		#DIV/0!		#DIV/0!		#DIV/0!		#DIV/0!		#DIV/0!		#DIV/0!
FRINGE BENEFITS MD			#DIV/0!		#DIV/0!		#DIV/0!		#DIV/0!		#DIV/0!		#DIV/0!		#DIV/0!
PHYSICIAN FEES SALARIES CONTRACTS & FRINGES			#DIV/0!		#DIV/0!		#DIV/0!		#DIV/0!		#DIV/0!		#DIV/0!		#DIV/0!
HEALTH CARE PROVIDER TAX			#DIV/0!		#DIV/0!		#DIV/0!		#DIV/0!		#DIV/0!		#DIV/0!		#DIV/0!
DEPRECIATION AMORTIZATION			#DIV/0!		#DIV/0!		#DIV/0!		#DIV/0!		#DIV/0!	155,160	#DIV/0!	310,321	100.0%
INTEREST - LONG/SHORT TERM			#DIV/0!		#DIV/0!		#DIV/0!		#DIV/0!		#DIV/0!		#DIV/0!		#DIV/0!
OTHER OPERATING EXPENSE			#DIV/0!		#DIV/0!		#DIV/0!		#DIV/0!	15,000	#DIV/0!	35,470	136.5%	19,682	-44.5%
TOTAL OPERATING EXPENSE	-	-	#DIV/0!	-	#DIV/0!	-	#DIV/0!	-	#DIV/0!	15,000	#DIV/0!	190,630	1170.9%	330,003	73.1%
NET OPERATING INCOME (LOSS)	-	-	#DIV/0!	-	#DIV/0!	-	#DIV/0!	-	#DIV/0!	(15,000)	#DIV/0!	(190,630)	1170.9%	(330,003)	73.1%
NON-OPERATING REVENUE			#DIV/0!		#DIV/0!		#DIV/0!		#DIV/0!		#DIV/0!		#DIV/0!		#DIV/0!
EXCESS (DEFICIT) OF REVENUE OVER E	-	-	#DIV/0!	-	#DIV/0!	-	#DIV/0!	-	#DIV/0!	(15,000)	#DIV/0!	(190,630)	1170.9%	(330,003)	73.1%

Nuclear Medicine

Note: This table requires no "fill-in" as it is populated automatically

INCOME STATEMENT

Table 3C
WITH PROJECT

	2015	2016		2016		2017		Projected		Proposed Yr 2		Proposed Yr 2		Proposed Yr 3	
	Actual	Budget	% change	Actuals	% change	Budget	% change	2017	% change	2018	% change	2019	% change	2020	% change
REVENUES															
INPATIENT CARE REVENUE	170,343,832	176,547,476	3.6%	191,888,077	8.7%	180,666,477	-5.8%	205,322,090	7.0%	214,308,929	18.6%	228,018,452	6.4%	243,100,927	6.6%
OUTPATIENT CARE REVENUE	281,110,791	274,404,944	-2.4%	274,399,840	0.0%	257,142,036	-6.3%	255,704,927	-6.8%	264,354,189	2.8%	281,265,149	6.4%	299,869,672	6.6%
OUTPATIENT CARE REVENUE - PHYSICI	40,880,965	58,686,415	43.6%	62,566,398	6.6%	63,107,825	0.9%	49,400,399	-21.0%	52,275,189	-17.2%	55,619,277	6.4%	59,298,261	6.6%
CHRONIC/SNF PT CARE REVENUE	-	-	#DIV/0!	-	#DIV/0!	-	#DIV/0!	-	#DIV/0!	-	#DIV/0!	-	#DIV/0!	-	#DIV/0!
SWING BEDS PT CARE REVENUE	1,058,924	793,290	-25.1%	-	-100.0%	-	#DIV/0!	-	#DIV/0!	-	#DIV/0!	-	#DIV/0!	-	#DIV/0!
GROSS PATIENT CARE REVENUE	493,394,512	510,432,125	3.5%	528,854,315	3.6%	500,916,338	-5.3%	510,427,416	-3.5%	530,938,307	6.0%	564,902,878	6.4%	602,268,860	6.6%
DISPROPORTIONATE SHARE PAYMENTS	4,576,163	4,169,146	-8.9%	4,573,554	9.7%	5,724,870	25.2%	5,724,870	25.2%	4,579,237	-20.0%	4,837,858	5.6%	5,002,345	3.4%
BAD DEBT FREE CARE	(9,687,417)	(13,964,808)	44.2%	(10,022,419)	-28.2%	(10,196,810)	1.7%	(10,989,502)	9.6%	(11,431,102)	12.1%	(12,162,359)	6.4%	(12,955,849)	6.6%
DEDUCTIONS FROM REVENUE	(259,954,621)	(267,388,301)	2.9%	(277,582,498)	3.8%	(253,028,950)	-8.8%	(259,915,041)	-6.4%	(272,539,164)	7.7%	(297,478,492)	9.2%	(325,361,075)	9.4%
NET PATIENT CARE REVENUE	228,328,637	233,248,162	2.2%	245,822,952	5.4%	243,415,448	-1.0%	245,247,743	-0.2%	251,547,278	3.3%	260,099,885	3.4%	268,943,281	3.4%
OTHER OPERATING REVENUE	9,275,938	9,938,846	7.1%	8,598,283	-13.5%	11,017,731	28.1%	11,959,805	39.1%	12,290,310	11.6%	12,490,310	1.6%	12,690,310	1.6%
TOTAL OPERATING REVENUE	237,604,575	243,187,008	2.3%	254,421,235	4.6%	254,433,179	0.0%	257,207,548	1.1%	263,837,588	3.7%	272,590,195	3.3%	281,633,591	3.3%
OPERATING EXPENSE															
SALARIES NON MD	70,594,783	73,162,616	3.6%	78,446,783	7.2%	82,628,937	5.3%	79,468,595	1.3%	82,525,214	-0.1%	85,413,596	3.5%	88,403,072	3.5%
FRINGE BENEFITS NON MD	27,728,540	25,651,715	-7.5%	25,172,851	-1.9%	27,673,380	9.9%	25,223,283	0.2%	26,994,266	-2.5%	27,804,094	3.0%	28,638,217	3.0%
FRINGE BENEFITS MD	2,101,246	2,008,606	-4.4%	1,375,451	-31.5%	1,529,901	11.2%	1,380,112	0.3%	1,439,639	-5.9%	1,482,828	3.0%	1,527,313	3.0%
PHYSICIAN FEES SALARIES CONTRACT	30,053,013	30,114,342	0.2%	30,000,115	-0.4%	29,969,647	-0.1%	33,858,442	12.9%	35,060,044	17.0%	36,111,845	3.0%	37,195,201	3.0%
HEALTH CARE PROVIDER TAX	13,002,474	13,519,505	4.0%	14,052,304	3.9%	14,352,823	2.1%	14,740,749	4.9%	14,810,108	3.2%	15,254,411	3.0%	15,712,044	3.0%
DEPRECIATION AMORTIZATION	12,433,769	13,374,000	7.6%	13,596,263	1.7%	13,161,688	-3.2%	12,996,477	-4.4%	12,728,164	-3.3%	14,217,302	11.7%	16,849,963	18.5%
INTEREST - LONG/SHORT TERM	1,897,138	1,873,113	-1.3%	1,803,469	-3.7%	1,749,035	-3.0%	1,517,751	-15.8%	1,688,565	-3.5%	1,739,222	3.0%	1,791,399	3.0%
OTHER OPERATING EXPENSE	75,385,579	77,623,157	3.0%	79,195,624	2.0%	77,262,881	-2.4%	81,111,075	2.4%	82,318,323	6.5%	84,255,029	2.4%	85,131,540	1.0%
TOTAL OPERATING EXPENSE	233,196,542	237,327,054	1.8%	243,642,860	2.7%	248,328,292	1.9%	250,296,484	2.7%	257,564,323	3.7%	266,278,328	3.4%	275,248,748	3.4%
NET OPERATING INCOME (LOSS)	4,408,033	5,859,954	32.9%	10,778,375	83.9%	6,104,887	-43.4%	6,911,064	-35.9%	6,273,265	2.8%	6,311,867	0.6%	6,384,843	1.2%
NON-OPERATING REVENUE	(492,377)	5,973,111	-1313.1%	11,380,794	90.5%	7,136,913	-37.3%	9,727,331	-14.5%	8,905,374	24.8%	8,905,374	0.0%	8,905,374	0.0%
EXCESS (DEFICIT) OF REVENUE OVER E	3,915,656	11,833,065	202.2%	22,159,169	87.3%	13,241,800	-40.2%	16,638,395	-24.9%	15,178,639	14.6%	15,217,241	0.3%	15,290,217	0.5%

Operating Margin %	1.9%	2.4%	4.2%	2.4%	2.7%	2.4%	2.3%	2.3%
Bad Debt & Free Care%	2.0%	2.7%	1.9%	2.0%	2.2%	2.2%	2.2%	2.2%
Compensation Ratio	56.0%	55.2%	55.4%	57.1%	55.9%	56.7%	56.6%	56.6%
Capital Cost % of Total Expenses	6.1%	6.4%	6.3%	6.0%	5.8%	5.6%	6.0%	6.8%

RUTLAND REGIONAL MEDICAL CENTER

NUCLEAR MEDICINE
Balance Sheet
WITHOUT PROJECT

	2015 Actual	2016 Budget	% change	2016 Projection	% change	2017 Budget	% change	2017 Projected	% change	2018 Proposed Year 1	% change	2019 Proposed Year 2	% change	2020 Proposed Year 3	% change
ASSETS															
CURRENT ASSETS															
CASH & INVESTMENTS	12,803,315	23,680,313	85.0%	14,551,514	-38.6%	39,503,614	171.5%	15,386,482	-61.1%	14,576,141	-5.3%	13,593,130	-6.7%	14,471,783	6.5%
PATIENT ACCOUNTS RECEIVABLE, GROSS	65,671,511	66,814,488	1.7%	65,671,511	-1.7%	65,671,511	0.0%	67,802,702	3.2%	67,802,702	0.0%	67,802,702	0.0%	67,802,702	0.0%
LESS: ALLOWANCE FOR UNCOLLECTIBLE ACCTS	(45,002,495)	(42,592,168)	-5.4%	(45,002,495)	5.7%	(45,002,495)	0.0%	(45,270,950)	0.6%	(45,270,950)	0.0%	(45,270,950)	0.0%	(45,270,950)	0.0%
DUE FROM THIRD PARTIES	-	-	#DIV/0!	5,167,469	#DIV/0!	5,167,469	0.0%	5,260,001	1.8%	5,260,001	0.0%	5,260,001	0.0%	5,260,001	0.0%
OTHER CURRENT ASSETS	9,722,463	12,703,659	30.7%	9,722,463	-23.5%	9,722,463	0.0%	10,594,250	9.0%	10,594,250	0.0%	10,594,250	0.0%	10,594,250	0.0%
TOTAL CURRENT ASSETS	43,194,794	60,606,292	40.3%	50,110,462	-17.3%	75,062,562	49.8%	53,772,485	-28.4%	52,962,144	-1.5%	51,979,133	-1.9%	52,857,786	1.7%
BOARD DESIGNATED ASSETS															
FUNDED DEPRECIATION	61,639,087	114,778,672	86.2%	105,706,228	-7.9%	112,843,141	6.8%	120,526,972	6.8%	129,432,346	7.4%	138,337,720	6.9%	147,243,094	6.4%
ESCROWED BOND FUNDS	1,022,845	1,422,845	39.1%	-	-100.0%	-	#DIV/0!	-	#DIV/0!	-	#DIV/0!	-	#DIV/0!	-	#DIV/0!
OTHER	43,561,026	-	-100.0%	5,997,925	#DIV/0!	5,997,925	0.0%	6,201,912	3.4%	6,201,912	0.0%	6,201,912	0.0%	6,201,912	0.0%
TOTAL BOARD DESIGNATED ASSETS	106,222,958	116,201,517	9.4%	111,704,153	-3.9%	118,841,066	6.4%	126,728,884	6.6%	135,634,258	7.0%	144,539,632	6.6%	153,445,006	6.2%
PROPERTY, PLANT, AND EQUIPMENT															
LAND, BUILDINGS & IMPROVEMENTS	88,638,887	84,993,447	-4.1%	88,638,887	4.3%	88,638,887	0.0%	102,633,484	15.8%	102,633,484	0.0%	102,633,484	0.0%	102,633,484	0.0%
CONSTRUCTION IN PROGRESS	2,197,239	3,161,464	43.9%	2,197,239	-30.5%	2,197,239	0.0%	3,422,993	55.8%	3,422,993	0.0%	3,422,993	0.0%	3,422,993	0.0%
MAJOR MOVABLE EQUIPMENT	96,681,658	106,192,364	9.8%	113,784,698	7.1%	123,638,698	8.7%	119,875,161	-3.0%	135,200,943	12.8%	173,893,012	28.6%	190,893,012	9.8%
FIXED EQUIPMENT	29,597,080	30,016,498	1.4%	29,597,080	-1.4%	29,597,080	0.0%	33,456,193	13.0%	33,456,193	0.0%	33,456,193	0.0%	33,456,193	0.0%
TOTAL PROPERTY, PLANT AND EQUIPMENT	217,114,864	224,363,773	3.3%	234,217,904	4.4%	244,071,904	4.2%	259,387,831	6.3%	274,713,613	5.9%	313,405,682	14.1%	330,405,682	5.4%
LESS: ACCUMULATED DEPRECIATION															
LAND, BUILDINGS & IMPROVEMENTS	(44,966,451)	(49,171,122)	9.4%	(44,966,451)	-8.6%	(44,966,451)	0.0%	(53,095,223)	18.1%	(53,095,223)	0.0%	(53,095,223)	0.0%	(53,095,223)	0.0%
EQUIPMENT - FIXED	(22,872,018)	(23,795,284)	4.0%	(22,872,018)	-3.9%	(22,872,018)	0.0%	(24,755,689)	8.2%	(24,755,689)	0.0%	(24,755,689)	0.0%	(24,755,689)	0.0%
EQUIPMENT - MAJOR MOVEABLE	(75,558,526)	(84,163,325)	11.4%	(89,252,694)	6.0%	(102,414,382)	14.7%	(96,218,671)	-6.0%	(108,946,835)	13.2%	(123,008,977)	12.9%	(139,548,619)	13.4%
TOTAL ACCUMULATED DEPRECIATION	(143,396,995)	(157,129,731)	9.6%	(157,091,163)	0.0%	(170,252,851)	8.4%	(174,069,583)	2.2%	(186,797,747)	7.3%	(200,859,889)	7.5%	(217,399,531)	8.2%
TOTAL PROPERTY, PLANT AND EQUIPMENT, NET	73,717,869	67,234,042	-8.8%	77,126,741	14.7%	73,819,053	-4.3%	85,318,248	15.6%	87,915,866	3.0%	112,545,793	28.0%	113,006,151	0.4%
OTHER LONG-TERM ASSETS	9,289,915	9,834,219	5.9%	4,122,446	-58.1%	4,122,446	0.0%	5,266,689	27.8%	5,266,689	0.0%	5,266,689	0.0%	5,266,689	0.0%
TOTAL ASSETS	232,425,536	253,876,070	9.2%	243,063,802	-4.3%	271,845,127	11.8%	271,086,309	-0.3%	281,778,959	3.9%	314,331,248	11.6%	324,575,633	3.3%
LIABILITIES AND FUND BALANCE															
CURRENT LIABILITIES															
ACCOUNTS PAYABLE	2,818,694	4,265,502	51.3%	5,442,168	27.6%	5,442,168	0.0%	4,443,366	-18.4%	4,443,366	0.0%	4,443,366	0.0%	4,443,366	0.0%
SALARIES, WAGES AND PAYROLL TAXES PAYABLE	9,311,259	9,749,853	4.7%	10,113,344	3.7%	10,113,344	0.0%	11,234,778	11.1%	11,234,778	0.0%	11,234,778	0.0%	11,234,778	0.0%
ESTIMATED THIRD-PARTY SETTLEMENTS	8,592,533	7,847,454	-8.7%	8,592,533	9.5%	8,592,533	0.0%	9,152,712	6.5%	9,152,712	0.0%	9,152,712	0.0%	9,152,712	0.0%
OTHER CURRENT LIABILITIES	9,961,273	6,199,500	-37.8%	6,610,233	6.6%	6,610,517	0.0%	5,216,286	-21.1%	5,192,502	-0.5%	5,188,559	-0.1%	5,145,715	-0.8%
CURRENT PORTION OF LONG-TERM DEBT	2,283,260	1,871,793	-18.0%	1,727,223	-7.7%	2,133,373	23.5%	1,795,007	-15.9%	1,865,452	3.9%	1,938,661	3.9%	1,113,320	-42.6%
TOTAL CURRENT LIABILITIES	32,967,019	29,934,102	-9.2%	32,485,501	8.5%	32,891,935	1.3%	31,842,149	-3.2%	31,888,810	0.1%	31,958,076	0.2%	31,089,891	-2.7%
LONG-TERM DEBT															
BONDS & MORTGAGES PAYABLE	31,818,131	38,263,410	20.3%	38,263,410	0.0%	56,102,482	46.6%	36,469,153	-35.0%	34,603,702	-5.1%	54,357,110	57.1%	52,484,872	-3.4%
CAPITAL LEASE OBLIGATIONS	-	-	#DIV/0!	-	#DIV/0!	-	#DIV/0!	-	#DIV/0!	-	#DIV/0!	-	#DIV/0!	-	#DIV/0!
OTHER LONG-TERM DEBT	8,173,101	-	-100.0%	-	#DIV/0!	-	#DIV/0!								
TOTAL LONG-TERM DEBT	39,991,232	38,263,410	-4.3%	38,263,410	0.0%	56,102,482	46.6%	36,469,153	-35.0%	34,603,702	-5.1%	54,357,110	57.1%	52,484,872	-3.4%
OTHER NONCURRENT LIABILITIES	30,961,803	36,473,642	17.8%	32,450,125	-11.0%	29,744,143	-8.3%	32,865,815	10.5%	30,183,617	-8.2%	27,505,362	-8.9%	24,889,951	-9.8%
TOTAL LIABILITIES	103,920,054	104,671,154	0.7%	103,199,036	-1.4%	118,738,560	15.1%	101,177,117	-14.8%	96,676,129	-4.4%	113,820,548	17.7%	108,444,714	-4.7%
FUND BALANCE	128,505,482	149,204,916	16.1%	139,864,766	-6.3%	153,106,567	9.5%	169,909,191	11.0%	185,102,830	8.9%	200,510,700	8.3%	216,130,919	7.8%
TOTAL LIABILITIES AND FUND BALANCE	232,425,536	253,876,070	9.2%	243,063,802	-4.3%	271,845,127	11.8%	271,086,309	-0.3%	281,778,959	3.9%	314,331,248	11.6%	324,575,633	3.3%

RUTLAND REGIONAL MEDICAL CENTER

		PROJECT NAME					

Balance Sheet
PROJECT ONLY

	2015 Actual	2016 Budget	% change	2016 Projection	% change	2017 Budget	% change	2017 Projected	% change	2018 Proposed Year 1	% change	2019 Proposed Year 2	% change	2020 Proposed Year 3	% change
ASSETS															
CURRENT ASSETS															
CASH & INVESTMENTS			#DIV/0!		#DIV/0!		#DIV/0!		#DIV/0!	(1,692,958)	#DIV/0!	(2,891,067)	70.8%	(2,910,749)	0.7%
PATIENT ACCOUNTS RECEIVABLE, GROSS			#DIV/0!		#DIV/0!		#DIV/0!		#DIV/0!		#DIV/0!		#DIV/0!		#DIV/0!
LESS: ALLOWANCE FOR UNCOLLECTIBLE ACCTS			#DIV/0!		#DIV/0!		#DIV/0!		#DIV/0!		#DIV/0!		#DIV/0!		#DIV/0!
DUE FROM THIRD PARTIES			#DIV/0!		#DIV/0!		#DIV/0!		#DIV/0!		#DIV/0!		#DIV/0!		#DIV/0!
OTHER CURRENT ASSETS			#DIV/0!		#DIV/0!		#DIV/0!		#DIV/0!		#DIV/0!		#DIV/0!		#DIV/0!
TOTAL CURRENT ASSETS	-	-	#DIV/0!	-	#DIV/0!	-	#DIV/0!	0	#DIV/0!	(1,692,958)	#DIV/0!	(2,891,067)	70.8%	(2,910,749)	0.7%
BOARD DESIGNATED ASSETS															
FUNDED DEPRECIATION			#DIV/0!		#DIV/0!		#DIV/0!		#DIV/0!		#DIV/0!		#DIV/0!		#DIV/0!
ESCROWED BOND FUNDS			#DIV/0!		#DIV/0!		#DIV/0!		#DIV/0!		#DIV/0!		#DIV/0!		#DIV/0!
OTHER			#DIV/0!		#DIV/0!		#DIV/0!		#DIV/0!		#DIV/0!		#DIV/0!		#DIV/0!
TOTAL BOARD DESIGNATED ASSETS	-	-	#DIV/0!	-	#DIV/0!	-	#DIV/0!	0	#DIV/0!	-	#DIV/0!	-	#DIV/0!	-	#DIV/0!
PROPERTY, PLANT, AND EQUIPMENT															
LAND, BUILDINGS & IMPROVEMENTS			#DIV/0!		#DIV/0!		#DIV/0!		#DIV/0!		#DIV/0!	1,615,664	#DIV/0!	1,615,664	0.0%
CONSTRUCTION IN PROGRESS			#DIV/0!		#DIV/0!		#DIV/0!		#DIV/0!	1,677,958	#DIV/0!		-100.0%		#DIV/0!
MAJOR MOVABLE EQUIPMENT			#DIV/0!		#DIV/0!		#DIV/0!		#DIV/0!		#DIV/0!	1,224,932	#DIV/0!	1,224,932	0.0%
FIXED EQUIPMENT			#DIV/0!		#DIV/0!		#DIV/0!		#DIV/0!		#DIV/0!		#DIV/0!		#DIV/0!
TOTAL PROPERTY, PLANT AND EQUIPMENT	-	-	#DIV/0!	-	#DIV/0!	-	#DIV/0!	0	#DIV/0!	1,677,958	#DIV/0!	2,840,596	69.3%	2,840,596	0.0%
LESS: ACCUMULATED DEPRECIATION															
LAND, BUILDINGS & IMPROVEMENTS			#DIV/0!		#DIV/0!		#DIV/0!		#DIV/0!		#DIV/0!	(51,098)	#DIV/0!	(153,295)	200.0%
EQUIPMENT - FIXED			#DIV/0!		#DIV/0!		#DIV/0!		#DIV/0!		#DIV/0!		#DIV/0!		#DIV/0!
EQUIPMENT - MAJOR MOVEABLE			#DIV/0!		#DIV/0!		#DIV/0!		#DIV/0!		#DIV/0!	(104,062)	#DIV/0!	(312,186)	200.0%
TOTAL ACCUMULATED DEPRECIATION	-	-	#DIV/0!	-	#DIV/0!	-	#DIV/0!	-	#DIV/0!	-	#DIV/0!	(155,160)	#DIV/0!	(465,481)	200.0%
TOTAL PROPERTY, PLANT AND EQUIPMENT, NET	-	-	#DIV/0!	-	#DIV/0!	-	#DIV/0!	0	#DIV/0!	1,677,958	#DIV/0!	2,685,436	60.0%	2,375,115	-11.6%
OTHER LONG-TERM ASSETS			#DIV/0!		#DIV/0!		#DIV/0!		#DIV/0!		#DIV/0!		#DIV/0!		#DIV/0!
TOTAL ASSETS	-	-	#DIV/0!	-	#DIV/0!	-	#DIV/0!	-	#DIV/0!	(15,000)	#DIV/0!	(205,631)	1270.9%	(535,634)	160.5%
LIABILITIES AND FUND BALANCE															
CURRENT LIABILITIES															
ACCOUNTS PAYABLE			#DIV/0!		#DIV/0!		#DIV/0!		#DIV/0!		#DIV/0!		#DIV/0!		#DIV/0!
SALARIES, WAGES AND PAYROLL TAXES PAYABLE			#DIV/0!		#DIV/0!		#DIV/0!		#DIV/0!		#DIV/0!		#DIV/0!		#DIV/0!
ESTIMATED THIRD-PARTY SETTLEMENTS			#DIV/0!		#DIV/0!		#DIV/0!		#DIV/0!		#DIV/0!		#DIV/0!		#DIV/0!
OTHER CURRENT LIABILITIES			#DIV/0!		#DIV/0!		#DIV/0!		#DIV/0!		#DIV/0!		#DIV/0!		#DIV/0!
CURRENT PORTION OF LONG-TERM DEBT			#DIV/0!		#DIV/0!		#DIV/0!		#DIV/0!		#DIV/0!		#DIV/0!		#DIV/0!
TOTAL CURRENT LIABILITIES	-	-	#DIV/0!	-	#DIV/0!	-	#DIV/0!	-	#DIV/0!	-	#DIV/0!	-	#DIV/0!	-	#DIV/0!
LONG-TERM DEBT															
BONDS & MORTGAGES PAYABLE			#DIV/0!		#DIV/0!		#DIV/0!		#DIV/0!		#DIV/0!		#DIV/0!		#DIV/0!
CAPITAL LEASE OBLIGATIONS			#DIV/0!		#DIV/0!		#DIV/0!		#DIV/0!		#DIV/0!		#DIV/0!		#DIV/0!
OTHER LONG-TERM DEBT			#DIV/0!		#DIV/0!		#DIV/0!		#DIV/0!		#DIV/0!		#DIV/0!		#DIV/0!
TOTAL LONG-TERM DEBT	-	-	#DIV/0!	-	#DIV/0!	-	#DIV/0!	-	#DIV/0!	-	#DIV/0!	-	#DIV/0!	-	#DIV/0!
OTHER NONCURRENT LIABILITIES			#DIV/0!		#DIV/0!		#DIV/0!		#DIV/0!		#DIV/0!		#DIV/0!		#DIV/0!
TOTAL LIABILITIES	-	-	#DIV/0!	-	#DIV/0!	-	#DIV/0!	-	#DIV/0!	-	#DIV/0!	-	#DIV/0!	-	#DIV/0!
FUND BALANCE			#DIV/0!		#DIV/0!		#DIV/0!		#DIV/0!	(15,000)	#DIV/0!	(205,631)	1270.9%	(535,634)	160.5%

RUTLAND REGIONAL MEDICAL CENTER

TOTAL LIABILITIES AND FUND BALANCE	-	-	#DIV/0!	-	#DIV/0!	-	#DIV/0!	-	#DIV/0!	(15,000)	#DIV/0!	(205,631)	1270.9%	(535,634)	160.5%

RUTLAND REGIONAL MEDICAL CENTER

Note: This table requires no "fill-in" as it is populated automatically

Balance Sheet

WITH PROJECT

	2015 Actual	2016 Budget	% change	2016 Projection	% change	2017 Budget	% change	2,017 Projected	% change	2,018 Proposed Year 1	% change	2,019 Proposed Year 2	% change	2,020 Proposed Year 3	% change
ASSETS															
CURRENT ASSETS															
CASH & INVESTMENTS	12,803,315	23,680,313	85.0%	14,551,514	-38.6%	39,503,614	171.5%	15,386,482	-61.1%	12,883,183	-16.3%	10,702,063	-16.9%	11,561,034	8.0%
PATIENT ACCOUNTS RECEIVABLE, GROSS	65,671,511	66,814,488	1.7%	65,671,511	-1.7%	65,671,511	0.0%	67,802,702	3.2%	67,802,702	0.0%	67,802,702	0.0%	67,802,702	0.0%
LESS: ALLOWANCE FOR UNCOLLECTIBLE ACCTS	(45,002,495)	(42,592,168)	-5.4%	(45,002,495)	5.7%	(45,002,495)	0.0%	(45,270,950)	0.6%	(45,270,950)	0.0%	(45,270,950)	0.0%	(45,270,950)	0.0%
DUE FROM THIRD PARTIES	-	-	#DIV/0!	5,167,469	#DIV/0!	5,167,469	0.0%	5,260,001	1.8%	5,260,001	0.0%	5,260,001	0.0%	5,260,001	0.0%
OTHER CURRENT ASSETS	9,722,463	12,703,659	30.7%	9,722,463	-23.5%	9,722,463	0.0%	10,594,250	9.0%	10,594,250	0.0%	10,594,250	0.0%	10,594,250	0.0%
TOTAL CURRENT ASSETS	43,194,794	60,606,292	40.3%	50,110,462	-17.3%	75,062,562	49.8%	53,772,485	-28.4%	51,269,186	-4.7%	49,088,066	-4.3%	49,947,037	1.7%
BOARD DESIGNATED ASSETS					#DIV/0!		#DIV/0!								
FUNDED DEPRECIATION	61,639,087	114,778,672	86.2%	105,706,228	-7.9%	112,843,141	6.8%	120,526,972	6.8%	129,432,346	7.4%	138,337,720	6.9%	147,243,094	6.4%
ESCROWED BOND FUNDS	1,022,845	1,422,845	39.1%	-	-100.0%	-	#DIV/0!	-	#DIV/0!	-	#DIV/0!	-	#DIV/0!	-	#DIV/0!
OTHER	43,561,026	-	-100.0%	5,997,925	#DIV/0!	5,997,925	0.0%	6,201,912	3.4%	6,201,912	0.0%	6,201,912	0.0%	6,201,912	0.0%
TOTAL BOARD DESIGNATED ASSETS	106,222,958	116,201,517	9.4%	111,704,153	-3.9%	118,841,066	6.4%	126,728,884	6.6%	135,634,258	7.0%	144,539,632	6.6%	153,445,006	6.2%
PROPERTY, PLANT, AND EQUIPMENT															
LAND, BUILDINGS & IMPROVEMENTS	88,638,887	84,993,447	-4.1%	88,638,887	4.3%	88,638,887	0.0%	102,633,484	15.8%	102,633,484	0.0%	104,249,148	1.6%	104,249,148	0.0%
CONSTRUCTION IN PROGRESS	2,197,239	3,161,464	43.9%	2,197,239	-30.5%	2,197,239	0.0%	3,422,993	55.8%	5,100,951	49.0%	3,422,993	-32.9%	3,422,993	0.0%
MAJOR MOVABLE EQUIPMENT	96,681,658	106,192,364	9.8%	113,784,698	7.1%	123,638,698	8.7%	119,875,161	-3.0%	135,200,943	12.8%	175,117,944	29.5%	192,117,944	9.7%
FIXED EQUIPMENT	29,597,080	30,016,498	1.4%	29,597,080	-1.4%	29,597,080	0.0%	33,456,193	13.0%	33,456,193	0.0%	33,456,193	0.0%	33,456,193	0.0%
TOTAL PROPERTY, PLANT AND EQUIPMENT	217,114,864	224,363,773	3.3%	234,217,904	4.4%	244,071,904	4.2%	259,387,831	6.3%	276,391,571	6.6%	316,246,278	14.4%	333,246,278	5.4%
LESS: ACCUMULATED DEPRECIATION															
LAND, BUILDINGS & IMPROVEMENTS	(44,966,451)	(49,171,122)	9.4%	(44,966,451)	-8.6%	(44,966,451)	0.0%	(53,095,223)	18.1%	(53,095,223)	0.0%	(53,146,321)	0.1%	(53,248,518)	0.2%
EQUIPMENT - FIXED	(22,872,018)	(23,795,284)	4.0%	(22,872,018)	-3.9%	(22,872,018)	0.0%	(24,755,689)	8.2%	(24,755,689)	0.0%	(24,755,689)	0.0%	(24,755,689)	0.0%
EQUIPMENT - MAJOR MOVEABLE	(75,558,526)	(84,163,325)	11.4%	(89,252,694)	6.0%	(102,414,382)	14.7%	(96,218,671)	-6.0%	(108,946,835)	13.2%	(123,113,039)	13.0%	(139,860,805)	13.6%
TOTAL ACCUMULATED DEPRECIATION	(143,396,995)	(157,129,731)	9.6%	(157,091,163)	0.0%	(170,252,851)	8.4%	(174,069,583)	2.2%	(186,797,747)	7.3%	(201,015,049)	7.6%	(217,865,012)	8.4%
TOTAL PROPERTY, PLANT AND EQUIPMENT, NET	73,717,869	67,234,042	-8.8%	77,126,741	14.7%	73,819,053	-4.3%	85,318,248	15.6%	89,593,824	5.0%	115,231,229	28.6%	115,381,266	0.1%
OTHER LONG-TERM ASSETS	9,289,915	9,834,219	5.9%	4,122,446	-58.1%	4,122,446	0.0%	5,266,689	27.8%	5,266,689	0.0%	5,266,689	0.0%	5,266,689	0.0%
TOTAL ASSETS	232,425,536	253,876,070	9.2%	243,063,802	-4.3%	271,845,127	11.8%	271,086,308	-0.3%	281,763,959	3.9%	314,125,616	11.5%	324,039,998	3.2%
LIABILITIES AND FUND BALANCE															
CURRENT LIABILITIES															
ACCOUNTS PAYABLE	2,818,694	4,265,502	51.3%	5,442,168	27.6%	5,442,168	0.0%	4,443,366	-18.4%	4,443,366	0.0%	4,443,366	0.0%	4,443,366	0.0%
SALARIES, WAGES AND PAYROLL TAXES PAYABLE	9,311,259	9,749,853	4.7%	10,113,344	3.7%	10,113,344	0.0%	11,234,778	11.1%	11,234,778	0.0%	11,234,778	0.0%	11,234,778	0.0%
ESTIMATED THIRD-PARTY SETTLEMENTS	8,592,533	7,847,454	-8.7%	8,592,533	9.5%	8,592,533	0.0%	9,152,712	6.5%	9,152,712	0.0%	9,152,712	0.0%	9,152,712	0.0%
OTHER CURRENT LIABILITIES	9,961,273	6,199,500	-37.8%	6,610,233	6.6%	6,610,517	0.0%	5,216,286	-21.1%	5,192,502	-0.5%	5,188,559	-0.1%	5,145,715	-0.8%
CURRENT PORTION OF LONG-TERM DEBT	2,283,260	1,871,793	-18.0%	1,727,223	-7.7%	2,133,373	23.5%	1,795,007	-15.9%	1,865,452	3.9%	1,938,661	3.9%	1,113,320	-42.6%
TOTAL CURRENT LIABILITIES	32,967,019	29,934,102	-9.2%	32,485,501	8.5%	32,891,935	1.3%	31,842,149	-3.2%	31,888,810	0.1%	31,958,076	0.2%	31,089,891	-2.7%
LONG-TERM DEBT															
BONDS & MORTGAGES PAYABLE	31,818,131	38,263,410	20.3%	38,263,410	0.0%	56,102,482	46.6%	36,469,153	-35.0%	34,603,702	-5.1%	54,357,110	57.1%	52,484,872	-3.4%
CAPITAL LEASE OBLIGATIONS	-	-	#DIV/0!	-	#DIV/0!	-	#DIV/0!	-	#DIV/0!	-	#DIV/0!	-	#DIV/0!	-	#DIV/0!
OTHER LONG-TERM DEBT	8,173,101	-	-100.0%	-	#DIV/0!	-	#DIV/0!	-	#DIV/0!	-	#DIV/0!	-	#DIV/0!	-	#DIV/0!
TOTAL LONG-TERM DEBT	39,991,232	38,263,410	-4.3%	38,263,410	0.0%	56,102,482	46.6%	36,469,153	-35.0%	34,603,702	-5.1%	54,357,110	57.1%	52,484,872	-3.4%
OTHER NONCURRENT LIABILITIES	30,961,803	36,473,642	17.8%	32,450,125	-11.0%	29,744,143	-8.3%	32,865,815	10.5%	30,183,617	-8.2%	27,505,362	-8.9%	24,869,951	-9.6%
TOTAL LIABILITIES	103,920,054	104,671,154	0.7%	103,199,036	-1.4%	118,738,560	15.1%	101,177,117	-14.8%	96,676,129	-4.4%	113,820,548	17.7%	108,444,714	-4.7%
FUND BALANCE	128,505,482	149,204,916	16.1%	139,864,766	-6.3%	153,106,567	9.5%	169,909,191	11.0%	185,087,830	8.9%	200,305,069	8.2%	215,595,285	7.6%
TOTAL LIABILITIES AND FUND BALANCE	232,425,536	253,876,070	9.2%	243,063,802	-4.3%	271,845,127	11.8%	271,086,308	-0.3%	281,763,959	3.9%	314,125,616	11.5%	324,039,998	3.2%

RUTLAND REGIONAL MEDICAL CENTER

NUCLEAR MEDICINE

PAYER REVENUE REPORT

WITHOUT PROJECT

	2015 Actual	2016 Budget	% change	2016 Budget 201	% change	2017 Budget	% change	2017 Projection	% change	2018 Proposed Year 1	% change	2019 Proposed Year 2	% change	2020 Proposed Year 3	% change
Commercial															
Hospital	143,051,821	147,443,985	3.1%	147,443,985	0.0%	139,409,330	-5.4%	151,494,214	8.7%	156,967,020	3.6%	167,008,420	6.4%	178,055,335	6.6%
Physician	12,072,341	22,243,512	84.3%	22,243,512	0.0%	22,089,924	-0.7%	29,243,108	32.4%	30,883,026	5.6%	32,858,656	6.4%	35,032,120	6.6%
Total Revenue	155,124,162	169,687,497	9.4%	169,687,497	0.0%	161,499,254	-4.8%	180,737,322	11.9%	187,850,046	16.3%	199,867,077	6.4%	213,087,455	6.6%
Allowances - Hospital	-18,370,485	-18,391,078	0.1%	-18,391,078	0.0%	-14,221,966	-22.7%	(24,824,465)	74.6%	(25,352,171)	2.1%	(27,672,109)	9.2%	(30,265,808)	9.4%
Allowances - Physicians	-8,188,378	-13,044,557	59.3%	-13,044,557	0.0%	-10,904,655	-16.4%	(11,644,708)	6.8%	(12,298,792)	5.6%	(13,424,235)	9.2%	(14,682,485)	9.4%
Free Care	-4,167,120	-5,627,667	35.0%	-5,627,667	0.0%	-3,569,908	-36.6%	(5,885,228)	64.9%	(6,121,719)	4.0%	(6,512,943)	6.4%	(6,943,748)	6.6%
Bad Debt	-5,520,297	-8,337,141	51.0%	-8,337,141	0.0%	-6,626,902	-20.5%	(5,104,274)	-23.0%	(5,309,383)	0.04018378	(5,649,416)	6.4%	(6,023,101)	6.6%
Net Payer Revenue	118,877,882	124,287,054	4.6%	124,287,054	0.0%	126,175,823	1.5%	133,278,647	5.6%	138,767,981	4.1%	146,608,374	5.7%	155,172,312	5.8%
	77%	73%		73%		78%		74%		74%		73%		73%	
Medicaid															
Hospital	83,590,394	86,098,610	3.0%	86,098,610	0.0%	81,894,694	-4.9%	69,511,396	-15.1%	72,182,714	3.8%	76,800,343	6.4%	81,880,368	6.6%
Physician	12,296,675	13,941,441	13.4%	13,941,441	0.0%	14,755,924	5.8%	15,463,191	4.8%	16,324,134	5.6%	17,368,412	6.4%	18,517,260	6.6%
Total Revenue	95,887,069	100,040,051	4.3%	100,040,051	0.0%	96,650,618	-3.4%	84,974,587	-12.1%	88,506,848	4.2%	94,168,755	6.4%	100,397,628	6.6%
Allowances - Hospital	-60,388,738	-55,586,225	-8.0%	-55,586,225	0.0%	-59,357,279	6.8%	(49,176,923)	-17.2%	(51,874,244)	5.5%	(56,621,175)	9.2%	(61,928,263)	9.4%
Allowances - Physicians	-7,450,344	-9,105,509	22.2%	-9,105,509	0.0%	-9,044,966	-0.7%	(11,108,756)	22.8%	(11,943,660)	7.5%	(13,036,606)	9.2%	(14,258,523)	9.4%
Free Care	0	0	#DIV/0!	0	#DIV/0!	0	#DIV/0!		#DIV/0!		#DIV/0!		#DIV/0!		#DIV/0!
Bad Debt	0	0	#DIV/0!	0	#DIV/0!	0	#DIV/0!		#DIV/0!		#DIV/0!		#DIV/0!		#DIV/0!
Graduate Medical Education Payments Phys.	0	0	#DIV/0!	0	#DIV/0!	0	#DIV/0!		#DIV/0!		#DIV/0!		#DIV/0!		#DIV/0!
Graduate Medical Education Payments-Hosp	0	0	#DIV/0!	0	#DIV/0!	0	#DIV/0!		#DIV/0!		#DIV/0!		#DIV/0!		#DIV/0!
Net Payer Revenue	28,047,987	35,348,317	26.0%	35,348,317	0.0%	28,248,373	-20.1%	24,688,908	-12.6%	24,688,944	0.0%	24,510,975	-0.7%	24,210,841	-1.2%
	29%	35%		35%		29%		29%		28%		26%		24%	
Medicare															
Hospital	225,871,332	218,203,115	-3.4%	218,203,115	0.0%	216,504,489	-0.8%	214,294,322	-1.0%	222,519,471	3.8%	236,754,057	6.4%	252,414,355	6.6%
Physician	16,511,949	22,501,462	36.3%	22,501,462	0.0%	26,261,977	16.7%	30,421,185	15.8%	32,061,942	5.4%	34,112,989	6.4%	36,369,422	6.6%
Total Revenue	242,383,281	240,704,577	-0.7%	240,704,577	0.0%	242,766,466	0.9%	244,715,507	0.8%	254,581,413	4.0%	270,867,046	6.4%	288,783,778	6.6%
												6.4%			#DIV/0!
Allowances - Hospital	-154,393,417	-155,354,898	0.6%	-155,354,898	0.0%	-139,901,625	-9.9%	(141,436,420)	1.1%	(147,743,347)	4.5%	(161,262,368)	9.2%	(176,377,345)	9.4%
Allowances - Physicians	-11,163,259	-15,906,034	42.5%	-15,906,034	0.0%	-19,598,459	23.2%	(21,723,769)	10.8%	(23,327,227)	7.4%	(25,461,561)	9.2%	(27,848,066)	9.4%
Free Care	0	0	#DIV/0!	0	#DIV/0!	0	#DIV/0!		#DIV/0!		#DIV/0!		#DIV/0!		#DIV/0!
Bad Debt	0	0	#DIV/0!	0	#DIV/0!	0	#DIV/0!		#DIV/0!		#DIV/0!		#DIV/0!		#DIV/0!
Net Payer Revenue	76,826,605	69,443,645	-9.6%	69,443,645	0.0%	83,266,382	19.9%	81,555,318	-2.1%	83,510,839	2.4%	84,143,118	0.8%	84,558,367	0.5%
	32%	29%		28%		34%		33%		33%		31%		29%	
Disproportionate Share Payments	4,576,163	4,169,146	-8.9%	4,169,146	0.0%	5,724,870	37.3%	5,724,870	0.0%	4,579,237	-20.0%	4,837,858	5.6%	5,002,345	3.4%
Total Payer Revenue															
Hospital	452,513,547	451,745,710	-0.2%	451,745,710	0.0%	437,808,513	-3.1%	435,299,932	-0.6%	451,669,205	3.8%	480,562,820	6.4%	512,350,057	6.6%
Physician	40,880,965	58,686,415	43.6%	58,686,415	0.0%	63,107,825	7.5%	75,127,484	19.0%	79,269,102	5.5%	84,340,058	6.4%	89,918,803	6.6%
Total Revenue	493,394,512	510,432,125	3.5%	510,432,125	0.0%	500,916,338	-1.9%	510,427,416	1.9%	530,938,307	4.0%	564,902,878	6.4%	602,268,860	6.6%
Allowances - Hospital	-233,152,640	-229,332,201	-1.6%	-229,332,201	0.0%	-213,480,870	-6.9%	(215,437,808)	0.9%	(224,969,485)	4.4%	(245,556,091)	9.2%	(268,571,999)	9.4%
Allowances - Physicians	-26,801,981	-38,056,100	42.0%	-38,056,100	0.0%	-39,548,080	3.9%	(44,477,233)	12.5%	(47,569,679)	7.0%	(51,922,401)	9.2%	(56,789,075)	9.4%
Free Care	-4,167,120	-5,627,667	35.0%	-5,627,667	0.0%	-3,569,908	-36.6%	(5,885,228)	64.9%	(6,121,719)	4.0%	(6,512,943)	6.4%	(6,943,748)	6.6%
Bad Debt	-5,520,297	-8,337,141	51.0%	-8,337,141	0.0%	-6,626,902	-20.5%	(5,104,274)	-23.0%	(5,309,383)	0.04018378	(5,649,416)	6.4%	(6,023,101)	6.6%
Disproportionate Share Payments	4,576,163	4,169,146	-8.9%	4,169,146	0.0%	5,724,870	37.3%	5,724,870	0.0%	4,579,237	-20.0%	4,837,858	5.6%	5,002,345	3.4%
Graduate Medical Education Payments Phys.	0	0	#DIV/0!	0	#DIV/0!	0	#DIV/0!		#DIV/0!		#DIV/0!		#DIV/0!		#DIV/0!
Graduate Medical Education Payments-Hosp	0	0	#DIV/0!	0	#DIV/0!	0	#DIV/0!		#DIV/0!		#DIV/0!		#DIV/0!		#DIV/0!
Net Payer Revenue	228,328,637	233,248,162	2.2%	233,248,162	0.0%	243,415,448	4.4%	245,247,743	0.8%	251,547,278	2.6%	260,099,885	3.4%	268,943,282	3.4%
	46%	46%		46%		49%		48%		47%		46%		45%	

NUCLEAR MEDICINE

PAYER REVENUE REPORT

PROJECT ONLY

	2015 Actual	2016 Budget	% change	2016 Budget 201	% change	2017 Budget	% change	2017 Proposed Year 1	% change	2018 Proposed Year 1	% change	2019 Proposed Year 2	% change	2020 Proposed Year 3	% change
Commercial															
Hospital			#DIV/0!		#DIV/0!		#DIV/0!		#DIV/0!		#DIV/0!		#DIV/0!		#DIV/0!
Physician			#DIV/0!		#DIV/0!		#DIV/0!		#DIV/0!		#DIV/0!		#DIV/0!		#DIV/0!
Total Revenue			#DIV/0!		#DIV/0!		#DIV/0!	-	#DIV/0!	-	#DIV/0!	-	#DIV/0!	-	#DIV/0!
Allowances - Hospital			#DIV/0!		#DIV/0!		#DIV/0!		#DIV/0!		#DIV/0!		#DIV/0!		#DIV/0!
Allowances - Physicians			#DIV/0!		#DIV/0!		#DIV/0!		#DIV/0!		#DIV/0!		#DIV/0!		#DIV/0!
Free Care							#DIV/0!		#DIV/0!		#DIV/0!				#DIV/0!
Bad Debt							#DIV/0!		#DIV/0!		#DIV/0!				#DIV/0!
Net Payer Revenue			#DIV/0!		#DIV/0!		#DIV/0!		#DIV/0!	-	#DIV/0!	-	#DIV/0!	-	#DIV/0!
	#DIV/0!	#DIV/0!		#DIV/0!				#DIV/0!		#DIV/0!		#DIV/0!		#DIV/0!	
Medicaid															
Hospital			#DIV/0!		#DIV/0!		#DIV/0!		#DIV/0!		#DIV/0!		#DIV/0!		#DIV/0!
Physician			#DIV/0!		#DIV/0!		#DIV/0!		#DIV/0!		#DIV/0!		#DIV/0!		#DIV/0!
Total Revenue			#DIV/0!		#DIV/0!		#DIV/0!	-	#DIV/0!	-	#DIV/0!	-	#DIV/0!	-	#DIV/0!
Allowances - Hospital			#DIV/0!		#DIV/0!		#DIV/0!		#DIV/0!		#DIV/0!		#DIV/0!		#DIV/0!
Allowances - Physicians			#DIV/0!		#DIV/0!		#DIV/0!		#DIV/0!		#DIV/0!		#DIV/0!		#DIV/0!
Free Care							#DIV/0!		#DIV/0!		#DIV/0!				
Bad Debt							#DIV/0!		#DIV/0!		#DIV/0!				
Graduate Medical Education Payments_Phys.			#DIV/0!		#DIV/0!		#DIV/0!		#DIV/0!		#DIV/0!		#DIV/0!		#DIV/0!
Graduate Medical Education Payments-Hosp			#DIV/0!		#DIV/0!		#DIV/0!		#DIV/0!		#DIV/0!		#DIV/0!		#DIV/0!
Net Payer Revenue			#DIV/0!		#DIV/0!		#DIV/0!	-	#DIV/0!	-	#DIV/0!	-	#DIV/0!	-	#DIV/0!
	#DIV/0!	#DIV/0!		#DIV/0!				#DIV/0!		#DIV/0!		#DIV/0!		#DIV/0!	
Medicare															
Hospital			#DIV/0!		#DIV/0!		#DIV/0!		#DIV/0!		#DIV/0!		#DIV/0!		#DIV/0!
Physician			#DIV/0!		#DIV/0!		#DIV/0!		#DIV/0!		#DIV/0!		#DIV/0!		#DIV/0!
Total Revenue			#DIV/0!		#DIV/0!		#DIV/0!	-	#DIV/0!	-	#DIV/0!	-	#DIV/0!	-	#DIV/0!
															#DIV/0!
Allowances - Hospital			#DIV/0!		#DIV/0!		#DIV/0!		#DIV/0!		#DIV/0!		#DIV/0!		#DIV/0!
Allowances - Physicians			#DIV/0!		#DIV/0!		#DIV/0!		#DIV/0!		#DIV/0!		#DIV/0!		#DIV/0!
Free Care							#DIV/0!		#DIV/0!		#DIV/0!				
Bad Debt							#DIV/0!		#DIV/0!		#DIV/0!				
Net Payer Revenue			#DIV/0!		#DIV/0!		#DIV/0!		#DIV/0!	-	#DIV/0!	-	#DIV/0!	-	#DIV/0!
	#DIV/0!	#DIV/0!		#DIV/0!				#DIV/0!		#DIV/0!		#DIV/0!		#DIV/0!	
Disproportionate Share Payments			#DIV/0!		#DIV/0!		#DIV/0!		#DIV/0!		#DIV/0!		#DIV/0!		#DIV/0!
Total Payer Revenue															
Hospital			#DIV/0!		#DIV/0!		#DIV/0!		#DIV/0!		#DIV/0!		#DIV/0!		#DIV/0!
Physician			#DIV/0!		#DIV/0!		#DIV/0!		#DIV/0!		#DIV/0!		#DIV/0!		#DIV/0!
Total Revenue			#DIV/0!		#DIV/0!		#DIV/0!	-	#DIV/0!	-	#DIV/0!	-	#DIV/0!	-	#DIV/0!
Allowances - Hospital			#DIV/0!		#DIV/0!		#DIV/0!		#DIV/0!		#DIV/0!		#DIV/0!		#DIV/0!
Allowances - Physicians			#DIV/0!		#DIV/0!		#DIV/0!		#DIV/0!		#DIV/0!		#DIV/0!		#DIV/0!
Free Care			#DIV/0!		#DIV/0!		#DIV/0!		#DIV/0!		#DIV/0!		#DIV/0!		#DIV/0!
Bad Debt			#DIV/0!		#DIV/0!		#DIV/0!		#DIV/0!		#DIV/0!		#DIV/0!		#DIV/0!
Disproportionate Share Payments			#DIV/0!		#DIV/0!		#DIV/0!		#DIV/0!		#DIV/0!		#DIV/0!		#DIV/0!
Graduate Medical Education Payments_Phys,			#DIV/0!		#DIV/0!		#DIV/0!		#DIV/0!		#DIV/0!		#DIV/0!		#DIV/0!
Graduate Medical Education Payments-Hosp			#DIV/0!		#DIV/0!		#DIV/0!		#DIV/0!		#DIV/0!		#DIV/0!		#DIV/0!
Net Payer Revenue			#DIV/0!		#DIV/0!		#DIV/0!	-	#DIV/0!	-	#DIV/0!	-	#DIV/0!	-	#DIV/0!
	#DIV/0!	#DIV/0!		#DIV/0!				#DIV/0!		#DIV/0!		#DIV/0!		#DIV/0!	

RUTLAND REGIONAL MEDICAL CENTER

NUCLEAR MEDICINE
Note: This table requires no "fill-in" as it is populated automatically
PAYER REVENUE REPORT

WITH PROJECT

	2015 Actual	2016 Budget	% change	2016 Budget 201	% change	2017 Budget	% change	2017 Proposed Year 1	% change	2018 Proposed Year 1	% change	2019 Proposed Year 2	% change	2020 Proposed Year 3	% change
Commercial															
Hospital	143,051,821	147,443,985	3.1%	147,443,985	0.0%	139,409,330	-5.4%	151,494,214	8.7%	156,967,020	3.6%	167,008,420	6.4%	178,055,335	6.6%
Physician	12,072,341	22,243,512	84.3%	22,243,512	0.0%	22,089,924	-0.7%	29,243,108	32.4%	30,883,026	5.6%	32,858,656	6.4%	35,032,120	6.6%
Total Revenue	155,124,162	169,687,497	9.4%	169,687,497	0.0%	161,499,254	-4.8%	180,737,322	11.9%	187,850,046	16.3%	199,867,077	6.4%	213,087,455	6.6%
Allowances - Hospital	-18,370,485	-18,391,078	0.1%	-18,391,078	0.0%	(14,221,966)	-22.7%	(24,824,465)	74.6%	(25,352,171)	2.1%	(27,672,109)	9.2%	(30,265,808)	9.4%
Allowances - Physicians	-8,188,378	-13,044,557	59.3%	-13,044,557	0.0%	(10,904,655)	-16.4%	(11,644,708)	6.8%	(12,298,792)	5.6%	(13,424,235)	9.2%	(14,682,485)	9.4%
Free Care	-4,167,120	-5,627,667	35.0%	-5,627,667	0.0%	(3,569,908)	-36.6%	(5,885,228)	64.9%	(6,121,719)	4.0%	(6,512,943)	6.4%	(6,943,748)	6.6%
Bad Debt	-5,520,297	-8,337,141	51.0%	-8,337,141	0.0%	(6,626,902)	-20.5%	(5,104,274)	-23.0%	(5,309,383)	0.04018378	(5,649,416)	6.4%	(6,023,101)	6.6%
Net Payer Revenue	118,877,882	124,287,054	4.6%	124,287,054	0.0%	126,175,823	1.5%	133,278,647	5.6%	138,767,981	4.1%	146,608,374	5.7%	155,172,312	5.8%
	77%	73%		73%		78%		74%		74%		73%		73%	
Medicaid															
Hospital	83,590,394	86,098,610	3.0%	86,098,610	0.0%	81,894,694	-4.9%	69,511,396	-15.1%	72,182,714	3.8%	76,800,343	6.4%	81,880,368	6.6%
Physician	12,296,675	13,941,441	13.4%	13,941,441	0.0%	14,755,924	5.8%	15,463,191	4.8%	16,324,134	5.6%	17,368,412	6.4%	18,517,260	6.6%
Total Revenue	95,887,069	100,040,051	4.3%	100,040,051	0.0%	96,650,618	-3.4%	84,974,587	-12.1%	88,506,848	4.2%	94,168,755	6.4%	100,397,628	6.6%
Allowances - Hospital	-60,388,738	-55,586,225	-8.0%	-55,586,225	0.0%	(59,357,279)	6.8%	(49,176,923)	-17.2%	(51,874,244)	5.5%	(56,621,175)	9.2%	(61,928,263)	9.4%
Allowances - Physicians	-7,450,344	-9,105,509	22.2%	-9,105,509	0.0%	(9,044,966)	-0.7%	(11,108,756)	22.8%	(11,943,660)	7.5%	(13,036,606)	9.2%	(14,258,523)	9.4%
Free Care	0	0	#DIV/0!	0	#DIV/0!	-	#DIV/0!	-	#DIV/0!	-	#DIV/0!	-	#DIV/0!	-	#DIV/0!
Bad Debt	0	0	#DIV/0!	0	#DIV/0!	-	#DIV/0!	-	#DIV/0!	-	#DIV/0!	-	#DIV/0!	-	#DIV/0!
Graduate Medical Education Payments_Phys.	0	0	#DIV/0!	0	#DIV/0!	-	#DIV/0!	-	#DIV/0!	-	#DIV/0!	-	#DIV/0!	-	#DIV/0!
Graduate Medical Education Payments-Hosp	0	0	#DIV/0!	0	#DIV/0!	-	#DIV/0!	-	#DIV/0!	-	#DIV/0!	-	#DIV/0!	-	#DIV/0!
Net Payer Revenue	28,047,987	35,348,317	26.0%	35,348,317	0.0%	28,248,373	-20.1%	24,688,908	-12.6%	24,688,944	0.0%	24,510,975	-0.7%	24,210,841	-1.2%
	29%	35%		35%		29%		29%		26%		26%		24%	
Medicare															
Hospital	225,871,332	218,203,115	-3.4%	218,203,115	0.0%	216,504,489	-0.8%	214,294,322	-1.0%	222,519,471	3.8%	236,754,057	6.4%	252,414,355	6.6%
Physician	16,511,949	22,501,462	36.3%	22,501,462	0.0%	26,261,977	16.7%	30,421,185	15.8%	32,061,942	5.4%	34,112,989	6.4%	36,369,422	6.6%
Total Revenue	242,383,281	240,704,577	-0.7%	240,704,577	0.0%	242,766,466	0.9%	244,715,507	0.8%	254,581,413	4.0%	270,867,046	6.4%	288,783,778	6.6%
															#DIV/0!
Allowances - Hospital	-154,393,417	-155,354,898	0.6%	-155,354,898	0.0%	(139,901,625)	-9.9%	(141,436,420)	1.1%	(147,743,347)	4.5%	(161,262,368)	9.2%	(176,377,345)	9.4%
Allowances - Physicians	-11,163,259	-15,906,034	42.5%	-15,906,034	0.0%	(19,598,459)	23.2%	(21,723,769)	10.8%	(23,327,227)	7.4%	(25,461,561)	9.1%	(27,848,066)	9.4%
Free Care	0	0	#DIV/0!	0	#DIV/0!	-	#DIV/0!	-	#DIV/0!	-	#DIV/0!	-	#DIV/0!	-	#DIV/0!
Bad Debt	0	0	#DIV/0!	0	#DIV/0!	-	#DIV/0!	-	#DIV/0!	-	#DIV/0!	-	#DIV/0!	-	#DIV/0!
Net Payer Revenue	76,826,605	69,443,645	-9.6%	69,443,645	0.0%	83,266,382	19.9%	81,555,318	-2.1%	83,510,839	2.4%	84,143,118	0.8%	84,558,367	0.5%
	32%	29%		29%		34%		33%		33%		31%			
Disproportionate Share Payments	4,576,163	4,169,146	-8.9%	4,169,146	0.0%	5,724,870	37.3%	5,724,870	0.0%	4,579,237	-20.0%	4,837,858	5.6%	5,002,345	3.4%
Total Payer Revenue															
Hospital	452,513,547	451,745,710	-0.2%	451,745,710	0.0%	437,808,513	-3.1%	435,299,932	-0.6%	451,669,205	3.8%	480,562,820	6.4%	512,350,057	6.6%
Physician	40,880,965	58,686,415	43.6%	58,686,415	0.0%	63,107,825	7.5%	75,127,484	19.0%	79,269,102	5.5%	84,340,058	6.4%	89,918,803	6.6%
Total Revenue	493,394,512	510,432,125	3.5%	510,432,125	0.0%	500,916,338	-1.9%	510,427,416	1.9%	530,938,307	4.0%	564,902,878	6.4%	602,268,860	6.6%
Allowances - Hospital	-233,152,640	-229,332,201	-1.6%	-229,332,201	0.0%	(213,480,870)	-6.9%	(215,437,808)	0.9%	(224,969,485)	4.4%	(245,556,091)	9.2%	(268,571,999)	9.4%
Allowances - Physicians	-26,801,981	-38,056,100	42.0%	-38,056,100	0.0%	(39,548,080)	3.9%	(44,477,233)	12.5%	(47,569,679)	7.0%	(51,922,401)	9.2%	(56,789,075)	9.4%
Free Care	-4,167,120	-5,627,667	35.0%	-5,627,667	0.0%	(3,569,908)	-36.6%	(5,885,228)	64.9%	(6,121,719)	4.0%	(6,512,943)	6.4%	(6,943,748)	6.6%
Bad Debt	-5,520,297	-8,337,141	51.0%	-8,337,141	0.0%	(6,626,902)	-20.5%	(5,104,274)	-23.0%	(5,309,383)	0.04018378	(5,649,416)	6.4%	(6,023,101)	6.6%
Disproportionate Share Payments	4,576,163	4,169,146	-8.9%	4,169,146	0.0%	5,724,870	37.3%	5,724,870	0.0%	4,579,237	-20.0%	4,837,858	5.6%	5,002,345	3.4%
Graduate Medical Education Payments_Phys.	0	0	#DIV/0!	0	#DIV/0!	-	#DIV/0!	-	#DIV/0!	-	#DIV/0!	-	#DIV/0!	-	#DIV/0!
Graduate Medical Education Payments-Hosp	0	0	#DIV/0!	0	#DIV/0!	-	#DIV/0!	-	#DIV/0!	-	#DIV/0!	-	#DIV/0!	-	#DIV/0!
Net Payer Revenue	228,328,637	233,248,162	2.2%	233,248,162	0.0%	243,415,448	4.4%	245,247,743	0.8%	251,547,278	2.6%	260,099,885	3.4%	268,943,282	3.4%
	46%	46%		46%		49%		48%		47%		46%		45%	

Rutland Regional Medical Center

NUCLEAR MEDICINE

UTILIZATION PROJECTIONS--TABLE 8

WITHOUT PROJECT

	2015 Actual	2016 Budget	% change	2016 Actuals	% change	2017 Budget	% change	Projected 2017	% change	Proposed Yr 1 2018	% change	Proposed Yr 2 2019	% change	Proposed Yr 3 2020	% change
Inpatient Utilization															
Acute Beds (Staffed)	118	118	0.0%	118	0.0%	115	-2.5%	117	-0.8%	117	1.7%	117	0.0%	117	0.0%
Acute Admissions	5,941	5,541	-6.7%	6,495	17.2%	6,272	-3.4%	6,275	-3.4%	6,275	0.0%	6,275	0.0%	6,275	0.0%
Acute Patient Days	27,200	27,302	0.4%	30,815	12.9%	29,954	-2.8%	31,627	2.6%	31,700	5.8%	31,700	0.0%	31,700	0.0%
Acute Average Length Of Stay	4.58	4.93	7.6%	4.74	-3.7%	4.78	0.7%	5.04	6.2%	5.05	5.8%	5.05	0.0%	5.05	0.0%
Outpatient															
All Outpatient Visits	233,187	231,618	-0.7%	244,330	5.5%	230,700	-5.6%	241961	-1.0%	241389	4.6%	241,389	0.0%	241389	0.0%
Physician Office Visits	-	-	#DIV/0!	-	#DIV/0!	-	#DIV/0!		#DIV/0!		#DIV/0!		#DIV/0!		#DIV/0!
Ancillary															
All Operating Room Procedure	4,539	4,990	9.9%	4,885	-2.1%	4,978	1.9%	5037	3.1%	5037	1.2%	5,037	0.0%	5037	0.0%
All Operating Room Cases	-	4,990	#DIV/0!	-	-100.0%	4,978	#DIV/0!	5037	#DIV/0!	5037	1.2%	5,037	0.0%	5037	0.0%
Emergency Room Visits	34,067	34,467	1.2%	33,831	-1.8%	31,558	-6.7%	32218	-4.8%	32218	2.1%	32,218	0.0%	32218	0.0%
Cat Scan Procedures	10,711	10,644	-0.6%	11,410	7.2%	10,941	-4.1%	11898	4.3%	11900	8.8%	11,900	0.0%	11900	0.0%
Magnetic Resonance Image Exams	4,694	4,472	-4.7%	5,085	13.7%	5,121	0.7%	4981	-2.0%	4981	-2.7%	4,981	0.0%	4981	0.0%
Nuclear Medicine Procedures	710	635	-10.6%	806	26.9%	730	-9.4%	757	-6.1%	757	3.7%	757	0.0%	757	0.0%
Radiology - Diagnostic Procedures	43,492	39,721	-8.7%	43,352	9.1%	39,928	-7.9%	31377	-27.6%	31377	-21.4%	31,377	0.0%	31377	0.0%
Laboratory Tests	505,126	508,366	0.6%	510,930	0.5%	499,627	-2.2%	522573	2.3%	519824	4.0%	519,824	0.0%	519824	0.0%
			#DIV/0!		#DIV/0!		#DIV/0!		#DIV/0!		#DIV/0!		#DIV/0!		#DIV/0!
			#DIV/0!		#DIV/0!		#DIV/0!		#DIV/0!		#DIV/0!		#DIV/0!		#DIV/0!
Adjusted Statistics															
Adjusted Admissions	17,208	16,020	-6.9%	17,901	11.7%	17,390	-2.9%	15600	-12.9%	15558	-10.5%	15,558	0.0%	15558	0.0%
Adjusted Days	78,784	78,935	0.2%	84,928	7.6%	83,051	-2.2%	78624	-7.4%	78535	-5.4%	78,535	0.0%	78535	0.0%

Rutland Regional Medical Center

NUCLEAR MEDICINE

UTILIZATION PROJECTIONS--TABLE 8

PROJECT ONLY

	2015 Actual	2016 Budget	% change	2016 Actuals	% change	2017 Budget	% change	Proposed Yr 1 2017	% change	Proposed Yr 1 2018	% change	Proposed Yr 2 2019	% change	Proposed Yr 3 2020	% change
Inpatient Utilization															
Acute Beds (Staffed)			#DIV/0!		#DIV/0!		#DIV/0!		#DIV/0!		#DIV/0!		#DIV/0!		#DIV/0!
Acute Admissions			#DIV/0!		#DIV/0!		#DIV/0!		#DIV/0!		#DIV/0!		#DIV/0!		#DIV/0!
Acute Patient Days			#DIV/0!		#DIV/0!		#DIV/0!		#DIV/0!		#DIV/0!		#DIV/0!		#DIV/0!
Acute Average Length Of Stay			#DIV/0!		#DIV/0!		#DIV/0!		#DIV/0!		#DIV/0!		#DIV/0!		#DIV/0!
Outpatient															
All Outpatient Visits			#DIV/0!		#DIV/0!		#DIV/0!		#DIV/0!		#DIV/0!		#DIV/0!		#DIV/0!
Physician Office Visits			#DIV/0!		#DIV/0!		#DIV/0!		#DIV/0!		#DIV/0!		#DIV/0!		#DIV/0!
Ancillary															
All Operating Room Procedure			#DIV/0!		#DIV/0!		#DIV/0!		#DIV/0!		#DIV/0!		#DIV/0!		#DIV/0!
All Operating Room Cases			#DIV/0!		#DIV/0!		#DIV/0!		#DIV/0!		#DIV/0!		#DIV/0!		#DIV/0!
Emergency Room Visits			#DIV/0!		#DIV/0!		#DIV/0!		#DIV/0!		#DIV/0!		#DIV/0!		#DIV/0!
Cat Scan Procedures			#DIV/0!		#DIV/0!		#DIV/0!		#DIV/0!		#DIV/0!		#DIV/0!		#DIV/0!
Magnetic Resonance Image Exams			#DIV/0!		#DIV/0!		#DIV/0!		#DIV/0!		#DIV/0!		#DIV/0!		#DIV/0!
Nuclear Medicine Procedures			#DIV/0!		#DIV/0!		#DIV/0!		#DIV/0!		#DIV/0!		#DIV/0!		#DIV/0!
Radiology - Diagnostic Procedures			#DIV/0!		#DIV/0!		#DIV/0!		#DIV/0!		#DIV/0!		#DIV/0!		#DIV/0!
Laboratory Tests			#DIV/0!		#DIV/0!		#DIV/0!		#DIV/0!		#DIV/0!		#DIV/0!		#DIV/0!
			#DIV/0!		#DIV/0!		#DIV/0!		#DIV/0!		#DIV/0!		#DIV/0!		#DIV/0!
			#DIV/0!		#DIV/0!		#DIV/0!		#DIV/0!		#DIV/0!		#DIV/0!		#DIV/0!
Adjusted Statistics															
Adjusted Admissions			#DIV/0!		#DIV/0!		#DIV/0!		#DIV/0!		#DIV/0!		#DIV/0!		#DIV/0!
Adjusted Days			#DIV/0!		#DIV/0!		#DIV/0!		#DIV/0!		#DIV/0!		#DIV/0!		#DIV/0!

Rutland Regional Medical Center

NUCLEAR MEDICINE

UTILIZATION PROJECTIONS--TABLE 8

Note: This table requires no "fill-in" as it is populated automatically

WITH PROJECT

	2015 Actual	2016 Budget	% change	2016 Actuals	% change	2017 Budget	% change	Proposed Yr 1 2017	% change	Proposed Yr 1 2018	% change	Proposed Yr 2 2019	% change	Proposed Yr 3 2020	% change
Inpatient Utilization															
Acute Beds (Staffed)	118	118	0.0%	118	0.0%	115	-2.5%	117	-0.8%	117	1.7%	117	0.0%	117	0.0%
Acute Admissions	5,941	5,541	-6.7%	6,495	17.2%	6,272	-3.4%	6,275	-3.4%	6,275	0.0%	6,275	0.0%	6,275	0.0%
Acute Patient Days	27,200	27,302	0.4%	30,815	12.9%	29,954	-2.8%	31,627	2.6%	31,700	5.8%	31,700	0.0%	31,700	0.0%
Acute Average Length Of Stay	4.58	4.93	7.6%	4.74	-3.7%	4.78	0.7%	5	6.2%	5	5.8%	5	0.0%	5	0.0%
Outpatient															
All Outpatient Visits	233,187	231,618	-0.7%	244,330	5.5%	230,700	-5.6%	241,961	-1.0%	241,389	4.6%	241,389	0.0%	241,389	0.0%
Physician Office Visits	-	-	#DIV/0!	-	#DIV/0!	-	#DIV/0!	-	#DIV/0!	-	#DIV/0!	-	#DIV/0!	-	#DIV/0!
Ancillary															
All Operating Room Procedure	4,539	4,990	9.9%	4,885	-2.1%	4,978	1.9%	5,037	3.1%	5,037	1.2%	5,037	0.0%	5,037	0.0%
All Operating Room Cases	-	4,990	#DIV/0!	-	-100.0%	4,978	#DIV/0!	5,037	#DIV/0!	5,037	1.2%	5,037	0.0%	5,037	0.0%
Emergency Room Visits	34,067	34,467	1.2%	33,831	-1.8%	31,558	-6.7%	32,218	-4.6%	32,218	2.1%	32,218	0.0%	32,218	0.0%
Cat Scan Procedures	10,711	10,644	-0.6%	11,410	7.2%	10,941	-4.1%	11,898	4.3%	11,900	8.8%	11,900	0.0%	11,900	0.0%
Magnetic Resonance Image Exams	4,694	4,472	-4.7%	5,085	13.7%	5,121	0.7%	4,981	-2.0%	4,981	-2.7%	4,981	0.0%	4,981	0.0%
Nuclear Medicine Procedures	710	635	-10.6%	806	26.9%	730	-9.4%	757	-6.1%	757	3.7%	757	0.0%	757	0.0%
Radiology - Diagnostic Procedures	43,492	39,721	-8.7%	43,352	9.1%	39,928	-7.9%	31,377	-27.6%	31,377	-21.4%	31,377	0.0%	31,377	0.0%
Laboratory Tests	505,126	508,366	0.6%	510,930	0.5%	499,627	-2.2%	522,573	2.3%	519,824	4.0%	519,824	0.0%	519,824	0.0%
	-	-	#DIV/0!	-	#DIV/0!	-	#DIV/0!		#DIV/0!		#DIV/0!		#DIV/0!		#DIV/0!
	-	-	#DIV/0!	-	#DIV/0!	-	#DIV/0!		#DIV/0!		#DIV/0!		#DIV/0!		#DIV/0!
Adjusted Statistics															
Adjusted Admissions	17,208	16,020	-6.9%	17,901	11.7%	17,390	-2.9%	15,600	-12.9%	15,558	-10.5%	15,558	0.0%	15,558	0.0%
Adjusted Days	78,784	78,935	0.2%	84,928	7.6%	83,051	-2.2%	78,624	-7.4%	78,535	-5.4%	78,535	0.0%	78,535	0.0%

RUTLAND REGIONAL MEDICAL CENTER

							NUCLEAR MEDICINE									

STAFFING REPORT
WITHOUT PROJECT

	2015 Actual	2016 Budget	% change	2016 Actuals	% change	2017 Budget	% change	Projected 2017	% change	Proposed Year 1 2018	% change	Proposed Year 2 2019	% change	Proposed Year 3 2020	% change
PHYSICIAN FTEs	88.2	93.3	5.8%	68.2	-26.9%	71.0	4.1%	69.5	1.9%	69.4	-2.2%	69.4	0.0%	69.4	0.0%
TRAVELERS	93.0	73.7	-20.8%	91.7	24.5%	71.9	-21.6%	95.5	4.1%	77.8	8.2%	77.8	0.0%	77.8	0.0%
Residents & Fellows	-	-	#DIV/0!	-	#DIV/0!	-	#DIV/0!		#DIV/0!		#DIV/0!		#DIV/0!		#DIV/0!
MLPs	-	-	#DIV/0!	-	#DIV/0!	-	#DIV/0!		#DIV/0!		#DIV/0!		#DIV/0!		#DIV/0!
Non-MD FTEs	1,165.8	1,191.3	2.2%	1,242.8	4.3%	1,283.8	3.3%	1,270.2	2.2%	1,301.3	1.4%	1,301.3	0.0%	1,301.3	0.0%
TOTAL NON-MD FTEs	1,165.8	1,191.3	2.2%	1,242.8	4.3%	1,283.8	3.3%	1,270.2	2.2%	1,301.3	1.4%	1,301.3	0.0%	1,301.3	0.0%

Note: Mid-Level Providers and Residents are now included in Non-MD Employees, prior to 2013 Actual they were included in Physician FTEs

STAFFING REPORT
PROJECT ONLY

	2015 Actual	2016 Budget	% change	2016 Actuals	% change	2017 Budget	% change	Proposed Year 1 2017	% change	Proposed Year 1 2018	% change	Proposed Year 2 2019	% change	Proposed Year 3 2020	% change
PHYSICIAN FTEs			#DIV/0!		#DIV/0!		#DIV/0!		#DIV/0!		#DIV/0!		#DIV/0!		#DIV/0!
TRAVELERS			#DIV/0!		#DIV/0!		#DIV/0!		#DIV/0!		#DIV/0!		#DIV/0!		#DIV/0!
Residents & Fellows			#DIV/0!		#DIV/0!		#DIV/0!		#DIV/0!		#DIV/0!		#DIV/0!		#DIV/0!
MLPs			#DIV/0!		#DIV/0!		#DIV/0!		#DIV/0!		#DIV/0!		#DIV/0!		#DIV/0!
Non-MD FTEs			#DIV/0!		#DIV/0!		#DIV/0!		#DIV/0!		#DIV/0!		#DIV/0!		#DIV/0!
TOTAL NON-MD FTEs	-	-	#DIV/0!	-	#DIV/0!	-	#DIV/0!	-	#DIV/0!	-	#DIV/0!	-	#DIV/0!	-	#DIV/0!

Note: Mid-Level Providers and Residents are now included in Non-MD Employees, prior to 2013 Actual they were included in Physician FTEs

Note: This table requires no "fill-in" as it is populated automatically

STAFFING REPORT
WITH PROJECT

	2015 Actual	2016 Budget	% change	2016 Actuals	% change	2017 Budget	% change	Proposed Year 1 2017	% change	Proposed Year 1 2018	% change	Proposed Year 2 2019	% change	Proposed Year 3 2020	% change
PHYSICIAN FTEs	88.2	93.3	5.8%	68.2	-26.9%	71.0	4.1%	69.5	1.9%	69.4	-2.2%	69.4	0.0%	69.4	0.0%
TRAVELERS	93.0	73.7	-20.8%	91.7	24.5%	71.9	-21.6%	95.5	4.1%	77.8	8.2%	77.8	0.0%	77.8	0.0%
Residents & Fellows	-	-	#DIV/0!	-	#DIV/0!	-	#DIV/0!	-	#DIV/0!	-	#DIV/0!	-	#DIV/0!	-	#DIV/0!
MLPs	-	-	#DIV/0!	-	#DIV/0!	-	#DIV/0!	-	#DIV/0!	-	#DIV/0!	-	#DIV/0!	-	#DIV/0!
Non-MD FTEs	1,165.8	1,191.3	2.2%	1,242.8	4.3%	1,283.8	3.3%	1,270.2	2.2%	1,301.3	1.4%	1,301.3	0.0%	1,301.3	0.0%
TOTAL NON-MD FTEs	1,165.8	1,191.3	2.2%	1,242.8	4.3%	1,283.8	3.3%	1,270.2	2.2%	1,301.3	1.4%	1,301.3	0.0%	1,301.3	0.0%

Note: Mid-Level Providers and Residents are now included in Non-MD Employees, prior to 2013 Actual they were included in Physician FTEs

AMERICAN SOCIETY OF NUCLEAR CARDIOLOGY POSITION STATEMENT

The initial evaluation of patients presenting to emergency departments with chest pain of suspected cardiac origin is critical in determining hospital admission or discharge. Clinical evaluation alone has been unsatisfactory as a complete triage tool in this setting. This has resulted in numerous unnecessary hospital admissions, as well as unfortunate hospital discharge of patients with coronary artery disease. The situation has become more critical as hospitals, particularly in large metropolitan centers, are above capacity, resulting in closing of hospital admitting and emergency departments to critically ill patients. Acute rest myocardial perfusion imaging has been clearly documented as an extremely useful tool in the evaluation of such patients. However, uniform standards have been lacking.

This position statement by an American Society of Nuclear Cardiology task force on chest pain centers clearly demonstrates the value of acute rest myocardial perfusion imaging in the triage of patients with suspected acute coronary syndromes. The document further elucidates steps necessary for such evaluation and the type of patients for whom this evaluation is best suited. As such, the document furthers our appreciation of acute rest myocardial perfusion imaging in the emergency setting.

Gary V. Heller, MD, PhD
President, American Society of Nuclear Cardiology

American Society of Nuclear Cardiology position statement on radionuclide imaging in patients with suspected acute ischemic syndromes in the emergency department or chest pain center

Frans J. Th. Wackers, MD, PhD, Kenneth A. Brown, MD, Gary V. Heller, MD, PhD, Michael C. Kontos, MD, James L. Tatum, MD, James E. Udelson, MD, and Jack A. Ziffer, PhD, MD

INTRODUCTION

The American Society of Nuclear Cardiology (ASNC), founded in 1993, is a professional medical society whose mission is to foster optimal delivery of nuclear cardiology services through professional education, leadership in the establishment of standards and guidelines for training and practice, and the promotion of research. ASNC will intermittently publish "position statements," which reflect the growth of knowledge and evidence in a specific, focused area of the application of radionuclide imaging techniques for the clinical care of patients with known or suspected heart disease. Policy/position statements define the official opinion of ASNC and are approved or endorsed by the ASNC Board of Directors. Previous ASNC position statements have included statements on electrocardiographic gating of myocardial perfusion scintigrams,[1] the clinical relevance of a normal myocardial perfusion scintigraphic study,[2] and the value and use of attenuation correction for single photon emission computed tomography (SPECT) imaging.[3]

This position statement will examine the role of myocardial perfusion imaging (MPI) for use in the early evaluation of patients with suspected acute coronary syndromes (ACS), specifically those who are being

Table 1. NPV of resting MPI for acute MI in the ED

Author	y	N (total)	N (normal rest MPI)	NPV
Varetto et al[4]	1993	64	34	100%
Hilton et al[5]	1994	102	70	99%
Tatum et al[6]	1997	438	338	100%
Kontos et al[7]	1997	532	361	99%
Heller et al[8]	1998	357	204	99%
Kontos et al[10]	1999	620	379	99%

evaluated in the emergency department (ED) setting or in a chest pain center.

The timely identification, triage, and management of the patient presenting with possible ACS remain problematic. Among the large number of patients (>6,000,000 in the United States annually) who present with nonspecific symptoms possibly due to ACS and nonischemic electrocardiographic changes, the actual incidence of ACS is relatively low. Yet, the clinical risk in patients with ACS is relatively high and may be mitigated by the use of effective but time-sensitive therapies. Moreover, large numbers of such patients are admitted to hospitals or chest pain centers for prolonged observation but ultimately are found not to have had an acute ischemic syndrome, resulting in substantial unnecessary resource utilization.

POSITION STATEMENT

It is the position of ASNC that evidence supports the use of acute rest SPECT MPI as a means for triaging selected patients with suspected ACS. Acute rest MPI in patients with suspected ACS has a high negative predictive value (NPV) for excluding myocardial infarction (MI), as well as predicting the absence of future adverse cardiac events. Thus, in most cases, patients with normal acute rest MPI results do not need to be hospitalized. Positive (abnormal) acute rest MPI results are associated with a high probability of ACS and justify hospital admission for early initiation of treatment. Effective implementation of acute rest MPI for detecting ACS requires high-quality MPI performed in a well-defined population with use of a systematic evaluation protocol.

BACKGROUND

Acute rest MPI is particularly useful in patients in the ED with acute chest pain and normal or nonischemic rest electrocardiogram (ECG) results. The NPV of acute rest MPI to exclude MI in these patients ranges from 99% to 100% (Table 1), and the NPV for excluding future cardiac events during medium-term follow-up is approximately 97%.[3-8] Acute rest MPI in this setting is highly sensitive for the detection of acute MI[4-11] and is capable of detecting myocardial ischemia in the absence of necrosis.[4,7,10,11] One study has shown incremental value of acute rest MPI data over demographic, clinical, ECG, and enzyme information in prediction of short-term cardiac events.[8] The consistently high NPV found in many studies suggests that patients with a normal acute rest SPECT perfusion study may be safely discharged from the ED and scheduled for outpatient follow-up at a later time.

Thus there is a large body of observational studies that support the use of acute rest SPECT MPI in patients presenting with suspected acute ischemia. There have been 2 prospective randomized studies that evaluated the impact of acute rest MPI on ED physicians' triage decision making, length of hospital stay, and health care costs.[12,13] In both studies patients were randomized to a strategy that incorporated SPECT MPI or a strategy without imaging. In the first trial, median hospital costs were $1843 less, median length of stay in the intensive care unit was 1.0 day shorter, and median hospital length of stay was 2.0 days shorter for patients who had MPI-guided management than for those who had conventional management. This study also demonstrated that physicians who had access to MPI results ordered fewer cardiac catheterizations without any difference in outcomes at hospital discharge or at 30 days' follow-up.

A much larger prospective randomized study[13] evaluated the role of acute rest MPI on triage decisions by ED physicians in patients who were randomly assigned to receive either the usual ED evaluation or the usual strategy supplemented with acute rest MPI data. The results demonstrated that unnecessary hospitalizations were significantly reduced in the imaging strategy group, with no differences in outcomes between the usual care and MPI groups. Thus these 2 prospective randomized trials showed that acute rest MPI in patients presenting to the ED with low-to-intermediate–risk chest pain and nondiagnostic ECG results can improve the overall clinical effectiveness of the initial triage process and potentially provide cost savings.

Appropriate Selection of Patients for Evaluation

Patients with obvious clinical and ECG evidence for ACS should be admitted to the hospital for appropriate aggressive treatment and do not benefit from rest SPECT MPI. The patient populations best suited for an ED triage strategy that incorporates acute rest MPI are those in whom the initial history and ECG do not suggest a high or very low probability of ACS. These are patients with symptoms suggestive but not typical for ACS and normal or nonischemic rest ECG results. In this patient cohort, further evaluation is necessary before a confident triage decision can be made. Importantly, other nonischemic and noncardiac causes for chest discomfort, such as pulmonary embolism, infection, arrhythmia, or aortic dissection, should always be considered. Patients with prior MI, especially those with Q waves on the ECG, are likely to have resting myocardial perfusion defects and therefore will require subsequent repeat MPI after a pain-free period to differentiate new ischemia from old MI. Therefore the utility of the initial rest SPECT MPI in this patient cohort is limited unless a prior study is available for comparison.

Image Interpretation

In a minority of patients the results of acute rest MPI will be equivocal, neither clearly normal nor clearly abnormal. Only one fully published report has separately evaluated such patients, who were found to have an event rate slightly higher than patients with normal MPI results but lower than those with abnormal MPI results.[5] Thus, for the purpose of optimizing the sensitivity of detecting ACS and minimizing the "missed MI" rate, it is recommended that equivocal MPI be categorized as mildly abnormal and that further evaluation, such as stress

testing, be completed. The use of attenuation correction in this setting has not been elucidated but might be useful.

Presence of Symptoms During Injection of Radiopharmaceutical

One issue not completely resolved is the importance of injecting the radiopharmaceutical during ongoing chest discomfort. In the largest published experience, patients were studied after injection as long as 6 hours after cessation of symptoms.[6,8] Even at this time point, normal acute rest MPI was associated with a very low risk of a cardiac event over the subsequent 12-month period. Theoretically, a delay between the cessation of symptoms and the time of radionuclide injection may result in a missed diagnosis of ischemia and should be taken into account during image interpretation. This was convincingly demonstrated in patients with unstable angina.[11,14] Therefore it is recommended that a radiopharmaceutical preferably be injected during ongoing pain and not more than 2 hours after symptoms have abated.

Comparison of Acute Rest MPI and Cardiac Biomarkers

Two studies have compared the results of acute rest MPI with serial creatine kinase–MB and troponin analysis.[10,15] The sensitivity for detecting acute MI was similar between the two strategies, but acute resting MPI was positive earlier after presentation. These studies confirmed what could be expected based on the known release kinetics of the various widely used cardiac markers and the underlying pathophysiology of acute MPI. Whereas cardiac markers require 6 to 12 hours to become positive, rest MPI immediately reflects the status of regional myocardial blood flow at the time of radiopharmaceutical injection.

Choosing an Evaluation Strategy

For an ED staff or a multidisciplinary clinical group considering optimal strategies for evaluating patients with suspected acute ischemia, the choice of strategies, as well as the decision on whether to include resting MPI, involves a careful evaluation of local nuclear cardiology imaging expertise and the ability of the local imaging laboratory to provide imaging services and reports in a timely fashion. A strategy of observation with serial cardiac enzyme analysis and subsequent stress testing is widely applicable and widely practiced.[16]

Although published observational and randomized trial data regarding acute rest MPI are strong (Table 1), this approach is not as widely practiced. This may reflect the necessity of significant cooperation between the multiple stakeholders in the process, including ED physicians, providers of nuclear cardiology services (who may be radiologists, nuclear medicine physicians, or cardiologists), cardiologists who may be involved in consulting on clinical decision making, and other health care professionals including nursing and transport personnel.

Follow-up After Initial Evaluation Strategy

The initial goal of evaluating patients with suspected acute ischemia and nonischemic ECG results in the ED, through use of either resting MPI or serial cardiac serum markers, is to determine the likelihood of ACS and to assign patients into a high- or low-risk category for acute MI or unstable angina. Subsequently, the presence of coronary disease as a possible contributor to symptoms usually needs to be determined (particularly in patients with a negative initial evaluation and those injected without symptoms), and this is generally done best with some form of stress testing.[17] Decisions about the type of stress used (treadmill exercise or pharmacologic stress) and the type of analysis performed (ECG testing alone or ECG testing in conjunction with perfusion or function imaging) can be made based on well-established clinical protocols such as those outlined in the American College of Cardiology/American Heart Association stable angina guidelines.[18] It is recommended either that such stress testing is performed in the chest pain center before the patient is discharged or that the patient is discharged with an appointment for an outpatient stress test within 1 week.

Acknowledgment

References

1. Bateman TM, Berman DS, Heller GV, Brown KA, Cerqueira MD, Verani MS, et al. American Society of Nuclear Cardiology position statement on electrocardiographic gating of myocardial perfusion SPECT scintigrams. J Nucl Cardiol 1999;6:470-1.

2. Bateman TM. Clinical relevance of a normal myocardial perfusion scintigraphic study. American Society of Nuclear Cardiology. J Nucl Cardiol 1997;4:172-3.

3. Hendel RC, Corbett JR, Cullom SJ, DePuey EG, Garcia EV, Bateman TB. The value and practice of attenuation correction for myocardial perfusion SPECT imaging. a joint position statement from the American Society of Nuclear Cardiology and the Society of Nuclear Medicine. J Nucl Cardiol 2002;9:135-43.

4. Varetto T, Cantalupi D, Altieri A, Orlandi C. Emergency room technetium-99m sestamibi imaging to rule out acute myocardial ischemic events in patients with nondiagnostic electrocardiograms. J Am Coll Cardiol 1993;22:1804-8.

5. Hilton TC, Thompson RC, Williams HJ, Saylors R, Fulmer H, Stowers SA. Technetium-99m sestamibi myocardial perfusion imaging in the emergency room evaluation of chest pain. J Am Coll Cardiol 1994;23:1016-22.

6. Tatum JL, Jesse RL, Kontos MC, Nicholson CS, Schmidt KL, Roberts CS, et al. Comprehensive strategy for the evaluation and triage of the chest pain patient. Ann Emerg Med 1997;29:116-23.

7. Kontos MC, Jesse RL, Schmidt KL, Ornato JP, Tatum JL. Value of acute rest sestamibi perfusion imaging for evaluation of patients admitted to the emergency department with chest pain. J Am Coll Cardiol 1997;30:976-82.

8. Heller GV, Stowers SA, Hendel RC, Herman SD, Daher E, Ahlberg AW, et al. Clinical value of acute rest technetium-99m tetrofosmin tomographic myocardial perfusion imaging in patients with acute chest pain and nondiagnostic electrocardiograms. J Am Coll Cardiol 1998;31:1011-7.

9. Kontos MC, Arrowood JA, Jesse RL, Ornato JP, Paulsen WH, Tatum JL, et al. Comparison of echocardiography and myocardial perfusion imaging for diagnosing emergency department patients with chest pain. Am Heart J 1998;136:724-33.

10. Kontos MC, Jesse RL, Anderson FP, Schmidt KL, Ornato JP, Tatum JL. Comparison of myocardial perfusion imaging and cardiac troponin I in patients admitted to the emergency department with chest pain. Circulation 1999;99:2073-8.

11. Bilodeau L, Theroux P, Gregoire J, Gagnon D, Arsenault A. Technetium-99m sestamibi tomography in patients with spontaneous chest pain. correlations with clinical, electrocardiographic and angiographic findings. J Am Coll Cardiol 1991;18:1684-91.

12. Stowers SA, Eisenstein EL, Th Wackers FJ, Berman DS, Blackshear JL, Jones AD Jr, et al. An economic analysis of an aggressive diagnostic strategy with single photon emission computed tomography myocardial perfusion imaging and early exercise stress testing in emergency department patients who present with chest pain but nondiagnostic electrocardiograms. results from a randomized trial. Ann Emerg Med 2000;35:17-25.

13. Udelson JE. The ERASE Chest Pain Trial. Presented at "Special Session: Clinical Trials" at the 72nd Scientific Sessions of the American Heart Association, Atlanta, Ga, November 10, 1999.

14. Wackers FJ, Lie KI, Liem KL, Sokole EB, Samson G, van der Schoot JB, et al. Thallium-201 scintigraphy in unstable angina pectoris. Circulation 1978;57:738-42.

15. Duca MD, Giri S, Wu AH, Morris RS, Cyr GM, Ahlberg A, et al. Comparison of acute rest myocardial perfusion imaging and serum markers of myocardial injury in patients with chest pain syndromes. J Nucl Cardiol 1999;6:570-6.

16. Farkouh ME, Smars PA, Reeder GS, Zinsmeister AR, Evans RW, Meloy TD, et al. A clinical trial of a chest-pain observation unit for patients with unstable angina. Chest Pain Evaluation in

the Emergency Room (CHEER) Investigators. N Engl J Med 1998;339:1882-8.

17. Abbott BG, Abdel-Aziz I, Nagula S, Monico EP, Schriver JA, Wackers FJT. Selective use of single-photon emission computed tomography (SPECT) myocardial perfusion imaging in a chest pain center. Am J Cardiol 2001;87:1351-5.

18. Gibbons RJ, Chatterjee K, Daley J, Douglas JS, Fihn SD, Gardin JM, et al. ACC/AHA/ACP-ASIM guidelines for the management of patients with chronic stable angina. a report of the American College of Cardiology/American Heart Association Task Force on Practice Guidelines (Committee on Management of Patients With Chronic Stable Angina). J Am Coll Cardiol 1999;33:2092-197.

| Home | Abstract | Current Issue | Archives | Ahead of Print |

Benefits of planar and SPECT/CT imaging in lymphscintigraphy for melanoma

Authors

Abstract

2703

Objectives Using lymphoscintigraphy to detect the sentinel lymph node in patients with melanoma for removal and examination has become an integral part of the testing and staging process. The SNMMI's Guideline for Lymphoscintigraphy in Melanoma recommends only planar imaging. SPECT/CT imaging for breast cancer lymphoscintigraphy is gaining more support, but it is still not common practice, according to literature. The purpose of this study is to determine the value of combining planar imaging with SPECT/CT imaging for patients with melanoma.

Methods Personal observation of patients undergoing lymphoscintigraphy, combined with a review of the most recent literature regarding using SPECT/CT imaging for patients with melanoma was used to evaluate the use of a combination protocol. All patients observed received the recommended dose of Tc-99m Filtered Sulfur Colloid, injected intradermally around the site of the melanoma. Dynamic imaging was done immediately post-injection, followed by static transmission images and SPECT/CT images.

Results Planar imaging is valuable for visualizing the lymphatic drainage patterns to find the sentinel lymph node. However, SPECT/CT has the advantage of providing attenuation correction data as well as the anatomical location of nodes. Because SPECT/CT cameras are becoming more available, both in the U.S. and outside, the additional imaging does not create undue expense for the provider, and there is only a small increase in the radiation dose to the patient from the CT.

Conclusions The addition of SPECT/CT imaging in lymphoscintigraphy procedures is a valuable tool for the surgeon, because it has been shown to give more anatomical data. It is recommended to combine the SPECT/CT imaging with dynamic planar imaging, giving the surgeon optimal information with which to create a plan of action.

doi:10.1007/s00259-008- 0910-2 Vermeeren, L., Valdés Olmos, R., Klop, W., van der Ploeg, I., Nieweg, O., Balm, A., & van den Brekel, M. (2011). SPECT/CT for sentinel lymph node mapping in head and neck melanoma. Head & Neck, 33(1), 1-6. doi:10.1002/hed.21392

No Related Web Pages

1. *J Nucl Med* **May 2013** vol. 54 no. supplement 2 **2703**

a. » Abstract

Email me this article

MAJOR ACHIEVEMENTS IN NUCLEAR CARDIOLOGY/ CME ARTICLE

Advances in SPECT camera software and hardware: Currently available and new on the horizon

E. Gordon DePuey, MD

INTRODUCTION

A long-standing limitation of radionuclide myocardial perfusion SPECT is its relatively lengthy acquisition time, as compared to stress echocardiography and cardiac CT. The American Society of Nuclear Cardiology (ASNC) and the Intersocietal Commission for the Accreditation of Nuclear Medicine Laboratories (ICANL) have rightfully insisted that acquisition times not be decreased below those set forth in the ASNC Guidelines so that adequate image counting statistics are maintained, thereby maintaining test sensitivity and minimizing artifacts associated with low count density studies. New software methods and new innovative hardware described below, however, now allow for significantly shortened SPECT acquisition times without a decrease in image quality.

More recently, the media, the public, and the medical community have drawn attention to patient radiation exposure associated with radiographic, nuclear medicine, and nuclear cardiology procedures and the potential-associated patient risk.[1,2] The radiology and nuclear imaging communities have responded rapidly and definitively by implementing a variety of guidelines to decrease patient radiation exposure and to avoid exposure in higher risk patient populations: Image Gently, Image Wisely, Choosing Wisely, and the ASNC Patient-Centered Imaging Guidelines,[3] among others. ASNC has set a goal to decrease patient radiation exposure associated with myocardial perfusion SPECT to <9 mSv per entire study in 50% of patients by 2014.[4] The new software and hardware methods described below will help us achieve this goal by providing the ability to maintain or improve SPECT image quality with the lower image counting statistics associated with significantly decreased injected radiopharmaceutical doses.

There have been several comprehensive reviews and editorials published highlighting innovations in cardiac SPECT hardware and software.[5-9] I hope the present review will serve to reinforce the importance and clinical significance of these technical advancements. Of note, advancements in hybrid SPECT/CT imaging are not covered in the present review.

TECHNICAL ADVANCEMENTS

New Software Methods

New SPECT reconstructions software methods have preserved or improved SPECT image quality despite lower count statistics. Consequently, SPECT acquisition time may be shortened. Alternately, the injected radiopharmaceutical dose may be decreased, thereby decreasing patient radiation exposure. These methods, described below, are all now commercially available. They are available on new computer systems, and some may also be implemented on older scintillation camera systems.

Iterative reconstruction. Iterative reconstruction has been available on the nuclear medicine computer systems for over a decade, although many users have hung tenaciously to an older processing method, filtered backprojection (FBP). FBP basically suppresses high-frequency image data, thereby decreasing noise. However, in doing so the technique results in image blurring, often obscuring small perfusion abnormalities and rendering the images of both objects, i.e., the myocardium and perfusion defects indistinct. The smoother the filter, i.e., the lower the critical frequency and the higher the order, the greater the degree of image blurring and the poorer the diagnostic sensitivity in detecting perfusion abnormalities. In contrast, iterative reconstruction provides an estimated reconstruction volume from which estimated projections are derived. The estimate may be simply a uniform flood field or a more complex heuristic algorithm with an estimate of the expected configuration of the heart. Actual measured SPECT projection data are compared to the estimated

projections. Based upon the "error", i.e., the difference between the estimated and the measured projection information, the estimated projection is updated. This process is repeated until the estimated and the measured projections converge, resulting in an implicit recovery of resolution. The initial version of iterative reconstruction was Maximum Likelihood Expectation Maximization (MLEM), whereby individual iterations were repeated until data converged. Subsequently, with higher speed computers Ordered Subset Expectation Maximization (OSEM) has become the reconstruction method of choice, whereby data are grouped into subsets, allowing more rapid and accurate data convergence.

Myocardial perfusion SPECT images reconstructed with OSEM are of higher quality than those processed with FBP. Perfusion defects, anatomic variants such as physiologic apical thinning and prominent posterior papillary muscles, and the right ventricular myocardium are better visualized with OSEM. Likewise, image contrast is improved, thereby better defining the left ventricular endocardial borders. Although differences in FBP and OSEM may be only slight in high count density myocardial perfusion SPECT scans, in lower count density studies the improvement with OSEM is often clinically significant. Another advantage of OSEM is that the Ramp filter, inherent to FBP, is not employed, thereby minimizing the possibility of a Ramp filter artifact, i.e., an artifactual decrease in inferior left ventricular myocardial count density when intense tracer concentration is present in extracardiac structures in the x-plane of the left ventricle (Figure 1). However, of note, for most commercially available implementations of OSEM, a post-processing filter is employed to further improve image quality. Therefore, the Ramp filter artifact may not be eliminated entirely.

Resolution recovery. The high-resolution, parallel-hole collimator used for myocardial perfusion SPECT maintains spatial resolution by accepting photons emitted from the myocardium, traveling directly perpendicular to the face of the camera and the parallel holes of the collimator. Photons emanating from voxels not directly perpendicular to the collimator hole are attenuated by the collimator's lead septa. Photons emanating from these voxels may undergo Compton scattering and may also subsequently travel perpendicular to the collimator hole. These are eliminated by the pulse height analyzer, which rejects photons losing more than 10%-15% of their initial photon energy. However, these advantages of the parallel-hole collimator are progressively compromised the more distant the voxel is from the camera face (Figure 2). The greater the distance of object from the camera face, the greater the likelihood that photons from adjacent voxels will pass through the parallel-hole collimator. Likewise, the

Figure 1. A This low-dose rest/high-dose stress Tc-99m ▶ sestamibi study, performed in an obese patient, was processed with FBP. Reconstructed tomograms are technically suboptimal with considerable noise and indistinct definition of the myocardial borders. Both at stress and at rest there is considerable tracer uptake in the left lobe of the liver, which lies in the x-plane of the inferior wall of the left ventricle. The fixed inferior perfusion defect could be secondary either to scar or a Ramp filter artifact. **B** The same study was processed with OSEM iterative reconstruction. SPECT image quality is significantly improved with less noise and sharper definition of the myocardial borders. The inferior perfusion abnormality is resolved, indicating that it was a Ramp filter artifact since OSEM does not incorporate the Ramp filter. Courtesy Gordon DePuey, St. Luke's-Roosevelt Hospital, New York, NY.

likelihood that Compton-scattered photons will be accepted progressively increases. For these reasons spatial resolution of a voxel/object decreases with distance from the camera face. Therefore, it has always been emphasized that when a patient is positioned for myocardial perfusion SPECT, the face of the scintillation detector should be as close as possible to the patient's chest wall. Likewise, an elliptical orbit is preferable because it allows the camera head to more closely approximate the chest wall in all projections. The magnitude of this loss of resolution is directly proportional to the width of the collimator hole and inversely proportional to the hole length (Figure 3). Septal penetration of photons is another cause of decreased the resolution of a parallel-hole collimator. However, for the relatively low-energy isotopes, Tc-99m and Tl-201, used for myocardial perfusion imaging the degree of septal penetration is minimal.

This distance-dependent collimator-detector blur, dependent upon the shape of the holes, their dimensions, and the thickness of the septa for each individual collimator has a major influence on image resolution.[10,11] It is the main factor affecting the resolution and noise properties of nuclear medicine images. In reconstructed SPECT images, these effects are strongly influenced by the applied reconstruction algorithm and its parameters. Resolution recovery models the physics and geometry of the emission and detection processes. It is thereby a means to compensation for the collimator-detector response (CDR) in iterative reconstruction.[12-14] The CDR consists of four main components: intrinsic response (the system without a collimator) and the geometric, septal penetration, and septal scatter components of the collimator parameters. By including an accurate model of CDR function in an iterative SPECT reconstruction algorithm, compensation for the blurring effect may be included in the iterative reconstruction process, resulting in improved spatial resolution. For each combination of acquisition system, radiopharmaceutical, and particular acquisition protocol, the CDR

a

b

STRESS_IRNC(G)	REST_IRNC
Date: 2008/06/02 10:57	Date: 2008/06/04 10:48
SA Pixel Size: 6.78mm	SA Pixel Size: 6.78mm
SA Thickness: 6.78mm	SA Thickness: 6.78mm
L/H Ratio: 0.70	L/H Ratio: 0.61

An object close to the collimator will have less blur.   An object farther from the collimator will have more blur.
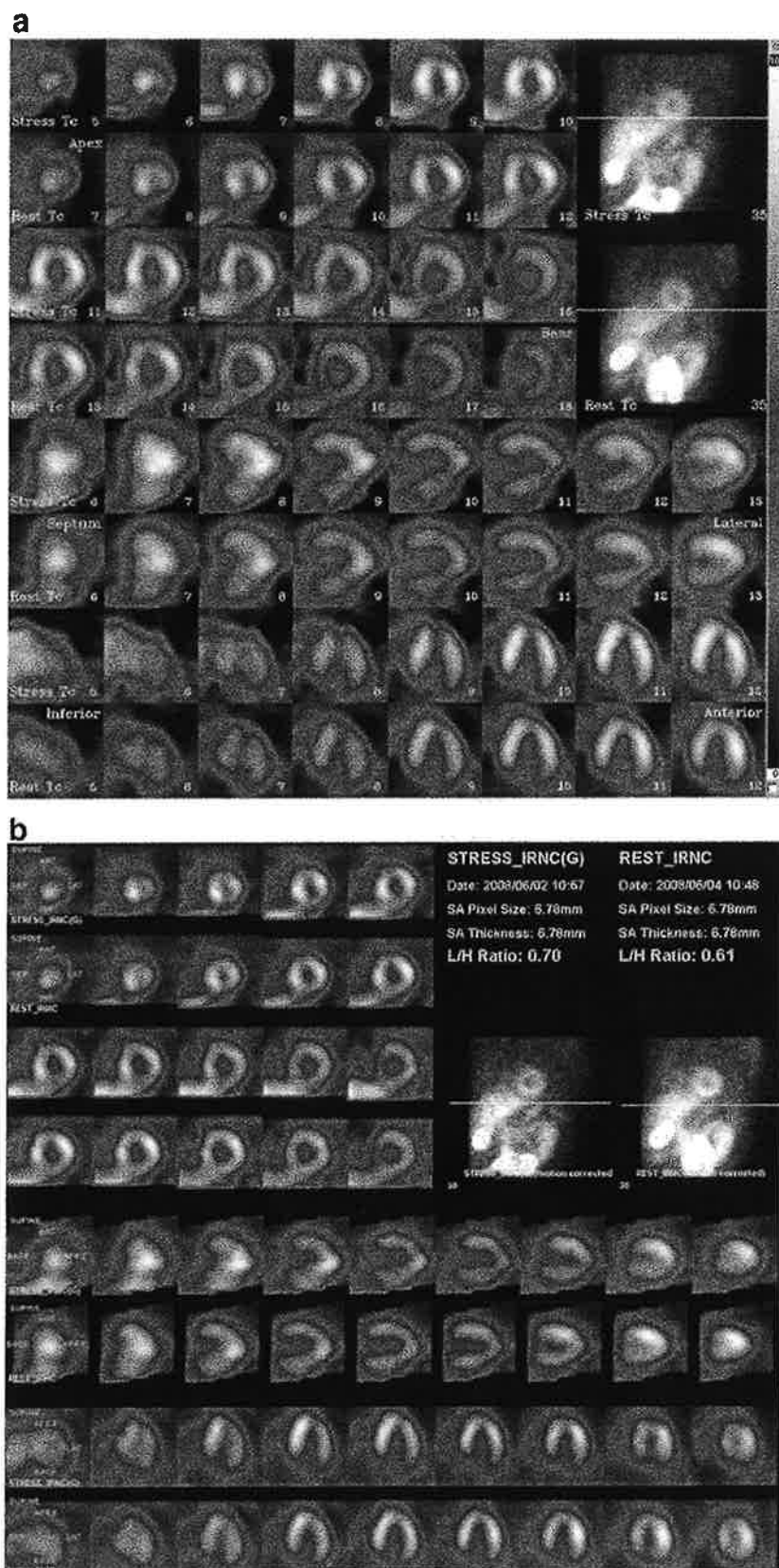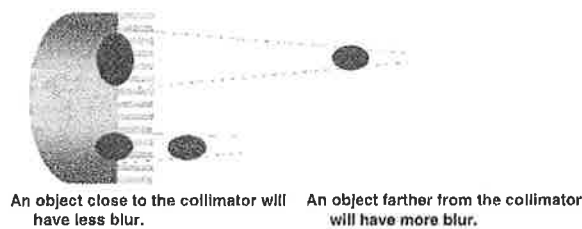
Figure 2. Depth-dependent loss of resolution. When an object is further from a parallel-hole collimator, photons emanating from the object pass through a greater number of parallel holes of the collimator, thereby blurring the object and decreasing spatial resolution. Courtesy Yossi Srour, UltraSPECT Ltd.

**Narrow, long collimator holes   Short, wide collimator holes
Slight septal penetration**

Figure 3. Loss of resolution with the depth from the parallel-hole collimator depends upon the collimator hole characteristics. For a collimator with narrow, long holes (*left*) the loss of resolution with depth is less than that of a collimator with short, wide holes (*right*). Septal penetration of photons also contributes to image blurring (*left*), although this factor is minor for low-energy isotopes such as Tc-99m.

function provides the probability that a photon emitted from any point of the imaged object will contribute to a pixel of the resulting image. Accurate predictions of the geometric response function for various collimator designs have been derived. Specifically, during iterative reconstruction each voxel is reconstructed according to the collimator's geometry. Pixel weights are calculated analytically, taking into account the solid angles subtended by the collimator between each detector pixel and each body voxel. This is accomplished by knowing the CDR for each particular scintillation camera/collimator system.

To implement resolution recovery acquisition parameters including the center-of-rotation and the collimator-to-voxel distances for every projection view acquired must be known. Additionally, in order to apply pixel weighting appropriately to the image matrix, which includes the heart and surrounding body structures, the distance from the detector to the patient's body must be determined. Newer cameras automatically provide this distance in the acquired parameters for each angular position. However, for cameras that do not provide this distance automatically from the acquisition parameters, a simple segmentation algorithm may be applied to the projections to estimate the detector-to-body distance.

One resolution recovery method, incorporated into Wide Beam Reconstruction® (WBR®) (UltraSPECT, Ltd.), models the CDR and the physics and geometry of the emission and detection processes.[15] As described above, the shape of the holes, their dimensions, and the thickness of the septa for each individual collimator have a major influence on image resolution. Therefore, during iterative reconstruction data are modified in each reconstructed voxel according to the collimator's geometry. Pixel weights are calculated analytically, taking into account the solid angles subtended by the collimator between each detector pixel and each body voxel (Figure 4). With knowledge of various scintillation detector systems and collimators, this resolution

Figure 4. During iterative reconstruction data are modified in each reconstructed voxel according to the collimator's geometry. Pixel weights are calculated analytically, taking into account the solid angles subtended by the collimator between each detector pixel and each body voxel. Also, in order to apply pixel weighting appropriately to the image matrix, the distance from the detector to the patient's body is accounted for.

recovery method can be implemented on both newer and older cameras.

Therefore, resolution recovery yields images of improved spatial resolution and with less noise as compared to conventional techniques.[15] Clinical images of lower count density acquired with resolution recovery have been demonstrated to be equivalent or superior to those acquired with conventional SPECT imaging, allowing for reduced SPECT acquisition time or reduced injected radiopharmaceutical dose (see below).

Noise compensation. Nuclear imaging data are inherently noisy due to relatively poor counting statistics. Low count density myocardial perfusion SPECT images are characterized by noise, which has similar or higher magnitude compared to the high-frequency portion of the true myocardial data. As

described above, FBP eliminates high-frequency data, thereby "smoothing" (i.e., blurring) the image. This filtering results in decreased image contrast, decreased spatial resolution, and potentially decreased diagnostic sensitivity in detecting perfusion and regional wall motion abnormalities. In contrast, with noise compensation methods signal-to-noise values are determined by the resolution and smoothness desired in the final cardiac SPECT image. High-frequency components of the image are suppressed while resolution is maintained (Figure 5).

One noise compensation technique, WBR® (Ultra-SPECT, Ltd.), suppresses noise and enhances the signal-to-noise ratio (SNR) by modeling the statistical characteristics of the emission process and of the detected data.[16] It accounts for the Poisson distribution of the emission data, as well as for the noise in the acquired data. To preserve or even enhance the SNR, WBR®
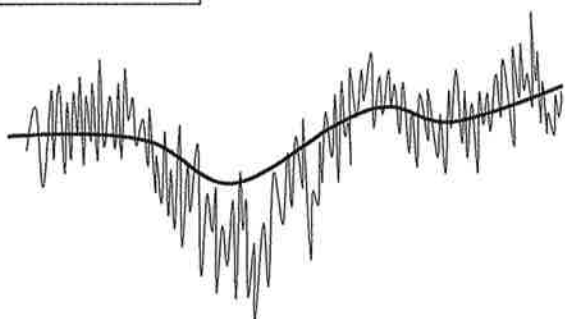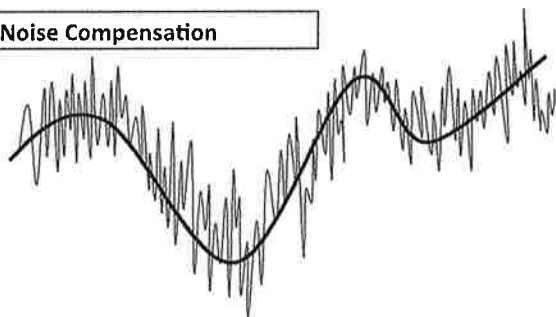
Figure 5. Comparison of the effects of filtering and noise compensation on a myocardial perfusion count-rate profile. A representative profile across an object demonstrates considerable high-frequency noise. Filtering, i.e., smoothing, the data (*top*) decreases noise, but at the same time considerably decreases image resolution and contrast. On the other hand, with noise compensation (*bottom*) signal-to-noise values are determined by the resolution and smoothness desired in the final SPECT image. High-frequency components of the image are suppressed while resolution and contrast are maintained. Concept courtesy of Ernest Garcia, Emory University, Atlanta, GA.

regularizes the likelihood objective function by adding a Gaussian component. Higher weight to the Gaussian component results in suppressed high-frequency components present in the projections, due to its fast vanishing tail. Higher weighting of the Poisson component results in recovery of high-frequency signal, or enhancement of noise if no appropriate weight is given. The balance between the two is determined adaptively and automatically according to the data analysis and desired smoothness. The reconstruction is iterative and automatic with all noise compensation parameters selected automatically and with no post-filter applied. The smoothness of the image is guided by the application's target SNR without applying filters during or post-reconstruction (Figure 6). For the WBR® method, incorporating iterative reconstruction, resolution recovery, and noise compensation, the spatial resolution (FWHM) for three line sources with scatter was reported to be 5.1 mm, as compared to 10.2 mm (coefficient of variation = 3.7% for both) for standard FBP processing. Contrast resolution from Data Spectrum phantom experiments (with scatter) was 0.67 compared to 0.53 for FBP (coefficient of variation = 12% for both).[15]

Of note, resolution recovery algorithms themselves may result in accentuation of noise in reduced-time acquired projections. This has a detrimental effect on image quality. One method, adopted in the General Electric Evolution® software suppresses the impact of noise by incorporating a Maximum A Posteriori (MAP) Algorithm.[17] The scheme used is a modified one step late (OSL) algorithm using a Green prior optimized for each clinical protocol, and for gated and attenuation corrected image.[18] The last iteration is performed using a Median root prior.[19] This scheme was found to give an image of equal or superior quality on clinical studies and on physical phantom data.[20]
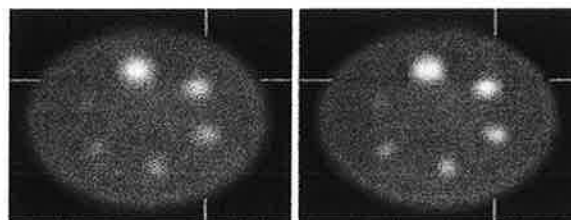
Figure 6. Tomographic slice through the Jaszczak phantom containing low-level Tc-99m background tracer concentration and spheres of various diameters containing higher level activity. With FBP reconstruction (*left*) there is moderate noise in the background area, and the edges of the spheres are blurred. With WBR® reconstruction (*right*), incorporating resolution recovery and noise compensation, background noise is suppressed, and resolution and contrast of the spheres are increased[15].

Vendors of conventional SPECT cameras as well as the new, innovative cameras described below have all adopted advanced software processing methods, including iterative reconstruction, resolution recovery, and some type of noise compensation. These software packages include Astonish®, Phillips; Shine®, Segami; Evolution®, General Electric Medical Systems; 3-D Flash®, Siemens Medical Solutions; n-SPEED®, Digirad, Inc.; and proprietary software developed by General Electric for the Discovery 530c camera and by Spectrum Dynamics for the D-SPECT camera. Users should be aware that these software programs each use different reconstruction algorithms, so results are by no means identical.

Pre-determined SPECT acquisition times to obtain optimal counts. The introduction of dual-head cameras more than a decade ago allowed us to halve acquisition times as compared to acquisition times for studies performed on older single-head cameras. Since their introduction, however, cardiac SPECT protocols have been rather rigid with regards to image acquisition times. For larger patients with soft tissue attenuation resulting in low count density studies ''weight-based dosing'' was recommended to increase cardiac SPECT counting statistics. However, by increasing the radiopharmaceutical dose, patient radiation exposure is likewise increased. As an alternative to increasing the radiopharmaceutical dose, it is possible to increase SPECT acquisition time in cooperative patients. Newer ''smart'' cameras allow optimal SPECT acquisition times to be predetermined in such patients. For example, TruACQ® software available on the Digirad Cardius® camera determines the count rate from regions of interest manually placed over the heart on each of its three detectors. An acquisition time is then pre-determined which will result in 22,000 counts in the heart (in the LAO projection) at stress and 10,000 counts at rest. The camera operator can accept or reject this suggested acquisition time, depending upon the patient's tolerance. By this means optimal counting statistics can be obtained in larger patients without increasing the radiopharmaceutical dose.

Phase analysis. Innovative software has been developed to measure left ventricular systolic dyssynchrony using phase analysis of gated myocardial perfusion SPECT.[21] Increasing myocardial counts during ventricular systole correlates with regional left ventricular wall thickening and may be used to assess the pattern of systolic contraction. Data from the entire myocardium are used to generate a phase distribution map that may be displayed as a histogram or polar map. By means of a sampling theorem, temporal changes in left ventricular myocardial contraction can be assessed using only 8 frames per cardiac cycle. This method provides temporal resolution equivalent only 1/64th of

the cardiac cycle. Left ventricular dyssynchrony assessed by this technique in 75 heart failure patients was compared to echocardiographic tissue Doppler imaging and was found to correlate well ($r = 0.89$, $P < .0001$).[22] It has been reported that left ventricular dyssynchrony measured by this method is useful to predict which patients will respond to cardiac resynchronization therapy (CRT).[23] Using a phase histogram bandwidth of approximately 140°, this method demonstrated a sensitivity of 70% and specificity of 74% in predicting patient response to CRT. Although this radionuclide method is quite promising, there have been parallel advancements in echocardiography, magnetic resonance imaging, and cardiac computed tomography in assessing left ventricular dyssynchrony and patient response to CRT.[24]

Hardware Developments

Optimized detector geometry and focused collimation.

Dedicated sodium Iodide detector cardiac SPECT cameras. Well over a decade ago scintillation camera designs were modified to better perform dedicated cardiac imaging. Phillips introduced the CardioMD® camera with two 90°-angled detectors that could be positioned close to the patient's chest wall to optimize detector geometry and minimize detector-to-voxel blurring. The open gantry design was patient-friendly, even for most claustrophobic patients. The design was compact, allowing the small footprint camera to fit easily into an 8' × 10' room. General Electric introduced the Optima® camera, with similar advantageous characteristics. Both of these cameras could be equipped with rod-source attenuation correction (AC). Subsequently, dedicated cardiac SPECT cameras were introduced to accommodate larger patients. One example is the General Electric Ventri® camera with two independent detectors positioned in a 90° geometry, mounted on a ring gantry. Patients are comfortably positioned on an imaging palate, sturdy enough to accommodate the patients up to 440 pounds, with supports engineered to relieve pressure on the arms, knees, low back, and neck. The palate slides into the ring detector of the gantry, and the detectors are then positioned close to the chest wall in an optimal geometry for cardiac SPECT. The advantages of such dedicated cardiac SPECT cameras are considerable. However, for a general Nuclear Medicine laboratory they lack the flexibility to perform other non-cardiac scans.

Dedicated upright and semi-reclining cardiac SPECT cameras. Patients are positioned upright with the Digirad camera and semi-upright/semi-reclining with the Siemens C-Cam® camera and the Data

Spectrum D-SPECT® camera. Each of these cameras has a small footprint and is designed for patient comfort. Upright or semi-reclining positioning allows the diaphragm to move inferiorly, thereby decreasing diaphragmatic attenuation and Compton scatter from sub-diaphragmatic structures. A second advantage of upright or semi-upright positioning is that pendulous breasts are less likely to assume different positions in the stress and the rest SPECT acquisitions, a problem occasionally encountered with supine SPECT, resulting in "shifting" breast artifacts mimicking ischemia. Photon attenuation artifacts involving the inferior wall due to an overlying pendulous left breast, however, are more likely with upright and semi-upright/reclining patient positioning. Patient motion was problematic for the long acquisition times required for earlier single-head versions of the Digirad upright camera. However, in the most recent release of the multi-head camera shorter acquisition times combined with Velcro straps/binders around the patient's waist and chest effectively minimize motion, particularly in the Y- and Z-directions.

Cardiocentric SPECT. Conventional myocardial perfusion SPECT performed with a single- or dual-head scintillation camera, as described above, employs a body-centered orbit. However, SPECT images acquired with such a 180° body-centered orbit may have significant erroneous inhomogeneity and may overestimate defect size, particularly when the target object is off the center of the orbit, as is commonly the case in clinical cardiac imaging.[25] Although, elliptical body-centered orbits minimize the distance between the heart and the detector in all tomographic projections, thereby minimizing distance-dependent image blurring and scatter, SPECT artifacts, particularly those at the left ventricular apex, may be more severe in scans using elliptical orbits than in those from circular acquisitions.[26]

Newer camera designs incorporate "cardiocentric" SPECT orbits. Detector design and/or translation of either the camera heads or the patient before or during SPECT acquisition allow the heart to remain in the center of the field-of-view. For example, the Digirad Cardius® camera uses a triple-head geometry. The patient sits on a translating chair. Immediately prior to the SPECT acquisition the patient's heart is positioned in the center of the field-of-view of each detector. The detector heads are pushed in as close as possible to the patient's chest to optimize image quality. For the SPECT acquisition the chair rotates 67.5°, allowing the triple-head camera to acquire data in a 202.5° cardiocentric orbit. This triple-head configuration used in combination with 3-dimensional OSEM nSPEED® reconstruction enables emission scans to be performed up to four times faster than with conventional dual-head SPECT systems.[27] Image quality is improved as

compared to body-centered orbits, and the severity of artifacts is reduced[27] (Figure 7). New collimator designs and other new cameras, described below, including the Spectrum Dynamics D-SPECT® camera and the General Electric Discovery 530c® camera, also incorporate cardiocentric SPECT.

Cardio-focused collimation. A cardio-focused collimator, IQ SPECT®, has been developed by Siemens Medical Solutions to improve the efficiency of myocardial perfusion imaging using conventional, large field-of-view SPECT and SPECT/CT systems (Figure 8).[28,29] This variable-focus collimator is designed to magnify the region of the myocardium and its immediate surroundings by means of converging collimation, while keeping the entire torso in the field-of-view by morphing the collimator holes to a near parallel-hole geometry at the edges of the collimator, thereby avoiding truncation. There are 48,000 hexagonal holes, each 1.9 mm in diameter and 40 mm in length. Spatial resolution progressively increases from the face of a camera to the cardiac "sweet-spot" at 28 cm. The scan orbit is cardiocentric, 28 cm from the center of rotation, as determined by the operator, so that the heart is maintained in the region of highest magnification throughout the scan. A scanning arc of 104° with 6° angular steps is used for each of the two 90°-angled camera heads.

Since the collimator has a response that is not only distance-dependent but also variable across the face of the collimator, it is crucial to accurately model both the
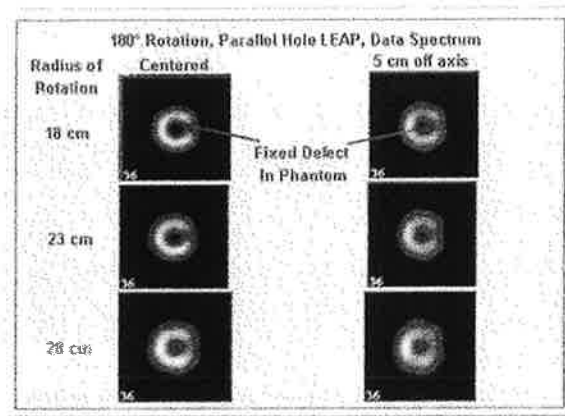
Figure 7. A data spectrum phantom, filled with Tc-99m, with a full-thickness insert in the posterior wall was imaged with a 180° cardio-centric orbit (*left*) and again with an off-center orbit (*right*), simulating a body-centered orbit. The radius of rotation of the orbit was progressively increased from 18 to 23 to 28 cm. The posterior defect is better resolved using a cardiocentric orbit, particularly with a smaller camera radius of rotation. Courtesy, Richard Conwell and Chuanyong Bai, Digirad Inc.

Magnifies in 2 Dimensions

5 cm   28 cm "sweet-spot"   40 cm

48,000 hexagonal holes
1.9 mm hole diameter
40 mm length, same as ME
HRES-like resolution response
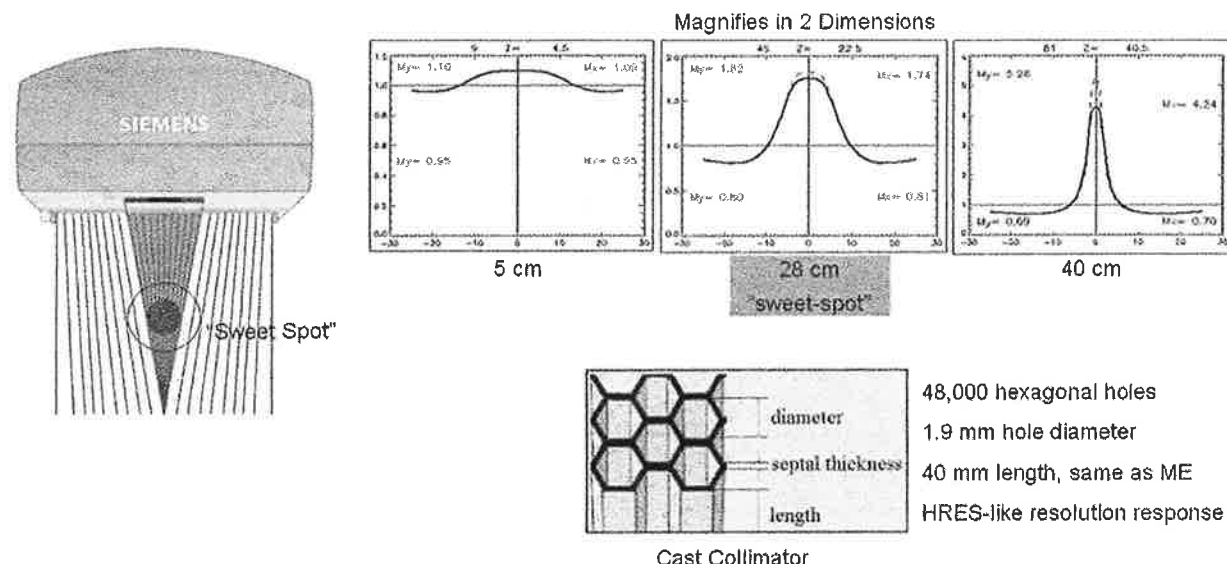
Cast Collimator

Figure 8. Diagram of the IQ SPECT® variable-focus collimator, demonstrating magnification of the region of the myocardium and its immediate surroundings by means of converging collimation, while keeping the entire torso in the field-of-view by morphing the collimator holes to a near-parallel-hole geometry at the edges of the collimator. Spatial resolution increases with depth from the central area of the collimator surface.[30] Courtesy Siemens Medical Solutions.

magnification and the point-response function of the collimator. Variable magnification results from the changing direction of each borehole with respect to the collimator surface normal vector, while the point response function depends on the finite size of the bore holes. Therefore, an advanced reconstruction engine based on a conjugate-gradient algorithm with ordered subsets that includes in the system matrix the view-angle dependent gantry deflections, a vector map of the collimator hole angles, and the system's point response function, is used for cardiac SPECT reconstruction. Based upon phantom experiments, as compared to a conventional low-energy high-resolution collimator, this novel cardio-focused collimator increases target sensitivity at 28 cm by a factor of ≥ 4 while maintaining comparable reconstructed resolution. The average resolution (FWHM) is 6.97 mm in the x-plane and 6.91 mm in the y-plane.[30] Therefore, with this novel collimator scan times, patient dose, or a combination thereof may be reduced by a factor of four while maintaining acceptable spatial resolution.[31]

Arc detector geometry with rotating slit-hole collimation. The CardiArc® scanner, dedicated to performing myocardial perfusion SPECT scans, manufactured by CardiArc Inc., uses a stationary curved camera head subtending a 180° angle, which is positioned centered over the patient's precordium.[6] The curved detector is composed of three adjacent curved sodium iodide crystals. Scintillation events are detected by an array of photomultiplier tubes mounted on the

back of these detectors. Vertical collimation is achieved using a unique curved lead sheet with six vertical slits that rotates back-and-forth during acquisition to obtain data over the 180° imaging arc (Figure 9). The movement of these six slits is synchronized electronically with the six areas of the crystal that are imaging the photons passing through the slits. Horizontal collimation is accomplished by a series of thin lead sheets that are stacked vertically, with the gaps between the slits defining the hole apertures. By means of this "slit-hole" method, collimation is focused at the depth of the heart, thereby increasing sensitivity and resolution. Counting statistics comparable to those obtained with a conventional parallel-hole collimator in 21 minutes can be achieved in only approximately 5 minutes with the CardiArc® scanner. The FWHM is 3.65 mm at a depth of 87 mm and 6.01 mm at 176 mm. To date, no clinical validation of this system has been published.

Multiple scanning parallel-hole collimators. The D-SPECT® camera, manufactured by Spectrum Dynamics incorporates nine pixilated cadmium zinc telluride (CZT) crystal detector columns situated vertically, spanning an L-shaped 90° geometry (Figure 10). The patient is positioned semi-reclining, in a posture similar to that assumed a dentist's chair. The L-shaped detector is positioned over the patient's chest, centered over the left precordium. Each of the CZT detectors is fitted with a square-hole tungsten collimator with an inherent high transmission efficiency. The collimator holes are 21.7 mm in length and measure 2.26 mm on
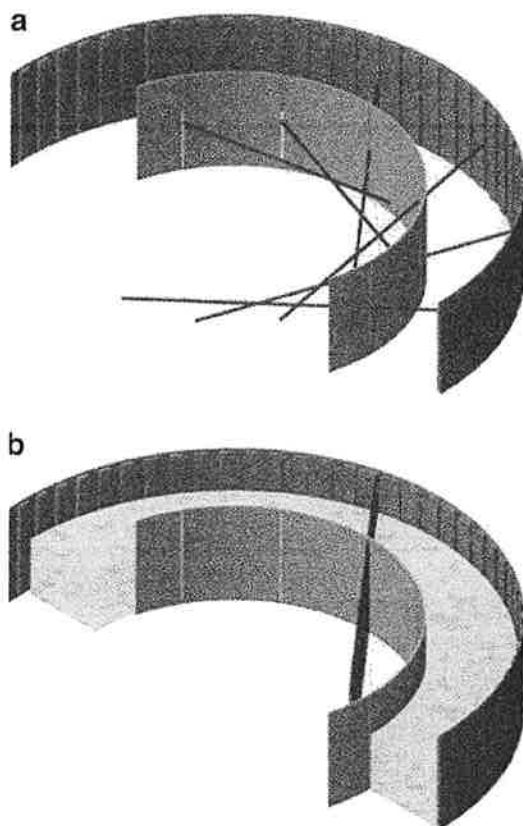
Figure 9. With the Cardiac Arc® Camera vertical collimation is achieved using a unique curved lead sheet with six vertical slits that rotates back-and-forth during acquisition to obtain data over the 180° imaging arc (**A**). Horizontal collimation is accomplished by a series of thin lead sheets that are stacked vertically (**B**). Courtesy Jack Juni, CardiArc Inc.

each side of each square hole.[32] These holes are shorter and wider than those used in conventional NaI detector low-energy, high-resolution collimators, which are typically 45-mm long and 1.6-mm wide. Consequently, the solid angle for acceptance of incident photons for the D-SPECT® collimator is more than 8 times that of the standard low-energy high-resolution lead parallel-hole SPECT collimator.

Emission data are first sampled by obtaining a 15-second scout scan to allow the nine detectors to identify the location of the heart. Each collimated detector column rotates and translates independently a maximum of 110°, allowing voxels to be viewed from hundreds of different viewing angles. Data are acquired in list mode, allowing physiologic markers such as the electrocardiographic R wave, to be recorded simultaneously. A sinogram is reconstructed and the location of the heart is derived, thereby setting the limits of the detectors' fanning motion for a subsequent diagnostic scan. The diagnostic scan, typically a 4-minute acquisition, is performed with 120 projections/detector and 2 seconds/projection. By this means for the diagnostic scan there is preferential sampling of photons emanating from the heart, whereby a greater proportion of imaging time is allocated to collecting data from the heart at the expense of collecting fewer data from less important surrounding and remote regions. Conceptually this design is equivalent to allowing pixels of a conventional parallel collimator to acquire scintigraphic emissions from the heart for a longer time than pixels acquiring data from background structures.

Although due to its unique L-shaped geometry, the D-SPECT® camera can be positioned very close to the
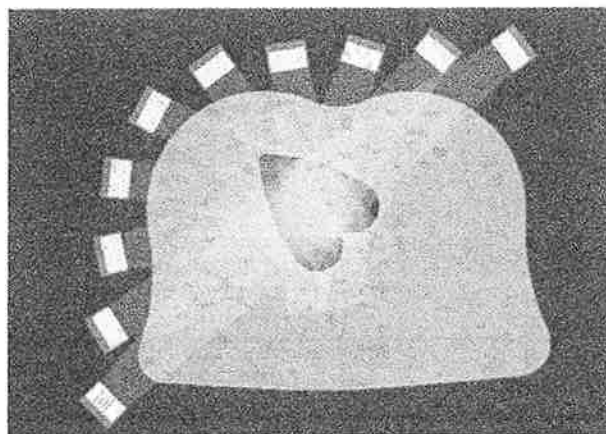
Figure 10. Schematic of the multiple scanning parallel-hole collimators of the D-SPECT® camera, focused on the region of the heart following a pre-scan to determine the heart's location. Courtesy, Spectrum Dynamics.

patient's chest wall, clearly the wide, short, square-hole collimator design described above would result in much poorer spatial resolution than that obtained using a conventional SPECT camera equipped with a high-resolution parallel-hole collimator. The loss of spatial resolution is compensated for by the use of a proprietary Broadview® software reconstruction algorithm based upon OSEM reconstruction, accurately modeling the probability function, supported by an increased number of viewing angles. Also, the reconstructed volume is fitted to a smooth ellipsoid-like surface, after which further iterations are performed, giving the myocardial walls a very thin appearance in typical D-SPECT® tomograms.[32]

Multi-pinhole collimation. The General Electric Discovery NM 530c® camera employees 19 8 × 8 cm detectors focused on the heart to sample photons emanating from the heart and the regions immediately around it (Figure 11). Each detector contains 32 × 32 pixilated 5-mm thick CZT elements. The detector assembly is mounted on a gantry that allows for patient positioning in either the supine or the prone position. The size of the CZT modules allows the camera to be positioned closely enough to the chest wall to ensure that the detectors provide 3-D sampling of the heart sufficient for tomographic reconstruction. The target volume is approximately a sphere of 19-cm diameter. The patient is positioned so that the heart is centered within this field-of-view. Each of the 19 detectors is composed of 4 solid-state CZT pixilated detectors mounted by a single tungsten pinhole collimator with a 5.1 mm effective diameter aperture.[33] Nine of the pinhole detectors are oriented perpendicular to the patient's long axis. Five are angled above, and five are angled below the axis, providing a 3-dimensional acquisition geometry. Each of the pinhole collimators simultaneously obtains an image of the heart, with no moving parts during data acquisition. Because the distance between the CZT detector and the pinhole is less than the distance between the pinhole and the heart, the cardiac image is minimized to preserve resolution, rather than maximized and distorted, as in the case of other nuclear medicine pinhole applications such as pinhole imaging of the thyroid or the hips.

Because the detectors and the patient are both stationary, there are no "rotating" planar projection images available to the interpreting physician to assess patient motion. Therefore, the location of the left breast and left hemidiaphragm as potential attenuators, and the location and intensity of subdiaphragmatic tracer concentration as a potential cause of Compton scatter into the inferior myocardial wall cannot be ascertained. However, a "scan QC" screen is provided that includes all pinhole views to aid the interpreting physician estimate the location of these attenuators. With multi-pinhole collimation the focal point of the collimators is within the thorax, so breast attenuation is less problematical than with parallel-hole collimation. However, the problems of diaphragmatic attenuation and subdiaphragmatic Compton scatter are not avoided. Since high counting statistics allow for dramatically reduced SPECT acquisition times (see below), several laboratories using the Discovery 530c® camera perform both supine and prone SPECT routinely on all patients to better assess inferior myocardial tracer distribution.

Solid-State Detectors

Conventional sodium iodide scintillation cameras employ an array of photomultiplier tubes mounted behind the scintillation crystal. Typically photomultiplier tubes are hexagonal or square and measure approximately 46 cm^2. In general, there are over 50 photomultiplier tubes in modern scintillation cameras. When a photon strikes the sodium iodide crystal, a flash of light is emitted, which is detected by all the photomultiplier tubes. Those tubes closest to the scintillation event receive more light than more distant tubes. Each photomultiplier tube is a photocathode, which emits electrons when impacted by light. By means of a cascading dynode array, the number of electrons is then multiplied, producing an electrical current output at the back end of the photomultiplier tube. Those photomultiplier tubes closest to the scintillation event therefore produce a stronger electrical signal than the more distant tubes. The location of the scintillation event is then determined by electrical

Figure 11. Schematic of the multiple focused pinhole collimator design of the Discovery NM 530c® camera, focused on the region of the heart. Spatial resolution is optimal at the focal depth of the collimators. Courtesy, General Electric Medical Systems.

positioning circuitry, which combines the analog output signals of all the photomultiplier tubes and computes a weighted average of all the signals as a function of position. This probabilistic method results in a Gaussian spatial distribution, estimating the location of the scintillation event.

As a result of this probabilistic approach, there is considerable uncertainty in localization of the scintillation event, resulting in blurring of the scintigraphic image and suboptimal spatial resolution. Also, the positioning circuitry is relatively slow, limiting the count-rate capabilities of conventional scintillation cameras. To compound this shortcoming, the efficiency of the photocathode of the photomultiplier tube in converting optical photons to electrons only about 20%. These combined factors result in relatively poor spatial resolution and sensitivity of conventional scintillation cameras.

In contrast, solid-state detectors are quantized, whereby the detector head is divided into an array of individual detector elements. Crosstalk between these pixilated detectors is minimal; therefore, when a scintigraphic event occurs each of the pixilated detectors produces an "all or none" output signal. The output is quantized and discrete rather than Gaussian, as in the case of conventional sodium iodide cameras. Therefore, the size and the spacing of the solid-state detector elements define the spatial resolution of the detector (Figure 12).

Indirect solid-state detectors. When gamma rays are converted to electrical charge indirectly, first with the gamma ray undergoing a scintillation event and being converted to light, then with the light converted to electron hole pairs, the conversion process is termed "indirect." Indirect solid-state detectors are used in a wide variety of medical imaging applications including CT scanners and PET cameras. The only scintillation specifically camera designed for nuclear cardiology that employs indirect solid-state technology is the Digirad camera. The scintillator is cesium iodide (CsI), which has a good stopping power for low-energy gamma rays and emits more optical photons than sodium iodide. Scintillation events are detected using a pixilated detector array.[27] Each individual detector element (pixel) measures 6 mm × 6 mm × 6 mm. These detectors are arranged in 24 modules, each containing two 4 × 4 arrays. Thus, each camera head is composed of an array of 768 6-mm detector elements. Each CsI detector element is interfaced to a wafer-thin (0.3 mm) silicon photodiode semiconductor detector. The silicon photodiode has a high efficiency in converting optical photons to electrons. A bias voltage is applied across the semiconductor detector, resulting in electrical output when the photodiode is impacted by optical photons created by a scintillation event.
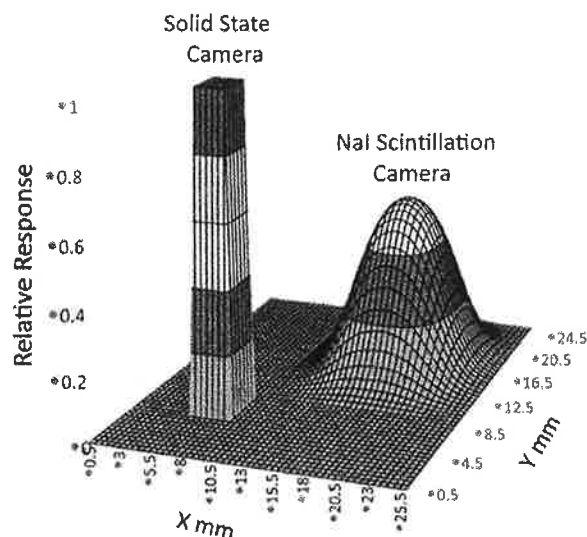
Figure 12. Schematic of the differences in spatial resolution provided by a solid-state detector as compared to a conventional NaI detector. With solid-state detectors the output is "all or none," with resulting optimal spatial resolution. In contrast, using probabilistic positioning circuitry to process signals from an array of photomultiplier tubes, spatial resolution is poorer for NaI detectors, with blurring of object edges. Courtesy, Richard Conwell, Digirad Inc.

Direct solid-state detectors. In contrast to indirect semiconductor detectors, CZT provides "direct" solid-state technology. The CZT semiconductor is a pixilated array approximately 5-mm thick with an effective Z of 50 and a density of 5.8 g/cm^3. Gamma rays enter the CZT semiconductor detector and are directly converted to electron hole pairs. These charges (electrons and holes) then drift towards positive and negative electrodes, respectively, producing electrical output signals. Because not all the holes and the electrons drift towards the negative and the positive electrodes at the same rate, some of the holes get delayed or "trapped" in the semiconductor material. This results in incomplete charge collection, in turn resulting in a broadening of the photopeak on the low-energy side. This "hole-tailing" effect varies from pixel to pixel within the array, but in general becomes more marked with increasing thicknesses of semiconductor material. For that reason, although CZT is more dense than sodium iodide (5.8 vs 3.7 gm/cm^3), the thickness of the CZT detector must be kept to a minimum (~ 5 mm). In this configuration, the CZT detector has excellent energy resolution (FWHM = 5.4%, compared to a FWHM = 9.4% for a conventional sodium iodide camera). With such improved energy resolution it is possible to clearly separate photons of Tc-99m (140 keV) and iodine-123 (160 keV) (Figure 13). Similarly, the composite 70 keV photopeak and 81 keV lines of thallium-

201 are clearly resolved.[34] However, due to the necessary thinness of the CZT detector, its intrinsic efficiency for detecting 140 keV gamma rays is only approximately equivalent to that of a conventional sodium iodide detector (88% vs 90%). Additionally, to overcome the effects of the variation of hole-tailing per pixel, energy windows in CZT cameras are often set relatively wide, as in conventional sodium iodide cameras, to ±10%, making their scatter fraction performance similar to conventional sodium iodide cameras.[35]

Attenuation Correction

AC for myocardial perfusion SPECT has been available for over a decade, and therefore cannot truly be considered a "new advancement." However, technical advancements in AC now allow for reduced patient radiation dose associated with x-ray emission scans. Diagnostic quality CT imaging of the chest is not necessary for AC. An attenuation map adequate for AC can be generated using a lower mA and kVp. By this means state-of-the-art technology for AC of myocardial perfusion SPECT affords the patient only approximately 0.2-0.4 mSv.

A novel, ultra-low-dose AC method has been incorporated into the Digirad Cardius X-ACT® camera.[27] After the emission scan has been acquired, the camera's three detectors are automatically reconfigured to form a single large 27-inch transaxial detector arc. The focal line of the collimator of each head co-aligns

Figure 13. Pulse height spectra for Tc-99m and I-123 obtained using a conventional NaI Anger camera and a CZT solid-state detector (Alcyone, Discovery NM 530c® camera). The two isotope peaks are discriminated much more effectively using the CZT detector. Courtesy, General Electric Medical Systems.

with the spatial location of a fluorescent x-ray transmission line source to form a fan-beam transmission acquisition geometry. During the transmission scan the chair on which the patient sits first rotates 206° for 60 seconds with the transmission source on in order to acquire the transmission data, then rotates 206° for 60 seconds in the reverse direction with the transmission source off to acquire the contamination data from emission sources in the patient to the transmission data. The resulting attenuation map is of poor spatial resolution (relative to a diagnostic CT machine), but adequate to correct the Tc-99m cardiac emission scan for soft tissue and blood pool attenuation. The associated patient radiation dose is only approximately 5 μSv. A limitation of this method, shared by all other x-ray attenuation techniques, is that the emission and subsequent transmission scans are sequential, allowing the possibility of patient motion between the emission and the transmission scans and misregistration of the two. Due to the longer acquisition time for the low-flux fluorescent x-ray transmission scan, the opportunity for patient motion is somewhat greater. Fortunately, however, software is available to easily register the emission and the transmission scans.

It should be emphasized that the increased count-rate statistics and improved image quality obtained with the new hardware methods described above are a result of combined advancements in both hardware and software. Spatial resolution for SPECT imaging of Tc-99m has been evaluated for the three new cameras described above, all of which combine hardware and software innovations. For the Digirad Cardius® detector head the extrinsic planar resolution (FWHM) at 10 cm with scatter was determined to be 9.9 mm with a LEHR collimator and 10.6 mm with a LEAP collimator. Defect contrast of the Data Spectrum phantom full defect was 0.528.[27] For the Spectrum Dynamics D-SPECT® camera, for a single line source the FWHM was demonstrated to be 3.5 mm in the x-axis and 4.2 mm in the y-axis, as compared to 9.2 and 12.5 mm, respectively, for conventional SPECT.[32] Compared to a standard SPECT system, the D-SPECT camera was demonstrated to have energy resolution ~2 times better, a point-source sensitivity ~5 times higher, and a superior count-rate capability.[36] For the General Electric Discovery NM 530c® camera SPECT resolution at 15 cm evaluated using three point sources with scatter was determined to be 5.4 mm, compared to 9.4 mm for conventional SPECT with a dual-head state-of-the-art NaI detector.[37] It should be emphasized that since these experiments evaluating system performance were performed independently for each of the cameras, not necessarily with settings used for clinical imaging, and since experimental parameters differed for each system,
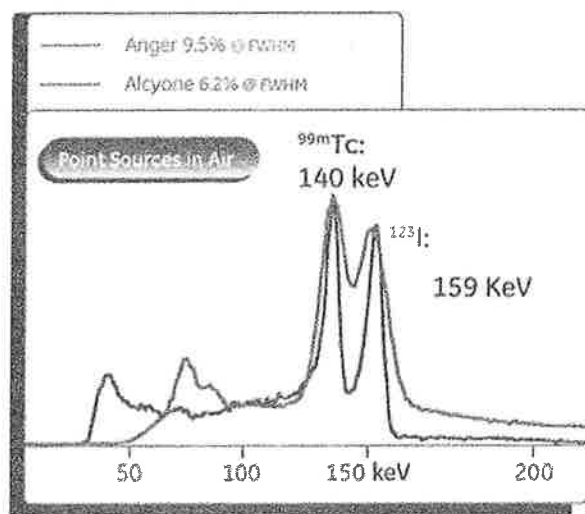
it is not possible to draw direct comparisons. In fact, efforts to perform a more representative comparisons show that the performance of these cameras are very similar.[38,39] Nevertheless, these innovative cameras, which combine advancements in detector characteristics, collimation, and SPECT processing software, represent a tremendous advancement in the field of Nuclear Cardiology, enabling a significant decrease in image acquisition time, radiopharmaceutical dose, or both.

CLINICAL RESULTS

Software Methods

In a single-center study of 50 patients, Borges-Neto et al[15] reported similar myocardial perfusion SPECT quality using WBR® (UltraSPECT, Ltd.) "half-time" software compared to standard "full-time" SPECT acquisitions acquired on a standard dual-head sodium iodide detector and processed with FBP. Subsequently, in a prospective series of 156 patients DePuey et al[16] reported that the image quality of gated perfusion SPECT obtained with both Evolution® software (General Electric Medical Systems), incorporating OSEM

and resolution recovery, and "half-time" WBR® software, incorporating these advancements as well as noise compensation, were both equivalent or superior to gated full-time FBP scans (Figures 14, 15). However, these authors observed that left ventricular functional parameters determined by both of these "half-time" methods differed significantly from those derived from "full-time" FBP processing. LVEF's averaged 3-9 points lower with "half-time" processing compared to those obtained using "full-time" FBP processing. Basso et al[40] reported similar results in a series of 47 patients. Reduced-time WBR® yielded image quality superior to that obtained with full-time FBP. In patients with perfusion defects summed difference scores (SDSs) were similar by both methods, but as reported by DePuey et al, LVEFs were 9%-10% lower with the WBR® method. In a prospective trial, Marcassa et al[41] studied 52 patients undergoing a rest/stress Tc-99m sestamibi protocol with "full-time" SPECT processed with FBP and "half-time" SPECT processed with WBR®. In addition, 40 other patients received half the usual radiopharmaceutical dose and underwent "double-time" SPECT processed with FBP and "full-time" SPECT processed with WBR®. These investigators reported that for either the "full-dose/half-time" or
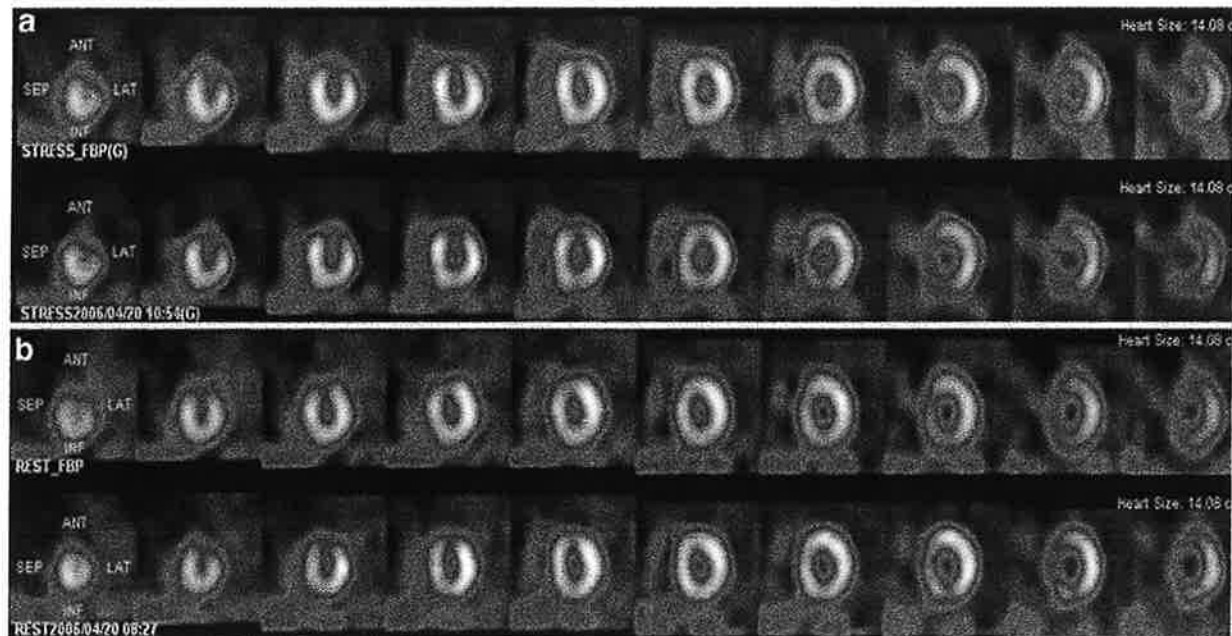
Figure 14. Comparison of myocardial perfusion stress (A) and rest (B) SPECT acquired "full-time" and processed with FBP (*top row*), compared to "half-time" SPECT processed with Evolution® software (*bottom row*), incorporating OSEM iterative reconstruction and resolution recovery. A single-day rest/stress 9/32 mCi Tc-99m sestamibi protocol was used. Image quality and resolution of the fixed anterior perfusion defect in this patient with a documented prior myocardial infarction is equivalent using the "full-time" and "half-time" acquisition and processing techniques. Courtesy Gordon DePuey, St. Luke's-Roosevelt Hospital, New York, NY.
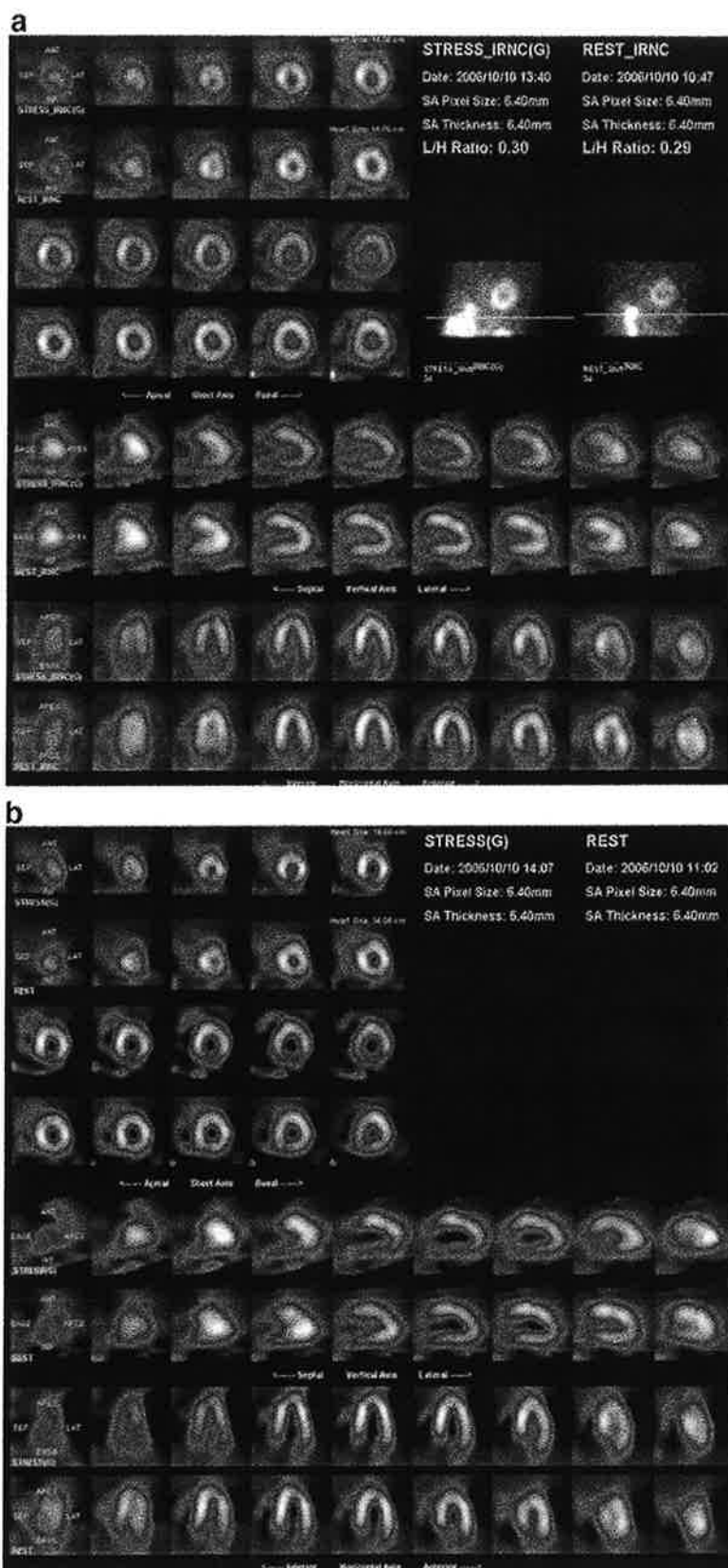
◄**Figure 15.** Comparison of myocardial perfusion stress SPECT acquired "full-time" and processed with FBP (**A**), compared to "half-time" SPECT processed with WBR® software, incorporating OSEM iterative reconstruction, resolution recovery, and noise compensation (**B**). A single-day rest/stress 9/32 mCi Tc-99m sestamibi protocol was used. Image quality and resolution of the reversible inferior perfusion defect in this patient with a documented RCA stenosis is superior using the "half-time" acquisition and processing techniques. Comparing gated post-stress SPECT image quality for the "full-time" (**C**) and "half-time" (**D**) techniques, the former provided better image quality with superior definition of the endocardial borders. Courtesy Gordon DePuey, St. Luke's-Roosevelt Hospital, New York, NY.

"half-dose/full-time" WBR® methods image quality and defect characteristics (SSSs) did not differ significantly from standard acquisition and FBP processing methods.

In a prospective study reported by Druz et al,[42] 434 patients underwent "full-time" (20 second/stop) dual-isotope Tl-201/Tc-99m sestamibi SPECT processed with FBP, followed by half-time (10 second/stop) SPECT processed with WBR®. For experienced nuclear cardiologist interpreting the scans diagnostic certainty was better for the "half-time" WBR® scans. The percentage of "equivocal" interpretations decreased from 35 to 9 ($P < .0001$). In a subgroup of patients who underwent coronary angiography, there were no differences in diagnostic sensitivity, specificity, or accuracy between the two methods.

Using Astonish® software developed by Phillips, incorporating resolution recovery and a different reduced-time software processing method, in a series of 221 patients in whom "half-time" acquisitions were simulated by dropping every other frame/stop of data during a 180° SPECT acquisition, Venero et al observed myocardial perfusion defect characteristics to be nearly identical to the "full-time" and simulated "half-time" techniques. Left ventricular functional parameters correlated well using the standard and reduced-time methods[43] (Figure 16). "Half-time" SPECT simulated with this "data stripping" method combined with Gd-153 line-source AC has also been reported to improve diagnostic certainty as compared to non-attenuation-corrected simulated "half-time" SPECT.[44]

In a later report, DePuey et al[45] imaged 209 patients prospectively at rest and following exercise or pharmacologic stress (9/32 mCi ^{99m}Tc-sestamibi) full-time processed with OSEM, and again "quarter-time" processed with a modified WBR® algorithm (Xpress-3®, UltraSPECT, Ltd.), incorporating a noise compensation technique more rigorous than the one employed for the previously described "half-time" technique (Figure 17). Blinded observers graded scan quality (1 = poor to 5 = excellent) based on myocardial

uniformity, endocardial/epicardial edge definition, and background noise. Perfusion defects were scored using a 17-segment model. Using three commercially available software methods, EDV, ESV, and LVEF were calculated. They demonstrated that by employing this more rigorous noise compensation algorithm "quarter-time" perfusion SPECT afforded image quality, defect characterization, and functional assessment equivalent to full-time OSEM, providing the potential for even more markedly decreased SPECT acquisition times and/or radiopharmaceutical doses. However, just as described above for WBR® "half-time" processing, these authors observed that left ventricular functional parameters determined by "quarter-time" WBR® averaged 3-9 points lower than those obtained using "full-time" OSEM processing. They postulated that the lower LVEFs obtained with "quarter-time" WBR® resulted from more accurate tracking of the motion of the left ventricular valve plane during ventricular systole, and therefore seemed to better correspond to visual estimation of LVEF. Consequently, they recommended that when following an individual patient, the same acquisition and processing methods should be used to determine functional parameters. Ideally, normal databases should be determined for each commercially available method used to determine left ventricular functional parameters.

Subsequently, using "half-time" WBR® software, DePuey et al[46] studied 156 consecutive patients in whom rest and 8-frame gated post-stress myocardial perfusion SPECT were performed following 9-12 mCi and 32-40 mCi Tc-99m sestamibi injections, respectively, with full-time (rest = 14 minutes; stress = 12.3 minute) acquisitions processed with OSEM, and also separate "half-time" acquisitions processed with WBR®. A separate group of 160 consecutive patients matched in gender, weight, and chest circumference received "half-dose" rest and stress injections (5.8 ± 0.6 and 17.5 ± 2.5 mCi) with full-time SPECT acquisitions. Image quality was again scored based upon myocardial count density and uniformity, endocardial edge definition, perfusion defect delineation, right ventricular visualization, and background noise. "Half-time" and "half-dose" WBR® non-gated and gated image quality were both superior to standard full-time OSEM (P's < .001). Mean image quality for rest, stress, and post-stress gated images were similarly excellent for "half-time" and "half-dose" WBR® (Figure 18). There was no significant difference between the summed stress and the rest scores for "full-time" OSEM versus "half-time" WBR® in 82 patients with perfusion defects. Therefore, these authors concluded that software methods that cope with reduced myocardial perfusion SPECT count density can be applied
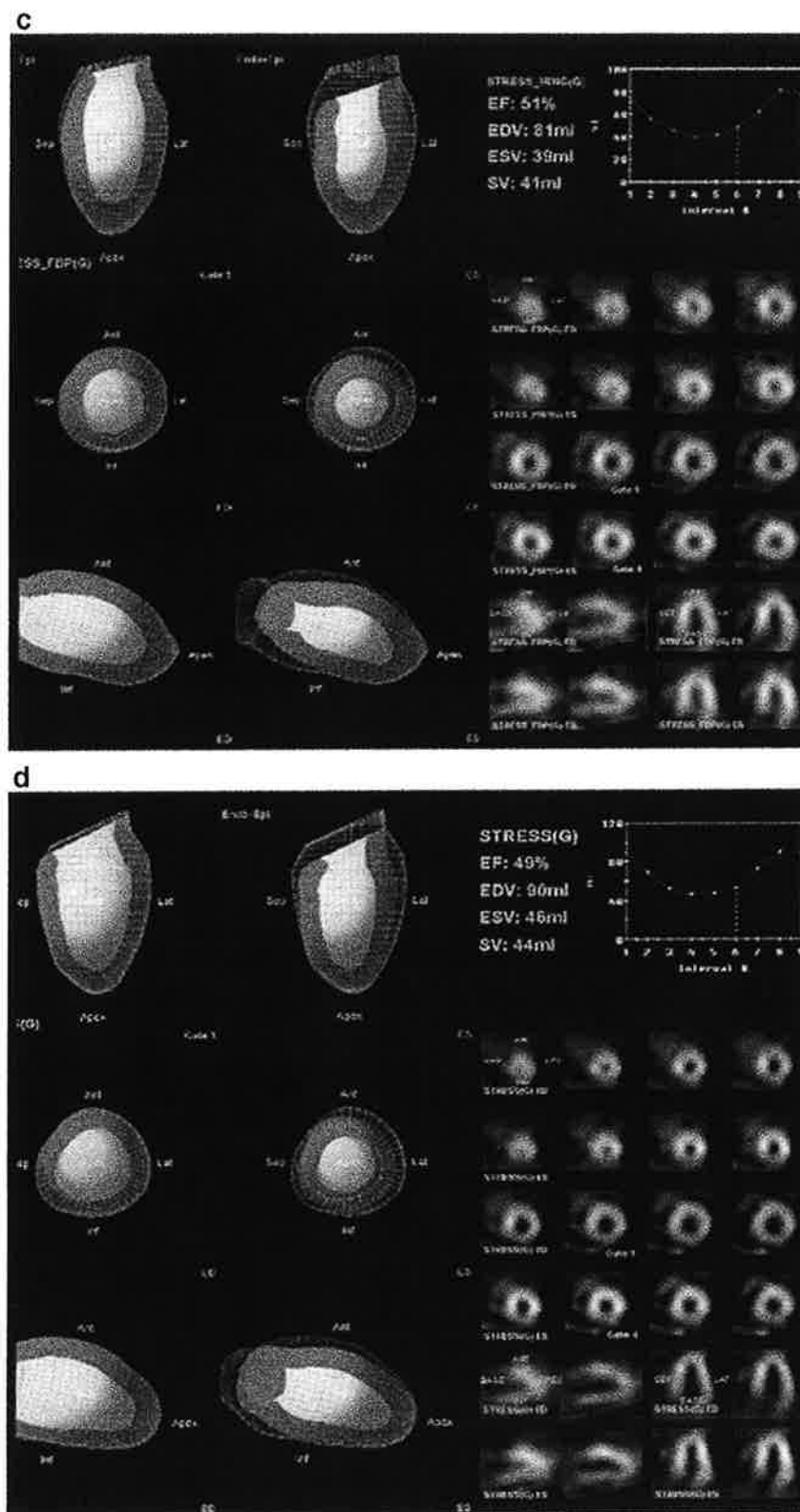
Figure 15. continued.
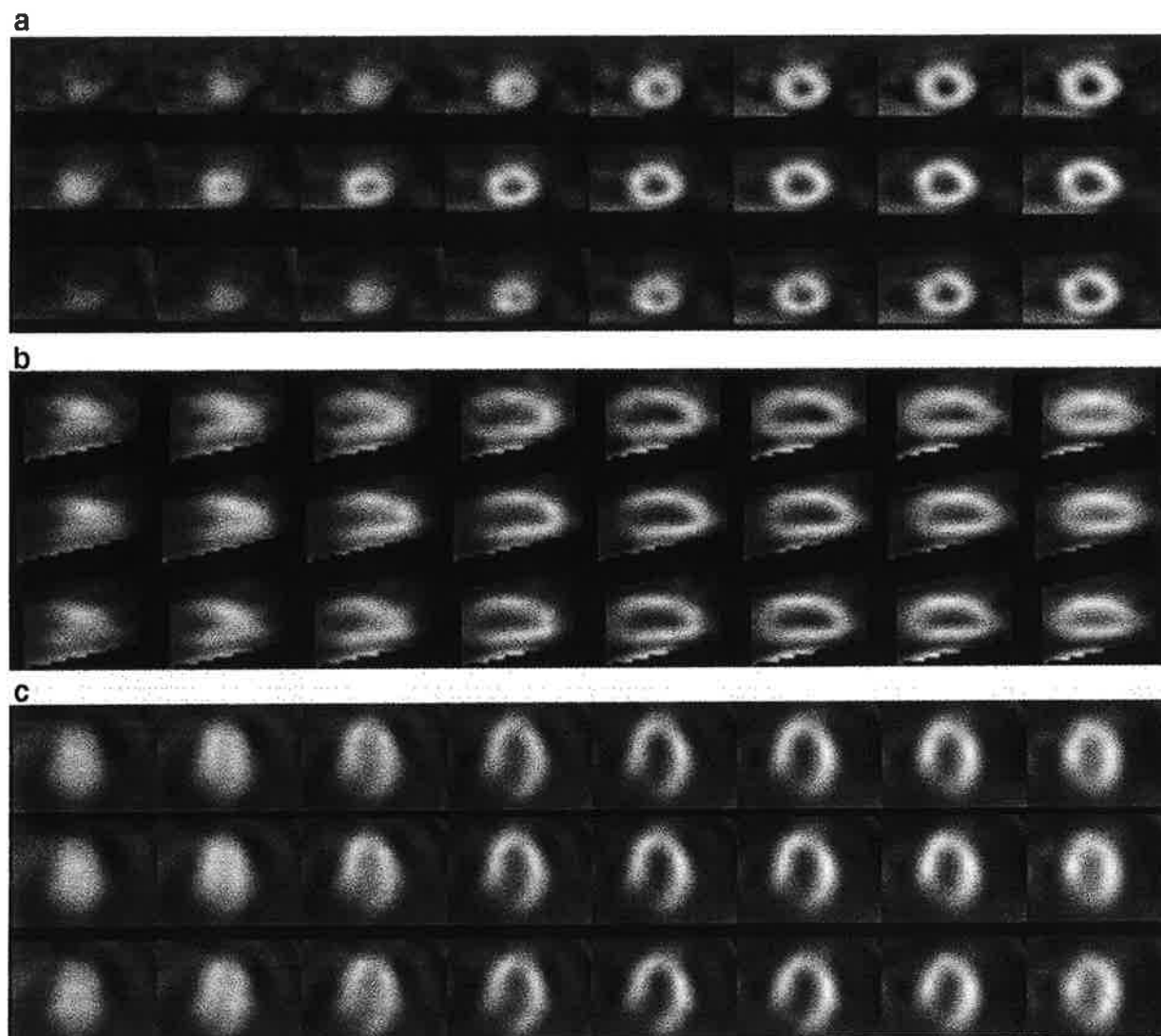
Figure 16. Comparison of myocardial perfusion stress SPECT from a normal subject acquired "full-time" and processed with FBP (*top row*), and with reduced count density Astonish® software, incorporating OSEM iterative reconstruction and resolution recovery (*middle row*). By means of "data stripping" a "half-time" SPECT acquisition was simulated, which was also processed with Astonish® software (*bottom row*). Short axis (A), vertical long axis (B), and horizontal long axis (C) tomograms are displayed. Image quality and resolution are equivalent for the "full-time" and "half-time" techniques.[42] Courtesy Gary Heller, Hartford Hospital, Hartford, CT.

equally well to reduced-time or reduced radiopharmaceutical dose scans.

Combined Hardware and Software Methods

Using the IQ SPECT® cardio-focused collimator in conjunction with Flash-3D® reduced count density reconstruction software (Siemens Medical Solution) and AC, Vija et al[28,29] demonstrated in Data Spectrum phantoms studies and one clinical patient example that

myocardial perfusion SPECT image quality was comparable in 4-minute IQ SPECT® scans as compared to standard 20-minute acquisitions acquired with a LEHR collimator (Figure 19).

In a prospective, multi-center trial of 448 patients in whom full-time gated SPECT acquisitions and simulated "half-time" acquisitions were compared qualitatively and quantitatively with regards to perfusion defect characteristics and functional parameters, Maddahi et al[47] reported the results of reduced-time myocardial perfusion SPECT acquired on the Cardius® upright

◀**Figure 17.** Comparison of myocardial perfusion stress and rest SPECT in a normal patient acquired "full-time" and processed with OSEM iterative reconstruction (A), compared to "quarter-time" stress SPECT processed with WBR® X-press 3® software, incorporating OSEM iterative reconstruction, resolution recovery, and a more rigorous noise compensation (B). A single-day rest/stress 9/32 mCi Tc-99m sestamibi protocol was used. Image quality and resolution are superior using the "quarter-time" acquisition and processing techniques. Comparing gated post-stress SPECT image quality for the "full-time" OSEM (C) and "half-time" WBR® (D) techniques, the former provided better image quality with superior definition of the endocardial borders. Courtesy Gordon DePuey, St. Luke's-Roosevelt Hospital, New York, NY.

camera employing CsI solid-state detectors and reduced count density nSPEED® software, incorporating OSEM reconstruction and resolution recovery (Digirad, Inc). They demonstrated that reduced-time acquisition image quality was at least as good as, and often superior to that obtained with full-time acquisitions. In 19.2% of stress tomograms and 19.4% of resting tomograms nSPEED® image quality was superior to standard SPECT image processing. The two techniques provided diagnostically equivalent images (Figure 20). Quantitative perfusion defect severity was not significantly different. These authors also observed an excellent correlation (r's $\geq$ 0.96) of functional parameters (LVEF, EDV, and ESV) comparing these two acquisition methods. The implication is that this new halftime method can be substituted reliably for full-time SPECT acquisition. Complementing the ability to preserve excellent image quality despite lower counting statistics, the Cardius X-ACT® upright camera incorporates advantages of upright, cardiocentric imaging, and low-dose AC (Figure 21).

The initial clinical validation of the D-SPECT® camera was reported by Sharir et al[48] in a single-center prospect of series of 44 patients who underwent a single-day stress/rest Tc-99m sestamibi protocol. Patients underwent conventional SPECT with 16- and 12-minute acquisitions and also high-speed D-SPECT® 4- and 2-minute acquisitions. Image quality of the D-SPECT® images acquired in much less time were excellent, and there was a close linear correlation between summed stress scores (SSSs) and summed rest scores (SRSs) (r's = 0.93, P's = .0001) determined by semiquantitative visual analysis (Figure 22). Diagnostic confidence in image interpretation was also similar for the two modalities.

This initial evaluation of the D-SPECT camera was followed by a large multi-center trial in which 238 patients underwent myocardial perfusion SPECT using a variety of exercise and pharmacologic stress single- and dual-isotope protocols.[49] A variety of commercially available standard scintillation cameras was used to

acquire rest and stress SPECT acquisitions for approximately 20 and 15 minutes, respectively. D-SPECT® acquisitions were also acquired on all patients for 4 and 2 minutes, respectively. An additional 63 patients with a low pre-test likelihood of coronary artery disease were studied to establish method- and gender-specific normal limits. These investigators demonstrated an excellent correlation between quantitative total perfusion stress and rest defect scores for the two separate imaging modalities (r's = 0.95 and 0.97, respectively, P's < .0001) and excellent correlations for post-stress ejection fraction and end-diastolic volumes (r's = 0.89 and 0.97, respectively). There was also a good concordance with regards to assignment of perfusion abnormalities to specific vascular territories (>90% agreement). They concluded that the D-SPECT® high-speed technology provides quantitative measures of myocardial perfusion and function comparable to those with conventional SPECT in approximately 1/7th of the acquisition time.

The initial clinical validation of the Discovery NM 530c® solid-state camera was reported by Esteves et al.[33] One hundred sixty-eight patients underwent a single-day rest/stress Tc-99m tetrofosmin protocol. All patients were imaged using conventional dual-detector cameras for 14 minutes for gated resting imaging and 12 minutes for gated post-stress imaging. Similar gated SPECT imaging datasets were acquired on the Discovery® camera but with acquisition times of only 4 and 2 minutes, respectively (Figure 23). There was a >90% correlation in interpretation of the presence or the absence of perfusion defects on a per-patient basis. Correlation coefficients of rest and stress left ventricular ejection fractions were 0.87 and 0.90, respectively. Similarly, excellent correlations were reported for rest and stress end-systolic and end-diastolic volumes (r's $\geq$ 0.94). These and other investigators concluded that the Discovery NM 530c® solid-state camera allows a more than 5-fold reduction in scan time and provides clinical perfusion and function information equivalent to conventional dual-head SPECT.[50]

Taking advantage of the Discovery® camera's list-mode capabilities, Herzog et al[51] reconstructed SPECT scans of varying duration from 1 to 6 minutes and compared results visually and semiquantitatively to full-time SPECT scans acquired on a standard dual-head NaI detector camera to determine an optimal scan acquisition time. Their results revealed that optimal imaging times are 3 minutes for resting SPECT and 2 minutes for post-stress SPECT using a conventional single-day low-dose rest/high-dose stress protocol. In a large retrospective study, Duval et al compared the myocardial count density and overall quality of low-dose Tc-99m sestamibi stress-only myocardial perfusion
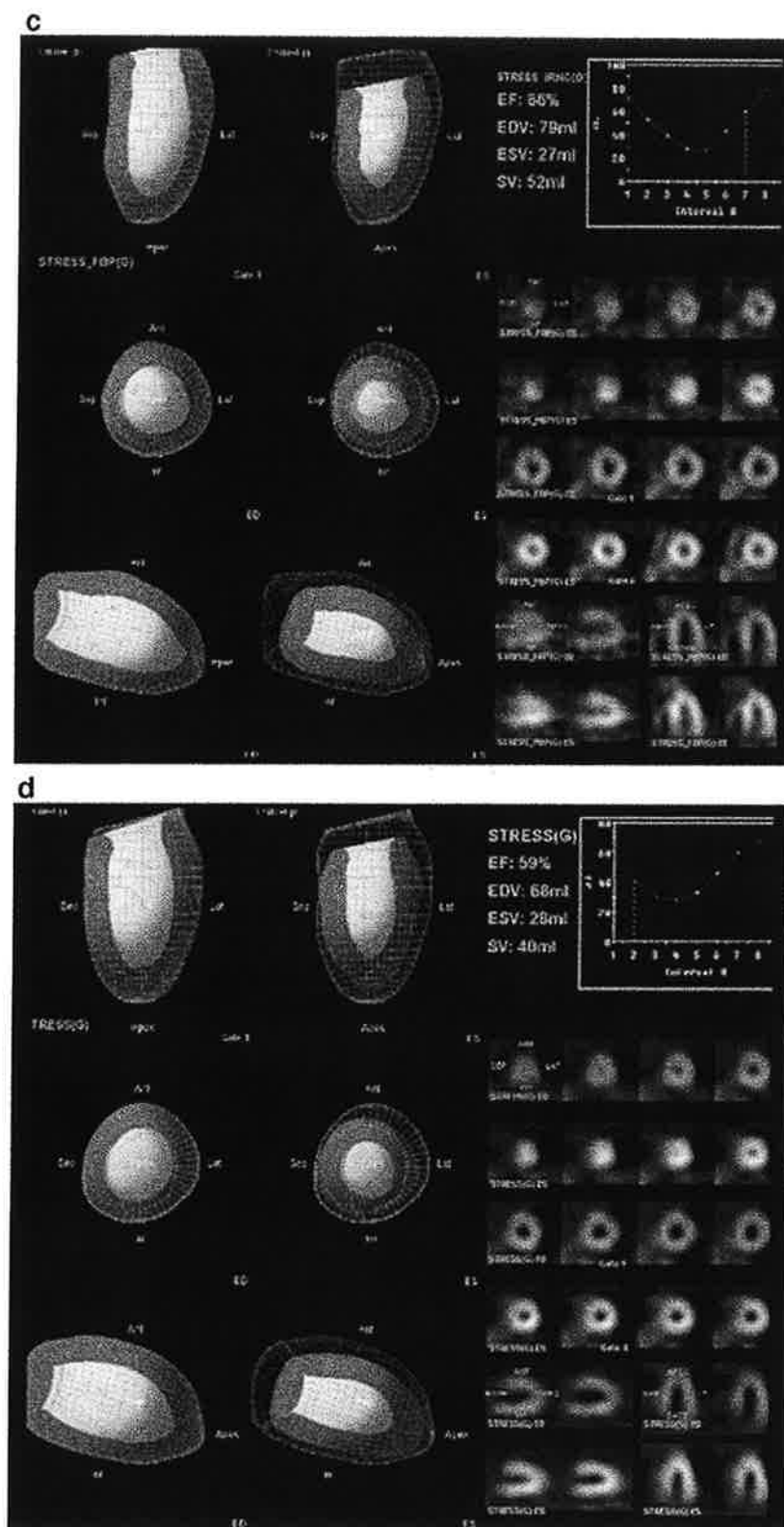
Figure 17. continued.

Figure 18. WBR® "half-time" Xpress® software was used to reconstruct this reduced-dose rest/stress (6.2/17.3 mCi) Tc-99m sestamibi "full-time" SPECT scan in a normal male patient with a 38" chest circumference. Image quality is excellent and comparable to a "full-dose," "full-time" study processed with OSEM iterative reconstruction[46].

SPECT (209 patients) with high-dose stress-only SPECT (140 patients) and with high-dose stress SPECT images acquired as part of a standard low-dose rest/high-dose stress protocol (368 patients).[52] The average injected Tc-99m sestamibi activities were 12.5, 29.2, and 41.7 mCi, respectively. SPECT imaging acquisition times were 3 minutes for the low-dose patients and 5 minutes for the other two patient groups. These authors observed that the myocardial count density and image quality of the low-dose 5-minute scans were equivalent to those in the other two groups in which the injected dose was higher and the image acquisition time was shorter. Moreover, as discussed below, using this protocol they documented the feasibility of performing a stress-only
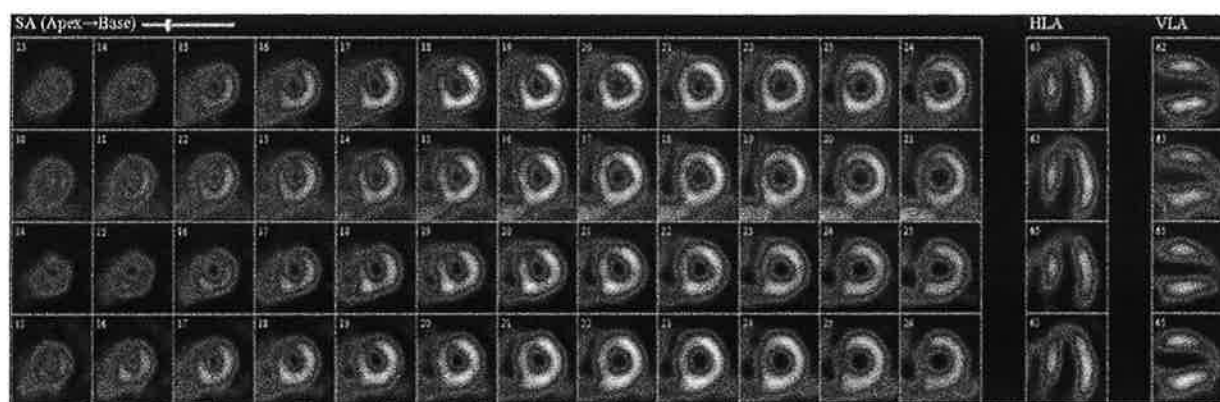
Figure 19. In this patient with an anterior/apical myocardial infarct SPECT was acquired first with a parallel-hole collimator with AC, and then with the IQ SPECT® collimator and AC. Stress and rest SPECT acquisition times were 15 and 20 minutes, respectively, for the parallel-hole collimator acquisitions; and 4 and 4 minutes, respectively, for the IQ SPECT® acquisitions. CT AC was performed with an exposure of 0.2-0.4 mSv. *Top row* parallel-hole stress with AC; *second row* parallel hole rest with AC; *third row* IQ SPECT® stress with AC; *fourth row* IQ SPECT® rest with AC. Courtesy James Corbett, University of Michigan, Ann Arbor, MI.
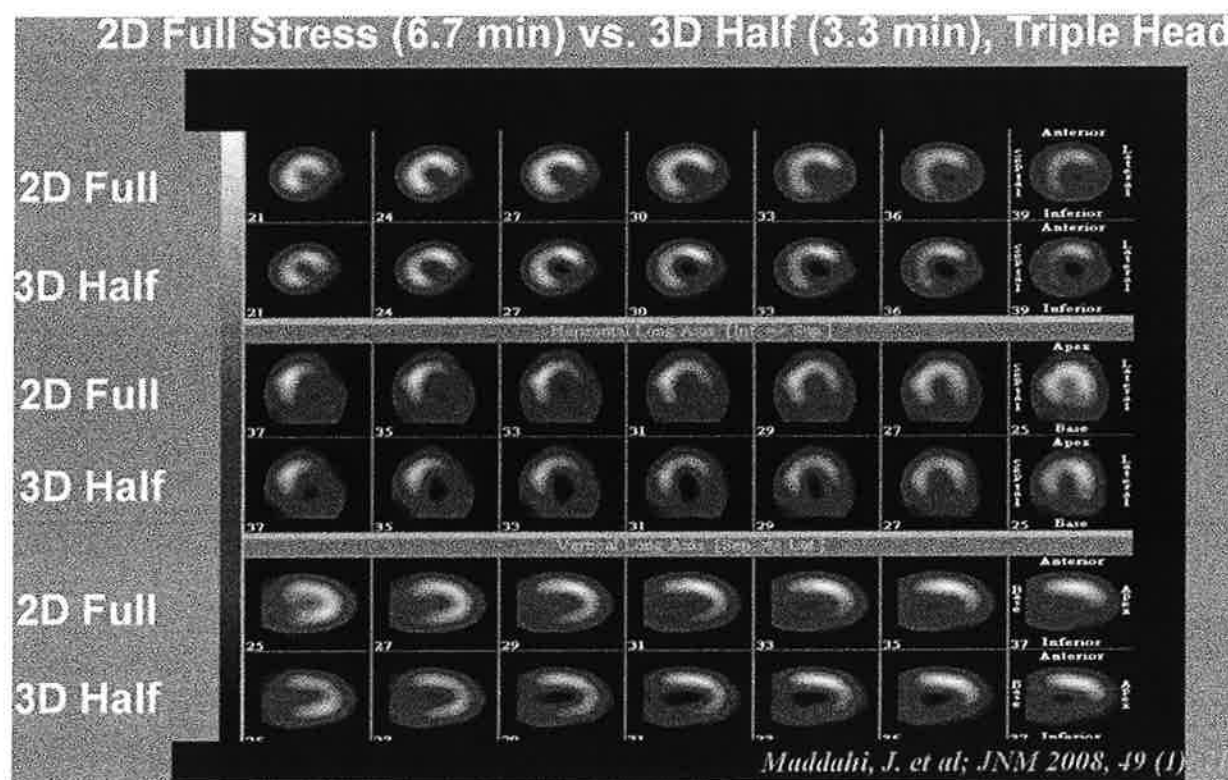
Figure 20. In this patient with an extensive inferolateral infarct SPECT was acquired on an upright Digirad solid-state detector camera. Images were acquired simultaneously "full-time" (*top row* of each orthogonal tomogram) and "half-time" (*bottom rows*). "Full-time" SPECT was processed with OSEM iterative reconstruction. "Half-time" SPECT was processed with nSPEED® software, incorporating resolution recovery and noise compensation. Image quality is slightly superior for the "half-time" technique. Courtesy Jamshid Maddahi, David Geffen School of Medicine at UCLA, Los Angeles, CA.
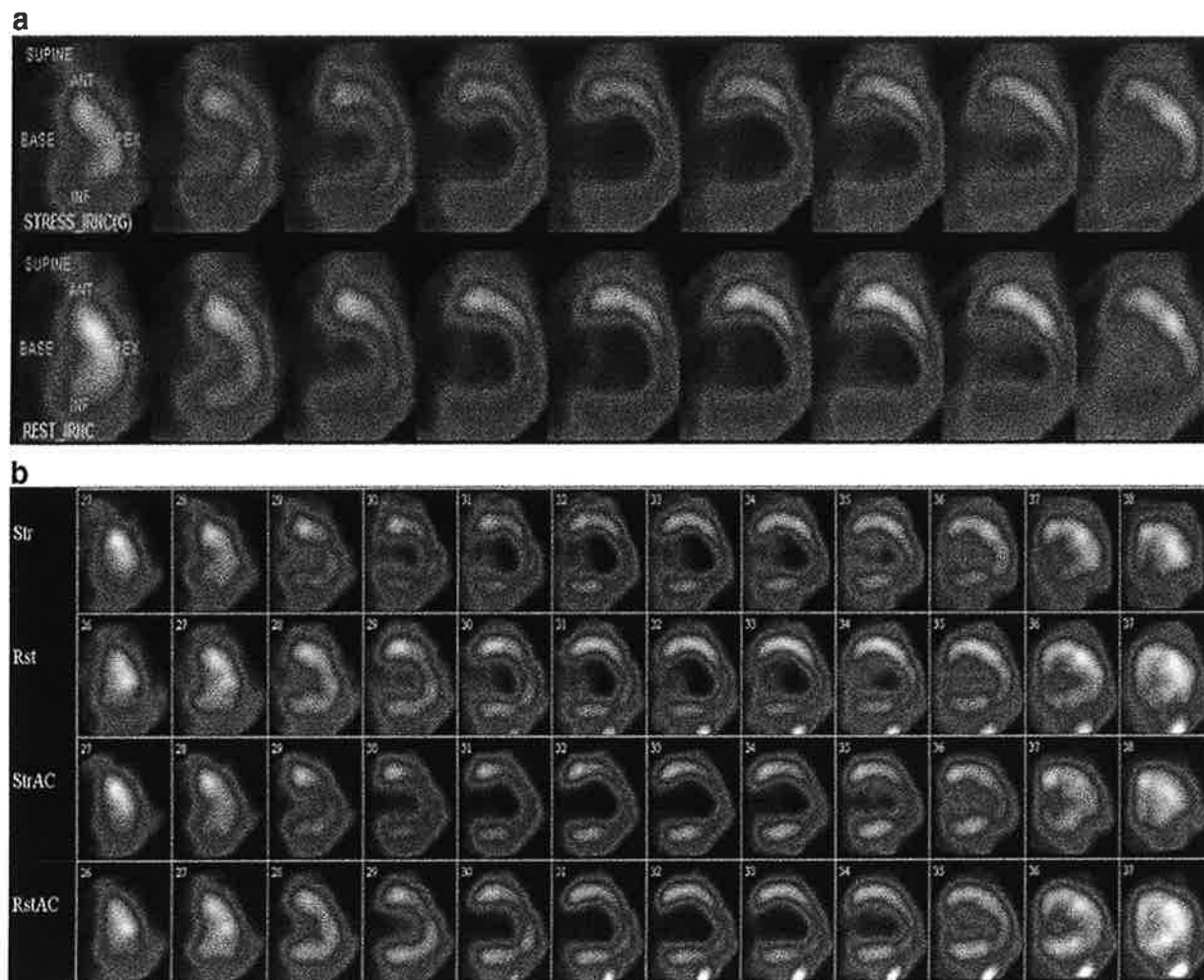
Figure 21. A Stress (*top row*) and rest (*bottom row*) supine SPECT was performed in this patient with an ischemic cardiomyopathy using a conventional dual-head NaI detector. In these vertical long axis tomograms the ventricle is markedly dilated, and there appear to be extensive, fixed perfusion abnormalities involving the apex and inferior wall. B The stress and rest (first and second rows, respectively) acquisitions were repeated on the Digirad X-ACT® camera with the patient sitting upright. There is partial resolution of the fixed inferior defect, indicating that with supine SPECT it was at least in part attributable to diaphragmatic attenuation. With additional AC (*third* and *fourth rows*) there is complete resolution of the inferior defect, indicating that with supine SPECT it was entirely attributable to diaphragmatic attenuation. There is also partial resolution of the resting apical defect, indicating some degree of stress-induced ischemia. Courtesy Gordon DePuey, St. Luke's-Roosevelt Hospital, New York, NY.

protocol with only 12.5 mCi and a 5-minute acquisition time using the new Discovery® camera, thereby significantly limiting patient radiation dose.

The very rapid imaging capability of the Discovery NM 530c® camera provides the opportunity for adjunctive techniques to potentially improve the diagnostic capabilities and accuracy of myocardial perfusion SPECT. Respiratory gating, which diminishes cardiac motion and potentially decreases diaphragmatic attenuation, thereby increasing diagnostic specificity, has been reported.[53] Buechel et al compared SPECT acquisitions triggered with breath-holding at deep inspiration to separate acquisitions acquired with x-ray AC but without breath-holding. Of 13 attenuation artifacts identified by AC, 4 (31%) were also partially unmasked by breath-holding. Pazhenkottil et al reported that by prolonging image acquisition time slightly to 5 minutes, gated image quality may be improved sufficiently to
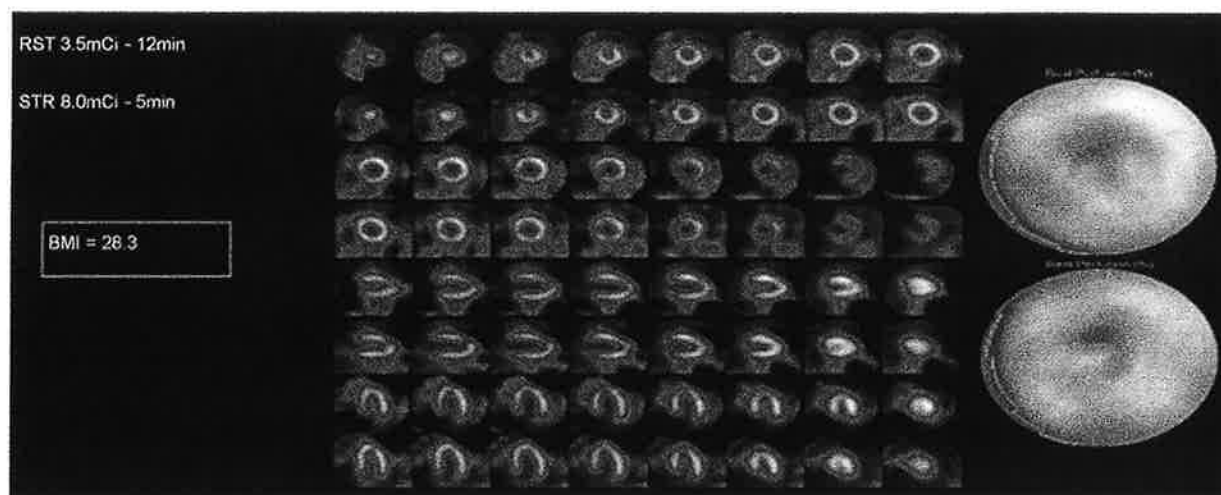
Figure 22. In this patient with a BMI of 28.3 a rest/stress SPECT scan was acquired on the D-SPECT® camera with significantly reduced Tc-99m sestamibi activity and image acquisition times. The patient received 3.5 mCi at rest and 8.0 mCi at stress. Acquisition times were 12 and 5 minutes, respectively. Image quality is excellent despite the reduced injected activity and scan acquisition times. Courtesy Spectrum Dynamics.

evaluate left ventricular dyssynchrony.[54] These investigators compared histogram bandwidth determined by phase analysis (Emory Toolbox®) of resting gated myocardial perfusion SPECT in 46 patients undergoing 15-minute SPECT on a standard dual-head NaI detector camera and 5-minute SPECT on the Discovery® camera and found no significant differences or the results obtained by the two methods. Hybrid imaging with x-ray CT, available with the Discovery® camera, allows for AC and image fusion with CT coronary angiography.[55,56]

ON THE HORIZON

Simultaneous Dual-Isotope SPECT

As described above, CZT solid-state detectors provide improved energy resolution as compared to NaI detectors. With improved discrimination of the photopeaks of Tc-99m and I-123, there is considerable future potential for simultaneous imaging of the radiopharmaceuticals labeled with these two isotopes. Similarly, Tl-201 emissions are better discriminated from Tc-99m photons using CZT detectors. Using the D-SPECT® camera, Berman et al[57] implemented a 20-minute sequential stress Tl-201/resting Tc-99m protocol, demonstrating similar image quality to that obtained using a standard rest/stress Tc-99m protocol. The advantage of using Tl-201 for stress imaging is its higher myocardial extraction, potentially allowing improved detection of stress-induced myocardial perfusion defects. Ben Haim et al[58] performed simultaneous

2.0 mCi resting Tl-201/6.8 mCi stress Tc-99m dual-isotope SPECT using the D-SPECT® camera in 27 consecutive patients and reported that image quality, diagnostic results, and SSS and SRS that were closely correlated with those obtained using a separate rest Tl-201/stress Tc-99m protocol in the same patients. Data were processed using a spill-over and scatter correction method, presumably minimizing the "hole-tailing" effect described above (Figure 24).

First-Pass Imaging and Evaluation of Coronary Flow Reserve

With high count-rate capabilities and list-mode acquisition the new CZT solid-state cameras provide the capability of performing high-quality first-pass radionuclide ventriculography.[37] Right ventricular function can be more accurately evaluated with first-pass imaging as compared to either planar equilibrium radionuclide ventriculography (MUGA) or gated myocardial perfusion SPECT. Assessment of left ventricular function during peak pharmacologic stress with either dobutamine or coronary vasodilators may be possible at the time of radiopharmaceutical injection. The adjunctive evaluation of left ventricular function at peak stress and at rest in conjunction with myocardial perfusion SPECT may increase diagnostic sensitivity and specificity of the latter.

An even more tantalizing potential capability is the assessment of coronary flow reserve.[8] Myocardial uptake of radiotracer is determined at stress and during peak pharmacologic coronary vasodilatation. It is now

possible to assess coronary flow reserve by this means using N-13 ammonia or Rb-82 PET. Quantification of coronary flow reserve has been demonstrated to provide adjunctive, prognostic value to myocardial perfusion PET.[59] The sensitivity of myocardial perfusion imaging is improved by the capability of detecting "balanced" ischemia, i.e., an equivalent, absolute decrease in myocardial perfusion in all vascular territories. Count-rate capabilities with the new solid-state detectors are now adequate to determine time-activity curves from the left ventricular cavity (input function) and from the myocardium (output function). Myocardial uptake is determined from these data using a two-compartment model, and a regional coronary flow reserve index is calculated as the ratio between myocardial uptake at stress versus rest. Although this technique has not yet been validated for SPECT systems, it seems promising. However, as compared to PET, SPECT methodology may be limited by the blunted myocardial extraction of Tc-99m sestamibi and tetrofosmin at high coronary flow rates. Moreover, to determine absolute myocardial blood flow AC, currently only available as an option on the Digirad X-ACT® and General Electric Discovery NM 530c® camera, is required.

Stress-Only Imaging

Stress-only myocardial perfusion SPECT has been demonstrated to be a practicable protocol in patients with no prior history of myocardial infarction and a relatively low pre-test likelihood of coronary artery disease. A normal stress-only scan confers the same favorable prognosis as a normal scan acquired using a conventional rest/stress protocol.[60] Stress myocardial perfusion SPECT with only a 5 mCi Tc-99m dose and a 12-16-minute acquisition time using a conventional dual-head NaI detector camera has been recently reported to be feasible in non-obese patients (Figure 25).[61] Apart from reducing the patient's time in the imaging laboratory and increasing laboratory efficiency by eliminating the resting scan, this protocol significantly decreases patient radiation exposure. Using the new software and hardware methods described above, which provide excellent image quality despite lower myocardial SPECT counting statistics in combination with a stress-only protocol, an even further reduction in patient radiation dose is feasible.

AC has been demonstrated to allow physicians to increase their confidence in interpreting stress-only studies as definitely normal or definitely abnormal and to reduce the need for resting imaging.[62] In a multi-center trial of 110 patients, Bateman et al[63] compared "full-time" myocardial perfusion SPECT acquired on a conventional dual-head NaI detector camera processed

with FBP to scans "stripped" of data to produce "half-time" scans, which underwent Gd-153 line-source AC and were then processed with Astonish® reduced-time software. These investigators demonstrated improved image quality, diagnostic certainty, diagnostic sensitivity, and diagnostic specificity using this advanced software processing method in conjunction with AC. Moreover, perfusion defect SSSs and gated LVEFs were similar using the "full-time" and attenuation corrected "half-time" methods. Therefore, it seems that a combination of new software and hardware methods that cope with lower counting statistics and AC is optimal for stress-only imaging both to decrease patient radiation dose and to improve diagnostic confidence and accuracy.

CONCLUSIONS AND COMMENTARY

The new software and hardware methods described above have been convincingly demonstrated to decrease SPECT acquisition time, injected radioactivity, or both. The potential advantages of shortening image acquisition time are considerable. Patient tolerance is improved, the opportunity for patient motion is decreased, and laboratory throughput is improved. Decreasing radiopharmaceutical doses while maintaining a longer acquisition time to decrease patient radiation exposure effectively addresses concerns of the public and the media and the latest recommendations by the American Society of Nuclear Cardiology. Combining these two potential advantages, there is the opportunity to "customize" scan protocols to meet specific patient requirements. For example, in a younger patient in whom radiation exposure is a concern, a reduced radiopharmaceutical dose and a relatively longer acquisition may be preferable. In an elderly, arthritic, or uncooperative patient unable to tolerate a 12-15-minute SPECT acquisition, a full radiopharmaceutical dose and reduced-time SPECT acquisition would be beneficial. In an obese patient, in order to increase image counting statistics, as an alternative to "weight-based" (e.g., increased) radiopharmaceutical doses, a standard or reduced dose could be given in combination with a "full-time" or even prolonged SPECT acquisition with an image acquisition time customized to provide adequate counting statistics.

Although reduced image acquisition time and/or decreased radiopharmaceutical dose(s) are obvious potential clinical advantages of the software and hardware methods described above, these method also may potentially hold promise in improving the diagnostic capabilities of myocardial perfusion SPECT due to their ability to cope with lower image counting statistics. For example, investigators have already reported improvement in image quality by adding respiratory gating.[53]

a

b
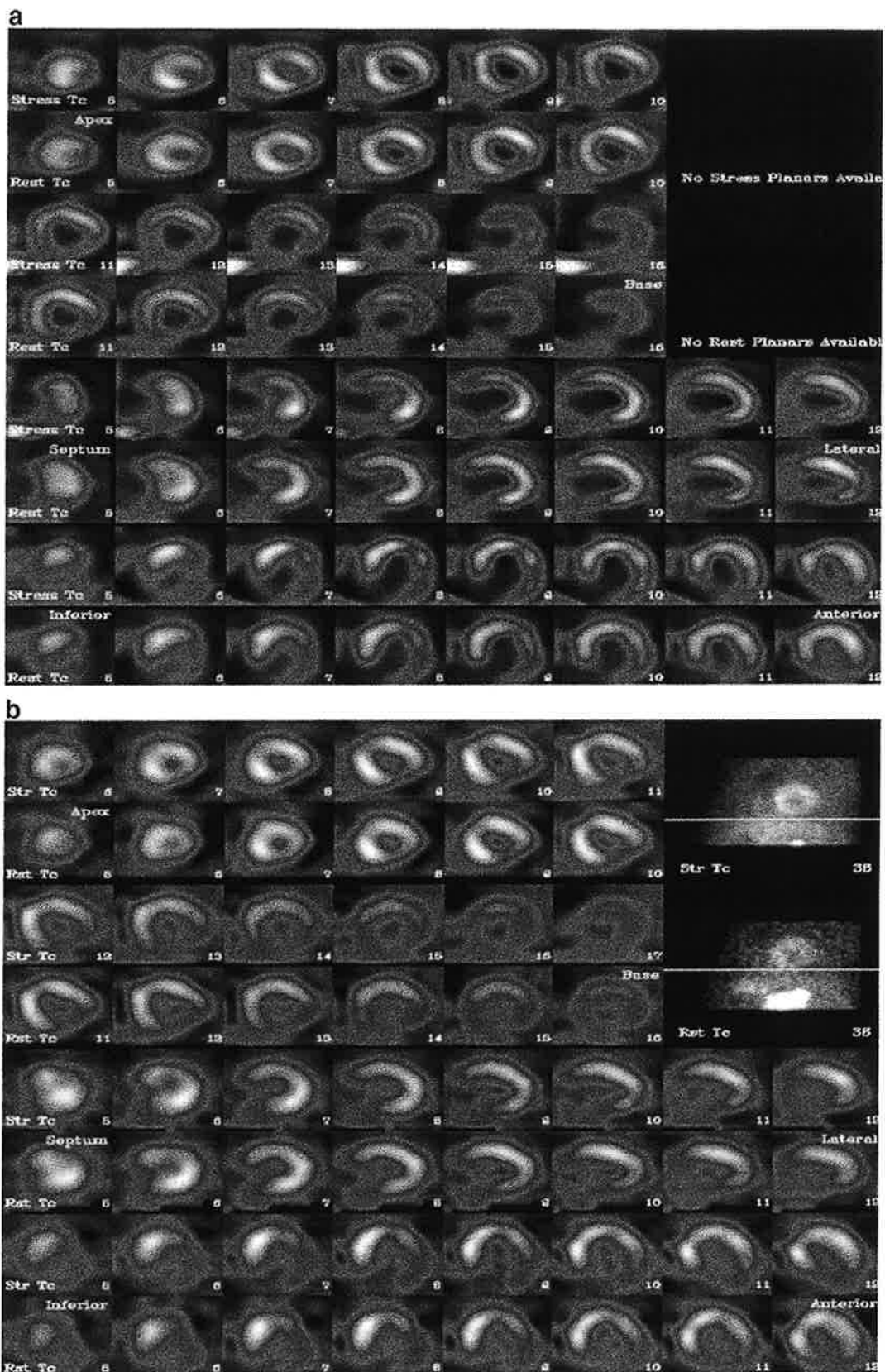
◄Figure 23. A Stress and rest standard-dose Tc-99m sestamibi myocardial perfusion SPECT was acquired on a conventional dual-detector NaI camera. SPECT acquisition times were 12 and 14 minutes, respectively. A severe and extensive fixed inferolateral perfusion defect is present. B Images were each reacquired on the Discovery NM 530c® camera with markedly reduced acquisition times: 2 and 4 minutes, respectively. Image quality is equivalent to that with the "full-time" conventional camera acquisition. Courtesy Ernest Garcia, Emory University, Atlanta, GA.

However, these potential capabilities to increase diagnostic accuracy should be explored much more fully. For example, it is very likely possible to increase the number of gated frames per cardiac cycle from 8 or 16 to ≥ 24, thereby providing both a more accurate ejection fraction and the potential for accurate quantitative analysis of systolic emptying and diastolic filling (i.e., peak systolic emptying rate and peak diastolic filling rate). Also, it would be highly desirable to "freeze"
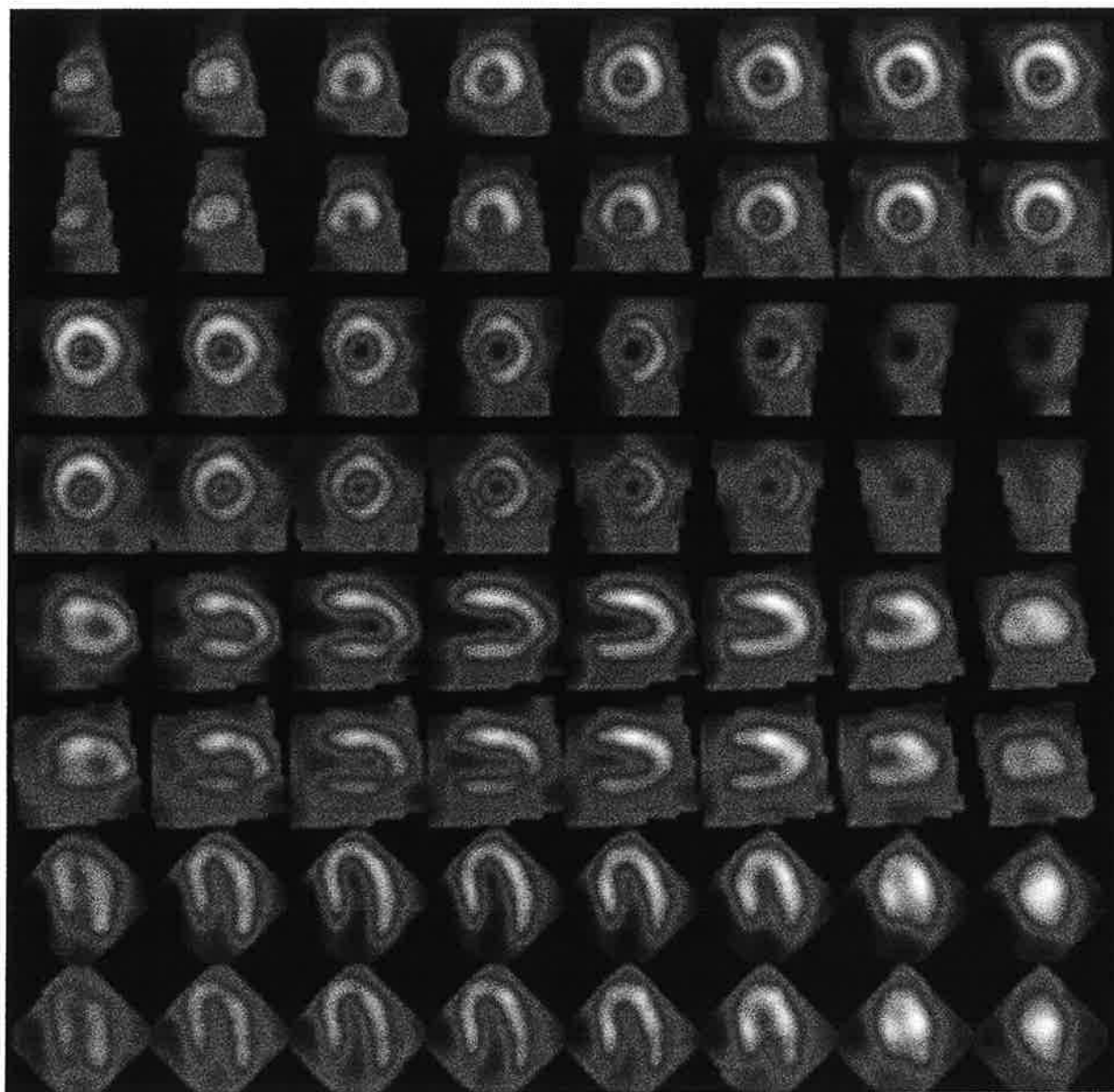
Figure 24. Simultaneous 2.0 mCi resting Tl-201/7.0 mCi stress Tc-99m sestamibi dual-isotope myocardial perfusion SPECT using the D-SPECT® CZT solid-state dedicated cardiac camera. Data were processed using a spill-over and scatter correction method.[58] Courtesy Spectrum Dynamics.
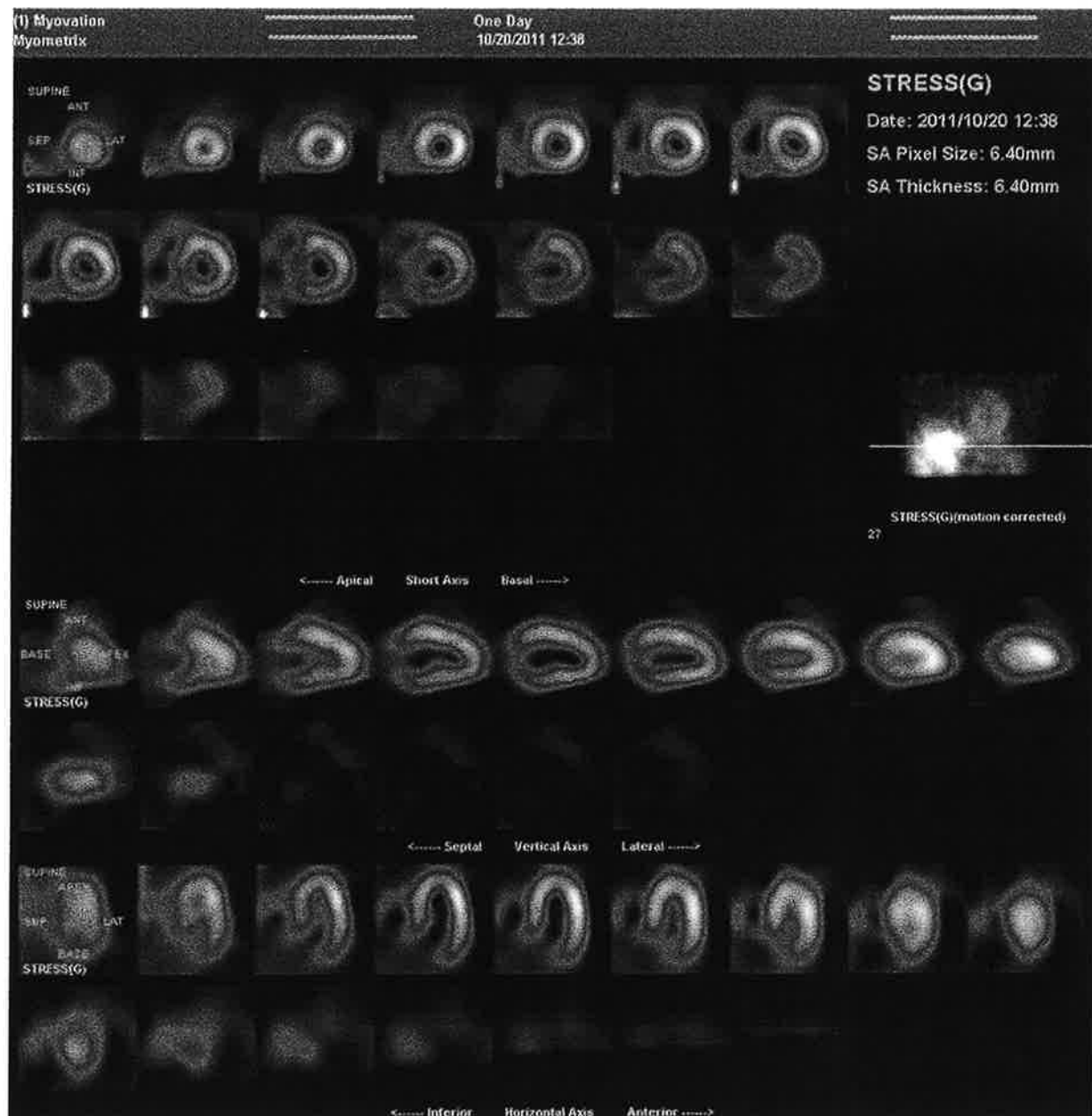
Figure 25. Stress-only myocardial perfusion SPECT was performed using a conventional dual-head NaI detector camera and only a 5 mCi Tc-99m sestamibi dose and a 16-minute acquisition time in this male patient with a 43″ chest circumference. Images were reconstructed using WBR Xpress3® "quarter-time" software. Because the SPECT images were unequivocally normal, a subsequent resting scan was unnecessary, thereby markedly decreasing patient radiation exposure. Courtesy Gordon DePuey, St. Luke's-Roosevelt Hospital, New York, NY.

cardiac motion by means of summing only end-diastolic gated frames in the summed perfusion tomograms, as describe more than a decade ago by Taillefer et al[64] to increase diagnostic sensitivity in detecting perfusion abnormalities. However, heretofore such techniques have not been practical because they significantly

decrease image counting statistics and thereby introduce noise and potential artifacts. For example, the diagnostic accuracy of end-diastolic imaging was confounded by more marked soft tissue attenuation artifacts. However, now by combining advanced techniques that cope with lower counting statistics and AC, end-diastolic

"freeze-frame" SPECT may be feasible. Other potential advantages of shorter acquisition times include the use of Tc-99m teboroxime, which is highly extracted by the myocardium but clears very rapidly, necessitating a rapid SPECT acquisition. There is also the possibility of performing gated SPECT acquisitions during dobutamine infusion to evaluate functional reserve as well as viability in a manner similar to that which is routinely accomplished with stress echocardiography. These applications most likely require SPECT acquisition times <5 minutes and list-mode acquisition, which are now clearly practical using a variety of the technical advancements described above.

If indeed the technical advancements reviewed in this article prove not only to decrease SPECT acquisition time and decrease radiation exposure but also to improve diagnostic accuracy in the detection of coronary artery disease, the Nuclear Cardiology community may be faced with the daunting task of reevaluating the diagnostic accuracy and prognostic value of myocardial perfusion SPECT. Such research would likely entail a prospective trial or trials with coronary angiographic correlation and extensive patient follow-up. Clearly, such an endeavor is too comprehensive and expensive to be undertaken by only one group of investigators or one instrumentation or software vendor. Such an effort will require sponsorship by national organizations and probably the Federal Government. However, if funding and sponsorship were available, before embracing this potential opportunity we should ask ourselves "Is now the time?" Are there radiopharmaceuticals on the horizon more highly extracted by the myocardium that will increase diagnostic accuracy? Do we anticipate further advancements in SPECT or PET technology that are worth waiting for? In the meantime, though, we should certainly embrace, tout, and clinically implement the remarkable myocardial perfusion SPECT technical advancements described above.

References

1. Einstein AJ, Moser KW, Thompson RC, Cerqueira MD, Henzlova MJ. Radiation dose from cardiac diagnostic imaging. Circulation 2007;116:1290-305.

2. Bogdanich W, Ruiz RR. FDA to increase oversight of medical radiation. New York Times, February 10, 2010;B7.

3. DePuey EG, Mahmarian JJ, Miller TD, Einstein AJ, Hansen CL, Holly TA, et al. Patient-centered imaging, ASNC Preferred Practice Statement. J Nucl Cardiol (in press).

4. Cerqueira MD, Allman KC, Ficaro EP, Hansen CL, Nichols KJ, Thompson RC, et al. Recommendations for reducing radiation exposure in myocardial perfusion imaging. J Nucl Cardiol 2010;17:709–18.

5. Patton JA, Slomka PJ, Germano G, Berman DS. Recent technological advances in nuclear cardiology. J Nucl Cardiol 2007;14:501-13.

6. Garcia EV, Faber TL. New trends in camera and software technology in nuclear cardiology. Cardiol Clin 2009;27:227-36.

7. DePuey EG. New software methods to cope with reduced counting statistics: Shorter SPECT acquisitions and many more possibilities. J Nucl Cardiol 2009;16:335-8.

8. Sharir T, Slomka PJ, Berman DS. Solid-state SPECT technology: Fast and furious. J Nucl Cardiol 2010;17:890-6.

9. Garcia EV, Faber TL, Esteves FP. Cardiac dedicated ultrafast SPECT cameras: New designs and clinical implications. J Nucl Med 2011;52:210-7.

10. Metz CE. The geometric transfer function component for scintillation camera collimators with straight parallel holes. Phys Med Biol 1980;25:1059-70.

11. Tsui BMW, Gullberg GT. The geometric transfer-function for cone and fan beam collimators. Phys Med Biol 1990;35:81-93.

12. Tsui BMW, Hu HB, Gillard DR, Gullberg GT. Implementation of simultaneous attenuation and detector response correction in SPECT. IEEE Trans Nucl Sci 1988;35:778-83.

13. Tsui BMW, Frey EC, Zhao X, Lalush DS, Johnston RE, McCartney WH. The importance and implementation of accurate three-dimensional compensation methods for quantitative SPECT. Phys Med Biol 1994;39:509-30.

14. Tsui BMW, Zhao XD, Frey EC, Gullberg GT. Characteristics of reconstructed point response in three-dimensional spatially variant detector response compensation in SPECT. In: Grangeat P, Amans J-L, editors. Three-dimensional image reconstruction in radiology and nuclear medicine. Dordrecht: Kluwer Academic Publishers; 1996. p. 509-30.

15. Borges-Neto S, Pagnanelli RA, Shaw LK, Honeycutt E, Shwartz SC, Adams GL, et al. Clinical results of a novel wide beam reconstruction method for shortenings can time of Tc-99m cardiac SPECT perfusion studies. J Nucl Cardiol 2007;14:555-65.

16. DePuey EG, Gadiraju R, Clark J, Thompson L, Anstett F, Shwartz SC. Ordered subset expectation that maximization and wide beam reconstruction "half-time" gated myocardial perfusion SPECT functional imaging: A comparison to "full-time" filtered backprojection. J Nucl Cardiol 2008;15:547-63.

17. Philipe P, Bruyant J. Analytic and iterative reconstruction algorithms in SPECT. J Nucl Med 2002;43:1343-58.

18. Green PJ. Bayesian reconstruction from emission tomography data using a modified EM algorithm. IEEE Trans Med Imaging 1990;9:84-93.

19. Alenius S, Ruotsalainen U. Bayesian image reconstruction for emission tomography based on medium root prior. Eur J Nul Med 1997;24:258-65.

20. Farkash G, Kenig K, Grabnic M, Yuzefovich B, Sachs J, Bocher M. Volumetric quantitation of left ventricular perfusion and function from myocardial perfusion SPECT: Validation of a new algorithm [abstract]. J Nucl Cardiol 2006;13:S5.

21. Chen J, Garcia EV, Folks RD, Cooke CD, Faber TL, Tauxe L, et al. Onset of left ventricular mechanical contraction as determined by phase analysis of ECG-gated myocardial perfusion SPECT imaging: Development of a diagnostic tool for assessment of cardiac mechanical dyssynchrony. J Nucl Cardiol 2005;12:687-95.

22. Henneman MM, Chen J, Ypenburg C, Dibbets P, Bleeker GB, Boersma E, et al. Phase analysis of gated myocardial perfusion single-photon emission computed tomography compared with tissue Doppler imaging for the assessment of left ventricular dyssynchrony. J Am Coll Cardiol 2007;49:1708-14.

23. Henneman MM, Chen J, Dibbets-Schneider P, Stokkel MP, Bleeker GB, Ypenburg C, et al. Can LV dyssynchrony as assessed with phase analysis on gated myocardial perfusion SPECT predict response to CRT? J Nucl Med 2007;48:1104-11.

24. Heydari B, Jerosch-Herold M, Kwong R. Imaging for planning of cardiac resynchronization therapy. J Am Coll Cardiovasc Imaging 2012;5:93-110.

25. Liu YH, Lam PT, Sinusas AJ, Wackers FJT. Different effect of 180° and 360° acquisition orbits on the accuracy of SPECT imaging: Quantitative evaluation of phantoms. J Nucl Med 2002;43:1115-24.

26. Abufadel A, Eisner RL, Schafer RW. Differences due to collimator blurring in cardiac images with use of circular and elliptical orbits. J Nucl Cardiol 2001;8:458-65.

27. Bai C, Conwell R, Kindem J, Babla H, Gurley M, De Los Santos R, et al. Phantom evaluation of a cardiac SPECT/VCT system that uses a common set of solid-state detectors for both emission and transmission scans. J Nucl Cardiol 2010;17:459-69.

28. Vija AH, Malmin R, Yahil A, Zeintl J, Bhattacharya M, Rempel TD, et al. A method for improving the efficiency of myocardial perfusion imaging using conventional SPECT and SPECT/CT imaging systems. Hoffman Estates: Molecular Imaging, Siemens Medical Solution USA, Inc; 2010.

29. Rajaram R, Bhattacharya M, Ding X, Malmin R, Rempel TD, Vija H, et al. Tomographic performance characteristics of the IQ-SPECT system. Hoffman Estates: Molecular Imaging, Siemens Medical Solution USA, Inc; 2011.

30. Zeintl J, Rempel TD, Bhattacharya M, Malmin RE, Vija AH. Performance characteristics of the SMARTZOOM® collimator. Hoffman Estates: Molecular Imaging, Siemens Medical Solution USA, Inc; 2011.

31. Corbett J, Meden J, Ficaro E. Clinical validation of attenuation corrected cardiac imaging with IQ-SPECT/CT [abstract]. J Nucl Med 2010;4:733.

32. Gambhir SS, Berman DS, Ziffer J, Nagler M, Sandler M, Patton J, et al. A novel high-sensitivity rapid-acquisition single-photon cardiac imaging camera. J Nucl Med 2009;50:635-43.

33. Esteves FP, Raggi P, Folks RD, Keidar Z, Askew W, Rispler S, et al. Novel solid-state-detector dedicated cardiac camera for fast myocardial perfusion imaging: Multicenter comparison with standard dual detector cameras. J Nucl Cardiol 2009;16:927-34.

34. Blevis I, Tsukerman L, Volokh L, Hugg J, Jansen F, Bouhnik JP. CZT gamma camera with pinhole collimator: Spectral measurements. In 2008 IEEE nuclear science symposium conference record. ISBN: 978-1-4244-2715-4/08.

35. Erlandsson K, Kacperski K, Van Gramberg D, Hutton B. Performance evaluation of D-SPECT: A novel dedicated cardiac SPECT scanner. Phys Med Biol 2009;54:2635-49.

36. Hutton B, Erlandsson K, Kacperski K, Van Gramberg D, Roth N. Performance evaluation of D-SPCT—a novel dedicated cardiac SPECT scanner. J Nucl Med 2008;49:124P.

37. Bocher M, Blevis IM, Tsukerman L, Shrem Y, Kovalski G, Volokh L. A fast cardiac gamma camera with dynamic SPECT capabilities: Design, system validation and future potential. Eur J Nucl Med Mol Imaging 2010;37:1887–902.

38. Gambhir SS, Berman DS, Ziffer J, Nagler M, Sandler M, Patton J, et al. A novel high-sensitivity rapid-acquisition single-photon cardiac imaging camera. J Nucl Med 2009;50:635-43 (On line supplemental material).

39. Hillel I, Hanney M, Redgate S, Taylor J, Randall D. Assessing the performance of a solid-state cardiac gamma camera prior to its introduction into routine clinical service. J Nucl Med 2011;52:1937.

40. Basso D, Passmore G, Holman M, Rogers W, Walters L, Zecchin T, et al. Semiqualitative visual and quantitative morphometric evaluations of reduced scan time and wide-beam reconstruction in rest-gated stress SPECT myocardial perfusion imaging. J Nucl Med Technol 2009;37:233-9.

41. Marcassa C, Campini R, Zoccarato O, Calza P. Wide beam reconstruction for half-dose or half-time cardiac gated SPECT acquisitions: Optimization of resources and reduction in radiation exposure. Eur J Nucl Med 2010;38:499-508.

42. Druz R, Phillips L, Chugkowski M, Boutis L, Rutkin B, Katz B. Wide-beam reconstruction half-time SPECT improves diagnostic certainty and preserves normalcy and accuracy: A quantitative perfusion analysis. J Nucl Cardiol 2011;18:52-61.

43. Venero CV, Heller GV, Bateman TM, McGhie AI, Ahlberg AW, Katten D, et al. A multicenter evaluation of a new post-processing method with depth-dependent collimator resolution applied to full-time and half-time acquisitions without and with simultaneously acquired attenuation correction. J Nucl Cardiol 2009;16:714-25.

44. Cullom SJ, Saha K, Heller GV, Bateman TV. An optimized iterative reconstruction and processing protocol for "half-time" (32 projections) REST/STRESS Tc99m-sestamibi myocardial perfusion SPECT. J Nucl Cardiol 2008;15:S6.

45. DePuey EG, Bommireddipalli S, Clark J, Thompson L, Srour Y. Wide beam reconstruction "quarter-time" gated myocardial perfusion SPECT functional imaging: A comparison to "full-time" ordered subset expectation maximum. J Nucl Cardiol 2009;16:736-52.

46. DePuey EG, Bommireddipalli S, Clark J, Leykekhman A, Thompson LB, Friedman M. A comparison of the image quality of full-time myocardial perfusion SPECT versus wide beam reconstruction half-time and half-dose SPECT. J Nucl Cardiol 2011;18:273-80.

47. Maddahi J, Mendez R, Mahmarian J, Thomas G, Bai C, Babla H, et al. Prospective multi-center evaluation of rapid gated SPECT myocardial perfusion and upright imaging. J Nucl Cardiol 2009;16:351-7.

48. Sharir T, Ben-Haim S, Merzon K, Prochorov V, Dickman D, Ben-Haim S, et al. High-speed myocardial perfusion imaging: Initial clinical comparison with conventional dual detector anger camera imaging. J Am Coll Cardiol Imaging 2008;1:156-63.

49. Sharir T, Slomka PJ, Hayes SW, DiCarli MF, Ziffer JA, Martin WH, et al. Multicenter trial of high-speed versus conventional single-photon emission computed tomography imaging: Quantitative of myocardial perfusion and left ventricular function. J Am Coll Cardiol 2010;55:1965-74.

50. Buechel RR, Herzog BA, Husmann L, et al. Ultrafast nuclear myocardial perfusion imaging on a new gamma camera with semiconductor detector technique: First clinical validation. Eur J Nucl Med Mol Imaging 2010;37:773-8.

51. Herzog BA, Buechel RR, Katz R, et al. Nuclear myocardial perfusion imaging with a cadmium-zinc-telluride detector technique; optimized protocol for scan time reduction. J Nucl Med 2010;51:46-51.

52. Duvall WL, Croft LB, Godiwala T, Ginsberg E, George T, Henzlova MJ. Reduced isotope dose with rapid SPECT MPI imaging: Initial experience with a CZT SPECT camera. J Nucl Cardiol 2010;17:1009-14.

53. Buechel RR, Pazhenkottil AP, Herzog BA, et al. Real-time breath-hold triggering of myocardial perfusion imaging with a novel cadmium-zinc-telluride detector gamma camera. Eur J Nucl Med Mol Imaging 2010;37:1903-8.

54. Pazhenkottil AP, Buechel RR, Herzog BA, et al. Ultrafast assessment of left ventricular dyssynchrony from nuclear myocardial perfusion imaging on a new high-speed gamma camera. Eur J Nucl Med Mol Imaging 2010;37:2086-92.

55. Herzog BA, Buechel RR, Husmann L, et al. Validation of CT attenuation correction for high-speed myocardial perfusion imaging using a novel cadmium-zinc-telluride detector technique. J Nucl Med 2010;51:1539-44.

56. Pazhenkottil AP, Husmann L, Kaufmann PA. Cardiac hybrid imaging with high-speed single-photon emission computed tomography/CT camera to detect ischemia and coronary artery obstruction. Heart 2010;96:2050.

57. Berman DS, Kang X, Tamarappoo B, Wolak A, Hayes SW, Nakazato R, et al. Stress thallium-201/rest technetium-99m sequential dual isotope high-speed myocardial perfusion imaging. JACC Cardivasc Imaging 2009;2:273-82.

58. Ben-Haim S, Kacperski K, Hain S, Van Gramberg D, Hutton BF, Erlandsson K, et al. Simultaneous dual-radionuclide myocardial perfusion imaging with a solid-state dedicated cardiac camera. Eur J Nucl Med Mol Imaging 2010;37:1710-21.

59. Herzog BA, Husmann L, Valenta I, Gaemperli O, Siegrist PT, Tay FM, et al. Long-term prognostic value of 13N-ammonia myocardial perfusion positron emission tomography added value of coronary flow reserve. J Am Coll Cardiol 2009;54:150-6.

60. Chang SM, Nabi F, Xu J, Raza U, Mahmarian JJ. Normal stress-only versus standard stress/rest myocardial perfusion imaging. J Am Coll Cardiol 2010;55:221-30.

61. DePuey G, Ata P, Wray R. 5 mCi stress myocardial perfusion SPECT with a conventional NaI camera [abstract]. J Nucl Med (submitted).

62. Heller GV, Bateman TM, Johnson LL, Cullom SJ, Case JA, Galt JR, et al. Clinical value of attenuation correction in stress-only Tc-99m sestamibi SPECT imaging. J Nucl Cardiol 2004;11:273-81.

63. Bateman TM, Heller GV, McGhie AI, Courter SA, Golub RA, Case JA, et al. Multicenter investigation comparing a highly efficient half-time stress-only attenuation correction approach against standard rest-stress Tc-99m SPECT imaging. J Nucl Cardiol 2009;16:726-35.

64. Taillefer R, DePuey EG, Udelson JE, Beller GA, Benjamin C, Gagnon A. Comparison between the end-diastolic images and the summed images of 99m-Tc sestamibi gated SPECT perfusion study in detection of coronary artery disease in women. J Nucl Cardiol 1999;6:169-76.

AMERICAN SOCIETY OF NUCLEAR CARDIOLOGY

CONTINUING EDUCATION INSTRUCTIONS: ADVANCES IN SPECT CAMERA SOFTWARE AND HARDWARE: CURRENTLY AVAILABLE AND NEW ON THE HORIZON

STATEMENT OF NEED

In order to maintain competence and improve performance, imaging professionals must assimilate and integrate knowledge spanning multiple areas, including clinical data, technical aspects of imaging, and appropriate application of imaging (e.g., clinical guidelines and appropriate use criteria). Each of these areas is constantly evolving, particularly as innovative technologies and novel pharmacologic agents are introduced.

The following issues in practice have been identified to demonstrate the learner's need for the skills and strategies presented in this journal continuing education activity:

- Studies consistently show that adequate awareness of radiation doses associated with procedures and the risk attributable to these doses is lacking among physicians. Physicians are encouraged to gain adequate knowledge on radiation exposure when performing MPI testing that result in lesser radiation exposure to patients.
- Evidence from the Intersocietal Commission for the Accreditation of Nuclear Laboratories (ICANL) accreditation process shows that a growing number of applications are cited for errors in their clinical protocols, in spite of ASNC's clinical guidelines and clinical updates indicating specific protocols required for nuclear cardiology procedures. ASNC guidelines and clinical updates include standardized nuclear cardiology protocols. Providers performing nuclear cardiology procedures need to reevaluate skills and competency in applying current guideline-based protocols.

TARGET AUDIENCE

This activity is targeted at imaging professionals and is intended to provide the latest information on clinical practice and cutting-edge scientific advances in nuclear cardiology and cardiac imaging.

OVERALL PURPOSE

The purpose of this CME activity in the *Journal of Nuclear Cardiology* is to increase the learners' competence in the application of nuclear cardiology strategies in clinical practice.

LEARNER OBJECTIVES

After reading and reflecting upon this article, the learner should be able to:

- Describe advances in software methods, including iterative reconstruction, resolution recovery, noise compensation, and phase analysis.
- Summarize developments in hardware, such as optimized detector geometry, focused collimation, solid-state detectors, and attenuation correction.
- Discuss potential future technological developments such as simultaneous dual-isotope SPECT, evaluation of coronary flow reserve, and stress-only imaging.

ACCREDITATION AND CONTINUING EDUCATION CREDIT

Physicians

The American Society of Nuclear Cardiology is accredited by the Accreditation Council for Continuing Medical Education to provide continuing medical education for physicians.

The American Society of Nuclear Cardiology designates this Journal-based CME activity for a maximum of 1 *AMA PRA Category 1 Credits*™. Physicians should only claim credit commensurate with the extent of their participation in the activity.

Technologists

The American Society of Nuclear Cardiology is a recognized provider of continuing education credit for technologists. ASNC's Continuing Education (ACE)

credit is accepted by both NMTCB and ARRT. This Journal-based activity has been approved for a maximum of 1 ACE credits for Technologists.

This program does not offer training or certification in the field.

Principal Faculty and their Credentials

Editor: George A. Beller, MD, Professor of Internal Medicine, University of Virginia
Author(s): E. Gordon DePuey, MD, Director of Nuclear Medicine, St. Luke's-Roosevelt Hospital

DISCLOSURES

As an accredited provider of the Accreditation Council for Continuing Medical Education (ACCME), The American Society of Nuclear Cardiology (ASNC) adheres to the ACCME's 2005 Standards for Commercial Support. In compliance with these standards, it is ASNC's policy to ensure balance, independence, objectivity, and scientific merit in all of its educational activities through the disclosure of relevant financial relationship with commercial companies and resolution of conflict of interest. The financial interest or relationships requiring disclosure are outlined in ASNC's CME Conflict of Interest Policy. All authors involved with this activity were required to disclose any relevant financial relationships. The American Society of Nuclear Cardiology has reviewed this activity's faculty disclosures and resolved or managed all identified conflicts of interest through a peer review process.

The following author reported the following financial relationships: E. Gordon DePuey, MD: Consultant/Advisory Board: Forest Laboratories, UltraSPECT Ltd; Speaker/Honoraria: Cardinal Health, Digirad; Research Support: Astellas, Digirad Inc., Lanthues, Michael J. Fox Foundation, UltraSpect Ltd.

The following members of the JNC Editorial Staff reported no financial relationships: George A. Beller, MD, FASNC and Wendy Passerell.

The following ASNC staff and article reviewers who were involved in the planning and development of this activity reported no financial relationships: J. Wells Askew, MD; Jamieson Bourque, MD; Beth Hodge; Barb Ziegner, CNMT.

The following article reviewer who was involved in the planning and development of this activity reported a financial relationship: Prem Soman, MD: Consultant: Astellas, GE Healthcare.

OFF LABEL USE

Articles may include discussion of drugs or devices, or uses of drugs or devices, which have not been approved by the Food and Drug Administration (FDA) or have been approved by the FDA for specific uses only. The FDA has stated that it is the responsibility of the physician to determine the FDA clearance status of each drug or device he or she wishes to use in clinical practice. ASNC is committed to the free exchange of medical education. Inclusion of any discussion in this program, including discussion on off-label uses, does not imply an endorsement by ASNC of the uses, products, or techniques presented. Authors are required to disclose to the learners, if there is any off-label usage within the article.

CONTINUING EDUCATION TERM OF APPROVAL

Release Date: May 15, 2012
Date of Last Review: April 2, 2012
Expiration Date: May 14, 2013

METHOD OF PARTICIPATION

To successfully complete this activity and receive a statement of credit, participants must:

1. Read the article and reflect upon its contents.
2. Successfully complete the Quiz and Evaluation questions. The participant must select the single most appropriate answer for each question. A score of 80% or higher is needed to pass the quiz and receive your credit certificate. If less than 80% of the questions were correct, the participant will be notified and may resubmit the quiz with modified answers up to three times. Tests will be graded by ASNC staff members.
3. Send your completed CE registration form, post-test and evaluation by mail, fax, or e-mail to:

   American Society of Nuclear Cardiology
   Attn: JNC Continuing Education
   4340 East-West Highway, Suite 1120
   Bethesda, MD 20814-4578
   Fax: (301) 215-7113
   E-mail: JournalCredit@asnc.org

After successfully completing the quiz and evaluation, participants will receive their certificate of credit via e-mail within 10 days. If an e-mail is not available, the certificate will be mailed.

ESTIMATED TIME OF COMPLETION

Estimated time of completion is one hour. Physicians will be asked to claim the actual amount of time spent on the activity.

BIBLIOGRAPHY

Bibliographic sources are cited throughout the article and a full bibliography is provided at the end of the article to provide you with further study resources on this topic.

MEDIUM OR COMBINATION OF MEDIUM USED

This article is available in print format only

PROCESSING FEES

ASNC members may claim continuing education credits at no charge. Non-members will be charged $25 per activity. Please fill out the payment area included on the evaluation form.

ACKNOWLEDGEMENT OF COMMERCIAL SUPPORT

This activity is not supported by commercial support.

For questions regarding CME content or obtaining CME credit, please contact ASNC at 301.215.7575 or info@asnc.org.

CE QUIZ & REGISTRATION FORM

In order to earn continuing education credit for this journal activity, you must read the article, reflect, and successfully pass the post-test. A passing grade of 80% is required to earn credit.

CME/ACE certificates will be sent within ten (10) business days.

Please mail or fax this form to:
American Society of Nuclear Cardiology
Attn: JNC Continuing Education
4340 East-West Highway, Suite 1120
Bethesda, MD 20814
Fax: (301) 215-7113
Email: Journalcredit@asnc.org
Please circle one response per question.

CE Quiz

1. Which of the following is NOT an advantage of iterative reconstruction software techniques over filtered back projection?

    a. Increased sensitivity to perfusion defects
    b. Elimination of artifacts related to extracardiac activity
    c. Improved spatial resolution
    d. Enhanced LV endocardial border definition

2. Which of the following is true about new advances in attenuation correction?

    a. Attenuation correction scans can be performed with as little as 0.2-0.4 mSv
    b. Misregistration is no longer an issue with new attenuation correction techniques
    c. Computed tomography is required for adequate attenuation correction
    d. Patient motion artifacts are not a limitation of the Digirad Cardius X-ACT® camera attenuation correction techniques

3. Clinical studies have shown all of the following benefits of SPECT image processing with wide beam reconstruction software as compared to filtered back projection EXCEPT:

    a. Similar or improved image quality

    b. Similar summed stress score
    c. Similar LV functional parameters
    d. Half-dose or half-time imaging

4. Which of the following is NOT a recent software technical advancement for SPECT reconstruction?

    a. Noise reduction
    b. Iterative reconstruction
    c. Resolution recovery
    d. Filtered back projection

5. Advantages of direct solid-state detectors (i.e. cadmium zinc telluride semiconductors) include:

    a. Improved intrinsic efficiency for detecting 140 KeV gamma rays compared to sodium iodide detectors
    b. Improved energy resolution compared to sodium iodide detectors
    c. Eliminated concern for "hole-tailing" effect related to increasing semiconductor thickness
    d. Use of probabilistic positioning circuitry to estimate a scintigraphic event

6. A normal stress-only myocardial perfusion scan can reduce the patient's time in the imaging laboratory, decrease patient radiation exposure, and have a similar favorable prognosis compared to a conventional rest/stress protocol.

    a. True
    b. False

7. Newer camera designs incorporating "cardiocentric" SPECT orbits:

    a. Allow the heart to remain in the center of the field-of-view
    b. Increase severity of artifacts
    c. Overestimate perfusion defect size compared to body-centered orbits
    d. Have equivocal image quality compared to body-centered orbits

CE Registration Form

In order to process the post-test and credit certificate, please complete the registration information below. A CME/ACE certificate will be issued once the test is processed.

PLEASE PRINT

I am requesting: ☐ CME   ☐ ACE

Time I spent on activity: ☐ .50hrs ☐ .75hrs ☐ 1 hour

_____

Last Name   First Name   Degree

_____

Phone Number   Fax Number

_____

E-mail

_____

Member ID (If Applicable)

BILLING

☐ Member ($0 fee)   ☐ Non-Member ($25 fee)

Non-Members please fill out the information below:

Type of Card: ☐ Visa ☐ MasterCard ☐ Amex

_____

Name on Card

_____

Card Number

_____/_____   _____

Exp Date   Security Code

_____

Billing Address

_____

City   State   Zip Code

_____

Cardholder Signature

EVALUATION FORM

Advances in SPECT Camera Software and Hardware: Currently Available and New on the Horizon

---

The American Society of Nuclear Cardiology appreciates and values your opinions. In order to assist us in evaluating the effectiveness of this program and to make recommendations for future online educational offerings, please take a moment to complete this evaluation form.

Directions: **Please select your responses to complete this evaluation form.**
Your comments and suggestions will aid in planning future activities.

Please rate how strongly you agree or disagree with these statements:	Strongly Agree 5	Agree 4	Neutral 3	Disagree 2	Strongly Disagree 1
1. *The following stated learning objectives were achieved: At the end of the activity I could:*					
Describe advances in software methods, including iterative reconstruction, resolution recovery, noise compensation, and phase analysis	O	O	O	O	O
Summarize developments in hardware, such as optimized detector geometry, focused collimation, solid-state detectors, and attenuation correction	O	O	O	O	O
Discuss potential future technological developments such as simultaneous dual-isotope SPECT, evaluation of coronary flow reserve, and stress-only imaging	O	O	O	O	O
2. *The activity met its overall purpose:* To increase the learners' competence in the application of nuclear cardiology strategies in clinical practice.	O	O	O	O	O
3. Please tell us at least one strategy you learned in this activity which you can apply in practice:					
4. Did you perceive any commercial bias throughout the article? If so, please list the author(s) and the perceived bias(es):					
5. Will any of the topics presented in the article improve the quality of care in your practice? If so, in what way?					
6. Do you feel future activities on this subject matter are necessary or important to your practice?	O Yes O No				
7. Please list any comments/suggestions for future activities:					

A review on the clinical uses of SPECT/CT

1st Giuliano Mariani

2nd Laura Bruselli
14.55 · Azienda Unità Sanitaria Lo...

3rd Torsten Kuwert
45.3 · Friedrich-Alexan...

+ 4

Last Naoyuki Watanabe

Show more authors

Abstract

In the era when positron emission tomography (PET) seems to constitute the most advanced application of nuclear medicine imaging, still the conventional procedure of single photon emission computed tomography (SPECT) is far from being obsolete, especially if combined with computed tomography (CT). In fact, this dual modality imaging technique (SPECT/CT) lends itself to a wide variety of useful diagnostic applications whose clinical impact is in most instances already well established, while the evidence is growing for newer applications. The increasing availability of new hybrid SPECT/CT devices with advanced technology offers the opportunity to shorten acquisition time and to provide accurate attenuation correction and fusion imaging. In this review we analyse and discuss the capabilities of SPECT/CT for improving sensitivity and specificity in the imaging of both oncological and non-oncological diseases. The main advantages of SPECT/CT are represented by better attenuation correction, increased specificity, and accurate depiction of the localization of disease and of possible involvement of adjacent tissues. Endocrine and neuroendocrine tumours are accurately localized and characterized by SPECT/CT, as also are solitary pulmonary nodules and lung cancers, brain tumours, lymphoma, prostate cancer, malignant and benign bone lesions, and infection. Furthermore, hybrid SPECT/CT imaging is especially suited to support the increasing applications of minimally invasive surgery, as well as to precisely define the diagnostic and prognostic profile of cardiovascular patients. Finally, the applications of SPECT/CT to other clinical disorders or malignant tumours is currently under extensive investigation, with encouraging results in terms of diagnostic accuracy.
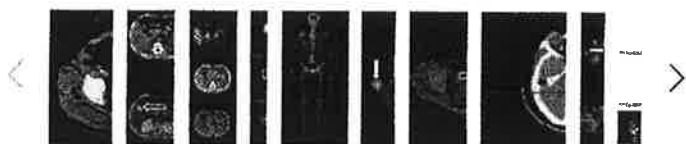
Cerenkov luminescence imaging: physics principles and potential applications in biomedical sciences

> "As discussed in the introduction, Cerenkov luminescence
> imaging is particularly promising to image β - emitters, which
> are widely used for example in internal radiotherapy but are
> difficult to visualize with other methods, such as
> Bremsstrahlung imaging. In addition, CLI is able to provide
> images in a fast, easy and cost-effective way compared to
> other methods in nuclear medicine, PET of β +-emitters[78]
> and single photon emission computed tomography (SPECT)
> of γ-emitters[79], and in this respect CLI would allow a larger
> employment of nuclear medicine probes also in facilities that
> do not have conventional tomographic systems available.
> Apart from these uses related to tumor diagnosis and
> treatment by injection of radionuclides, encouraging
> applications for CLI are endoscopic and intraoperative ones,
> as well as dosimetry in external beam therapy. "

[Show abstract]

Full-text · Article · Dec 2017

Esther Ciarrocchi   Nicola Belcari

Read full-text

An Overview of Multimodal Neuroimaging Using Nanoprobes

> "Bural et al. [40] highlighted the comparative advantages
> offered by SPECT-CT over the unimodal SPECT system in the
> problem of localizing endocrine and neuroendocrine tumors,
> thereby also implicitly emphasizing the significance of the
> multimodal imaging system. Mariani et al. [41] reviews the
> clinical applications of SPECT-CT and its importance, even
> with the emergence of PET as an advanced alternative. There
> are very few research models that focus on human brain
> imaging with SPECT-CT and radiotracers. "

[Show abstract]

Full-text · Article · Feb 2017

People who read this publication also read:

Article: Is the lung scan alive and well? Facts and controversies in defining the role of lung scintigraphy f...

Feb 2009 · European Journal of Nuclea...

Sriram Sridhar   Sachin Mishra   Miklós Gulyás   +1 more author ...

Parasuraman Padmanabhan

Read full-text

Targets and probes for non-invasive imaging of β-cells

"In, 123 I, and 131 I[79]. One additional point that has to be taken into account is that only 1–2% of the pancreas are βcells, meaning that the number of targets is limited. "

[Show abstract]

Full-text · Article · Dec 2016

Andreas Jodal   Roger Schibli   Martin Béhé

Read full-text

Show more

Recommended publications

Discover more publications, questions and projects in Endoc

Article

Is the lung scan alive and well? Facts and controversies in defining the role of lung scintigraphy f...

February 2009 · European Journal of Nuclear Medicine · Impact Factor: 5.38

John H Reid   Emmanuel Coche   Tomio Inoue   +3 more authors...   Giuliano Mariani

Read more

Chapter

Lung Scintigraphy in Pulmonary Embolism

January 2011

Giuliano Mariani   Laura Bruselli

Read more

People who read this publication also read:

Article: Is the lung scan alive and well? Facts and controversies in defining the role of lung scintigraphy f...

Feb 2009 · European Journal of Nuclea...

Article

Guest Editorial: IAEA Approach to Meet Nuclear Medicine Needs of the Emerging World

May 2013 · Seminars in nuclear medicine · Impact Factor: 3.34

Maurizio Dondi

Read more

Article

I-131 SPECT/CT in the Follow-Up of Patients With Differentiated Thyroid Carcinoma

June 2012 · Clinical nuclear medicine · Impact Factor: 3.93

Mareen Menges   Michael Uder   Torsten Kuwert   Daniela Schmidt

Read more

Discover more

Last Updated: 21 Apr 17

People who read this publication also read:

Article: Is the lung scan alive and well? Facts and controversies in defining the role of lung scintigraphy f...

Feb 2009 · European Journal of Nuclea...

MIRT Molecular Imaging and Radionuclide Therapy ⊘galenos
HOME
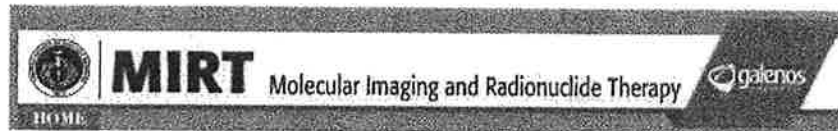
Improved Benefit of SPECT/CT Compared to SPECT Alone for the Accurate Localization of Endocrine and Neuroendocrine Tumors

Gonca G. Bural,[1] Ashok Muthukrishnan,[1] Matthew J Oborski,[1] and James M. Mountz[1,*]

[1] University of Pittsburgh Medical Center, Department of Radiology, Pittsburgh, PA, USA

[*] Address for Correspondence: University of Pittsburgh Medical Center, Department of Radiology, Pittsburgh, PA, USA Phone: +412 647 01 04 E-mail: mountzjm@upmc.edu

This article has been cited by other articles in PMC.

Abstract

Objective: To assess the clinical utility of SPECT/ CT in subjects with endocrine and neuroendocrine tumors compared to SPECT alone.

Material and Methods: 48 subjects (31 women;17 men; mean age 54±11) with clinical suspicion or diagnosis of endocrine and neuroendocrine tumor had 50 SPECT/CT scans (32 Tc-99m MIBI, 5 post treatment I-131, 8 In-111 Pentetreotide, and 5 I-123 MIBG). SPECT alone findings were compared to SPECT/CT and to pathology or radiological follow up.

Results: From the 32 Tc-99m MIBI scans, SPECT accurately localized the lesion in 22 positive subjects while SPECT/CT did in 31 subjects. Parathyroid lesions not seen on SPECT alone were smaller than 10 mm. In five post treatment I-131 scans, SPECT alone neither characterized, nor localized any lesions accurately. SPECT/CT revealed 3 benign etiologies, a metastatic lymph node, and one equivocal lesion. In 8 In-111 Pentetreotide scans, SPECT alone could not localize primary or metastatic lesions in 6 subjects all of which were localized with SPECT/CT. In five I-123 MIBG scans, SPECT alone could not detect a 1.1 cm adrenal lesion or correctly characterize normal physiologic adrenal uptake in consecutive scans of the same patient with prior history of adrenelectomy, all of which were correctly localized and characterized with SPECT/CT.

Conclusion: SPECT/CT is superior to SPECT alone in the assessment of endocrine and neuroendocrine tumors. It is better in lesion localization and lesion characterization leading to a decrease in the number of equivocal findings. SPECT/CT should be included in the clinical work up of all patients with diagnosis or suspicion of endocrine and neuroendocrine tumors.

Conflict of interest: None declared.

Keywords: tomography, emission-computed, single-photon, endocrine gland neoplasms, neuroendocrine tumors

INTRODUCTION

It has been a decade now since tomographic hybrid scanners including SPECT/CT (Single-photon emission computed tomography-computerized tomography) and PET/CT (positron emission tomography-computed tomography) have been introduced into nuclear medicine. These techniques provide a higher diagnostic accuracy than conventional non-tomographic scans ([1]). There has been a considerable emphasis on the benefits of PET/CT in oncology ([2,3,4,5,6,7]), but relatively less research proven emphasis on the SPECT/CT ([8]). Due to high investment expense and ongoing benefit to cost analysis, the clinical utility of SPECT/CT still warrants proof of data expressing its superiority. Incorporation of anatomic CT imaging with SPECT can increase the diagnostic capacity of these imaging modalities, predominantly in subjects presenting with the diagnosis or suspicion of endocrine and neuroendocrine tumors. Our aim was to assess the clinical utility of SPECT/CT compared with SPECT alone, in the assessment of subjects with endocrine and neuroendocrine tumors.

MATERIALS AND METHODS   Go to:

48 subjects (31 women; 17 men; mean age 54±11; age range 15-80 years) with clinical suspicion or diagnosis of endocrine and neuroendocrine tumors had 50 SPECT/CT scans performed on the dual head Siemens Symbia T6 SPECT/CT scanner between January 2010 and March 2012. Thirty-two of these scans were Tc 99m MIBI, 5 were post treatment I-131 scans, 8 were In-111 Pentetreotide scans, and 5 were I-123 MIBG scans.

SPECT/CT Protocols

All SPECT scans were performed using a 128x128 matrix, 30 seconds /stop, total of 64 stops obtaining 128 projections, using non circular orbit. All SPECT data was processed using filtered back projection, frequency cut off 0.5, order 5, and a second reconstruction using OSEM, 8 iterations and 16 subsets.

Tc-99m Sestamibi (MIBI) SPECT/CT scan: After intravenous administration of 1110 MBq Tc-99m sestamibi, immediate SPECT/CT images were obtained from the lower face to mid chest using a low energy collimator, energy setting at 140 KeV with 20% window. Following a 2-hour delay, repeat SPECT/CT images were obtained of the same level. MIP (maximum intensity projection) reconstructions were performed and the early and late images were compared side-by-side for distribution and retention of radiotracer.

I-131 Post treatment scan with SPECT/CT scan: One week after oral administration of therapeutic dose of I-131 raging between 1776–6031 MBq, anterior and posterior whole body planar images were obtained using a high energy collimator, energy settings at 364 KeV with 20% window and camera speed of 8 cm/min. SPECT/CT images of the neck as well as the regions with equivocal findings were obtained.

In-111 pentetreotide scan with SPECT/CT scan: 4 hours after the intravenous injection of the 222 MBq In-111 pentetreotide, whole body anterior and posterior planar images were obtained using a medium energy collimator, energy settings at 172 KeV and 247 KeV with 20% window and 10cm/min. Approximately 24 hours later, repeat whole body images in the anterior and posterior views, as well as SPECT/CT images of the regions with equivocal findings were obtained.

I-123 MIBG (Metaiodobenzylguanidine) scan with SPECT/CT scan: 24 hours after the intravenous injection of 400 MBq I-123 MIBG, whole body anterior and posterior images were obtained using a low energy high resolution collimator, energy settings at 159 KeV with 20% window, and 9cm/min. In addition SPECT/CT images of the regions with equivocal findings were obtained.

CT scan: After oral administration of 20 cc gastroview mixed with 900 cc clear non-carbonated liquid over the course of an hour, axial CT images of the area of interest were obtained using 2.5 mm

collimation, 130 kVp, mAs of 20-60 for neck, and mAs of 40-80 for chest, abdomen, pelvis and extremities, depending on body habitus, and pitch of 0.8 with a Siemens Symbia T6 SPECT/CT scanner.

Subjects

32 subjects with elevated parathyroid hormone levels had 32 MIBI scans, all of which were before a parathyroid surgery. In these subjects lesion detection and localization with SPECT alone was compared to SPECT/CT. Findings were correlated with pathology. For the other scans, including five post treatment I-131 scans in 5 subjects with papillary thyroid cancer, eight In-111 Pentetreotide scans (the primary tumor was well differentiated pancreatic endocrine neoplasm in 4 subjects, well differentiated neuroendocrine neoplasm of small bowel in one subject, carcinoid tumor of the small bowel in one subject, gastrinoma in one subject, and gastric carcinoid tumor in one subject), and five I-123 MIBG scans in 4 subjects with suspicion of primary or recurrent pheochromocytoma, lesion detection, characterization, and localization were compared between planar and SPECT and planar and SPECT/CT images. The planar images and the SPECT alone component of the studies were interpreted and the findings were recorded. Planar and SPECT/CT images were then evaluated and the findings were recorded. Planar image findings and SPECT findings were compared to planar and SPECT/CT findings. All findings were correlated with histopathology when available, or radiologic follow-up.

RESULTS   Go to:

48 subjects with clinical suspicion or diagnosis of endocrine and neuroendocrine tumors had 50 SPECT/CT scans. Localization or characterization of scan findings with SPECT alone and with SPECT/CT is summarized in Table 1.

Table 1
SPECT alone compared with SPECT/CT for accurate localizationand/or characterization of endocrine and neuroendocrine tumors

In 32 subjects who had a MIBI scan, SPECT correctly identified and localized the hyper functioning parathyroid tissues in 22 subjects (61%), while SPECT/CT correctly identified and localized the hyper functioning parathyroid tissues in 31 subjects (97%). Histopathology revealed adenoma in 29 subjects, 3 hyperplastic glands in 3 subjects. Parathyroid lesions not detected with SPECT alone in 10 subjects all had size less than 10 mm.

In 5 post treatment I-131 scans, SPECT alone neither characterized nor localized any malignant lesions or benign findings accurately. However, SPECT/CT correctly localized and/or characterized 3 benign etiologies in 3 different subjects, a malignant lesion in the 4th subject and an equivocal finding in the fifth subject. Figure 1 shows improved localization for a metastatic superior mediastinal lymph node. Figure 2 illustrates characterization advantage of SPECT/CT by showing an incidental submandibular gland duct stone causing obstruction which initially, on SPECT alone, was suspected to be a metastasis.

Figure 1
A 15 year-old girl with papillary thyroid cancer and totalthyroidectomy underwent radioiodine therapy with 3700 MBq I-131. The1 week post-therapy anterior (A) and posterior (B) whole body imagesshowed bilateral intense tracer uptake in the region of the ...
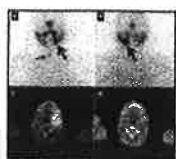
Figure 2

A 42 year-old woman with papillary thyroid cancer and totalthyroidectomy underwent radioiodine therapy with 6031 MBq I-131. 1week post-therapy anterior (A) and posterior (B) neck/chest images showedmild uptake in the thyroid bed (small arrow, image A) ...

In eight In-111 Pentetreotide scans, SPECT/CT was better than SPECT alone for lesion localization and characterization in the liver, pancreatic head, bones or lymph nodes. Pathologic confirmation was available for the 10 lesions (9 were malignant lesions one was benign), including liver metastases in 4 subjects, primary well differentiated endocrine tumor of the pancreas in one subject, retroperitoneal and superior mesenteric lymph node metastases in one subject and mediastinal and perirenal lymph node metastases in one subject and retroperitoneal lymph node in one subject. Two bone lesions did not have pathologic confirmation but, follow-up diagnostic CT scans confirmed the osseous metastases. Figures 3 illustrates detection and localization advantage for two osseous metastases. Figure 4 shows improved localization leading to better characterization of a 9 cm primary pancreatic head mass.

Figure 3

A 58 year-old woman with carcinoid tumor of the small bowel withknown liver metastases had an In-111 Pentetreotide scan. Anterior (A) andposterior (B) planar images of the abdominopelvic region show abnormal focaluptake is noted in the inferior right ...
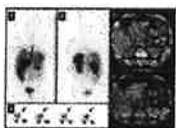

Figure 4

A 50 year-old man had a hyper vascular pancreatic head massdetected on an abdominal CT scan. The patient had an In-111 Pentetreotidescan to evaluate for tumor and to evaluate for distant metastases. Anterior(A) and posterior (B) whole body planar images ...

Four subjects had five I-123 MIBG scans as summarized in Table 1. In two subjects, large adrenal masses with intense I-123 MIBG uptake were visible on both planar whole body and SPECT scans. SPECT/CT did not reveal any additional abnormal findings. Surgical pathology was pheochromocytoma in both. In the third subject with suspicion of pheochromocytoma, a 1.1 cm left adrenal lesion had very mild asymmetric increased uptake, not very well identified on SPECT alone but better visualized on SPECT/CT images. The fourth subject with prior history of adrenelectomy, had normal physiologic adrenal uptake in consecutive scans. SPECT/CT correctly localized the uptake to the single hyperplasic adrenal gland and subsequently characterized this finding as benign normal finding.

DISCUSSION

Computerized tomography (CT) is a conventional high-resolution anatomical imaging modality that excels at providing details on lesion location, size, and morphology. However this modality does not provide information regarding tumor physiology (9). Despite its high sensitivity and specificity, SPECT alone is substantially limited by low spatial resolution and its inability to provide anatomical detail. Dual-modality imaging systems which allow both functional and structural imaging to be performed during a single imaging session improve image quality in comparison to functional imaging only (10). Fusion imaging resulting from hybrid devices has been reported to be clearly giving better localization

of disease and differentiation between physiologic and pathologic uptake (11,12,13,14). This study emphasizes the clinical utility of SPECT/CT over SPECT alone in the assessment of endocrine and neuroendocrine tumors.

In our study, the correct detection and localization of hyper functioning parathyroid lesions by SPECT/CT (31 of 32 subjects) was superior to SPECT (22 of 32 subjects) alone. All lesions which were not detected on SPECT alone in 10 subjects were smaller than 10 mm. SPECT/CT has a clear superiority over SPECT in the detection and localization of parathyroid lesions smaller than 10 mm. This is most likely secondary to poor spatial localization ability of SPECT alone in the absence of a precisely registered CT, leading to its inability to confidently detect small sized lesions. One out of 32 subjects who had an 8 mm adenoma in the left parathyroid gland detected in surgery was incorrectly localized by SPECT/CT to the right. The suspicious uptake in the right was most likely due to statistical noise. In this subject, 8 mm left parathyroid gland lesion could have been missed due to small size of the lesion or tumor characteristics.

Our patient based sensitivity for dual phase MIBI and SPECT/CT was 97% and for SPECT alone 61% respectively. In a retrospective study using dual phase MIBI and SPECT/CT in 94 patients the sensitivity of SPECT/CT was reported as 92%, which is similar to our findings (15). In another study with 116 patients, the sensitivity for SPECT/CT was slightly lower than our results with 88%, and the sensitivity for SPECT was similar to our findings with 59% (16).

In five subjects with post-therapy I-131 scans, SPECT/CT correctly characterized areas of suspicious uptake in three different subjects as physiologic or benign: physiologic thymic uptake, physiologic bowel uptake and a submandibular gland duct stone causing obstruction. In the fourth subject with post therapy I-131 scan, the suspicious uptake in the upper chest region localized to a right superior mediastinal lymph node which biopsy was proven to be metastatic thyroid tissue. In the last subject SPECT/CT localized the uptake to be within a small nodule in the mesentery of the upper abdomen. Follow-up surgical removal of this lesion was biopsy proven to be a benign epithelial cyst.

Previous studies in subjects who had post therapy I-131 scans and SPECT/CT reported similar findings to our results: including reduction or elimination in uncertain findings and better lymph node localization (17,18,19).

In 8 subjects who had In-111 Pentetreotide scans, SPECT/CT imaging improved lesion localization compared to planar and SPECT imaging in multiple metastatic lesions in various locations. Even for the very large lesions, SPECT alone was not helpful in lesion localization. A 9 cm pancreatic head mass had focal intense uptake in the mid upper abdomen on the whole body images. By SPECT alone, it was unclear if this was a large abdominal lymph node, an organ involvement or intense bowel uptake. SPECT/CT localized this to the pancreatic head, and showed no other evidence of abdominal disease. For the smaller lesions SPECT/CT was helpful both for detection and in almost all cases, characterization. Our findings are in keeping with the current literature, documenting the diagnostic value of SPECT/CT over planar and SPECT imaging in the assessment of neuroendocrine tumors with In-111 Pentetreotide (20,21,22). Despite the overall benefits of SPECT/CT with In-111 Pentetreotide scans in identifying and localizing disease in the majority of subjects, it was misinterpreted in one subject. This subject had a pelvic mesenteric lymph node with mild uptake, which was characterized as suspicious for residual disease or recurrence at the surgical site however, histopathology revealed chronic inflammation and fat necrosis.

In 4 subjects who had five I-123 MIBG scans, 2 had very large left adrenal masses identified equally well both on SPECT and SPECT/CT (one was 10 cm and other was 5 cm) consistent with pheochromocytoma. However SPECT/CT was additionally helpful in these cases, as it did not reveal any other metastatic foci elsewhere in these subjects. The third subject had a prior right adrenal

pheochromocytoma resection but remained symptomatic. In this case two SPECT/CT scans provided convincing evidence of an anatomically normal but minimally hyperplastic left adrenal gland. The fourth subject had mildly elevated vanillymandelic ascite (VMA) in the urine but normal plasma metanephrine levels. The I-123 MIBG scan with SPECT/CT detected a 1.1 cm left adrenal lesion with only mildly increased tracer uptake. Given these equivocal findings, a MRI scan was performed, which was normal. Clinically, the patient was diagnosed as having subclinical pheochromocytoma, and did not undergo surgery. A case report, with similar clinical picture to our subject, where subclinical pheochromocytoma was diagnosed on histopathology was published by Minako et al (23). Another study reported that I-123 MIBG SPECT or CT scanning alone were equally good for locating adrenal medullary pheochromocytoma but the combination of MIBG SPECT and CT makes it possible to distinguish between functioning and nonfunctioning adenomas (24).

Currently one major obstacle preventing routine clinical use of SPECT/CT is the high cost of SPECT/CT machines (25). However, we believe that as data continues to prove their clinical utility, this technology will become more widely available and a larger number of patients will be able to benefit from combined SPECT/CT imaging.

CONCLUSION Go to:

In this study we show that functional SPECT and anatomic CT data obtained as a single study have shown improvements in diagnostic imaging capability by improving lesion conspicuity, reducing false positives, and clarifying indeterminate lesions by better localization compared to SPECT alone. SPECT/CT is a very valuable and effective imaging tool in the assessment of patients with endocrine and neuroendocrine malignancies and should be included in the clinical work-up of these patients rather than SPECT alone.

References Go to:

1. Dongen TM, van, Waterval JJ, Willems P, Mottaghy F, Brans B. Combining CT and scintigraphy: SPECT-CT and PET-CT. Ned Tijdschr Geneeskd. 2011;155:2792–2792. [PubMed]

2. Kuehl H, Veit P, Rosenbaum SJ, Bockisch A, Antoch G. Can PET/CT replace separate diagnostic CT for cancer imaging? Optimizing CT protocols for imaging cancers of the chest and abdomen. J Nucl Med. 2007;45(Supll 1):45–57. [PubMed]

3. Weber WA, Figlin R. Monitoring cancer treatment with PET/CT: does it make a difference? J Nucl Med. 2007;48 (Suppl 1):36–44. [PubMed]

4. Czernin J, Allen-Auerbach M, Schelbert HR. Improvements in cancer staging with PET/CT: literature-based evidence as of September 2006. J Nucl Med. 2007;48 (Suppl 1):78–88. [PubMed]

5. Hutchings M, Barrington SF. PET/CT for therapy response assessment in lymphoma. J Nucl Med. 2009;50 (Suppl 1):21–30. [PubMed]

6. Vach W, Hoilund-Carlsen PF, Gerke O, Weber WA. Generating evidence for clinical benefit of PET/CT in diagnosing cancer patients. J Nucl Med. 2011;52 (Suppl 2):77–85. [PubMed]

7. Buck AK, Herrmann K, Stargardt T, Dechow T, Krause BJ, Schreyogg J. Economic evaluation of PET and PET/CT in oncology: evidence and methodologic approaches. J Nucl Med. 2010;51:401–412. [PubMed]

8. Chowdhury FU, and Scarsbrook AF. The role of hybrid SPECT-CT in oncology: current and emerging clinical applications. Clin Radiol. 2008;63:241–251. [PubMed]

9. Histed SN, Lindenberg ML, Mena E, Turkbey B, Choyke PL, Kurdziel KA. Review of functional/anatomical imaging in oncology. Nucl Med Commun. 2012;33:349–361. [PMC free article] [PubMed]

10. Hasegawa BH, Wong KH, Iwata K, Barber WC, Hwang AB, Sakdinawat AE, Ramaswamy M, Price DC, Hawkins RA. Dual-modality imaging of cancer with SPECT/CT. Technol Cancer Res Treat. 2002;1:449–458. [PubMed]

11. Castaldi P, Rufini V, Treglia G, Bruno I, Perotti G, Stifano G, Barbaro B, Giordano A. Impact of 111In-DTPAoctreotide SPECT/CT fusion images in the management of neuroendocrine tumours. Radiol Med. 2008;113:1056–1067. [PubMed]

12. Even-Sapir E, Keidar Z, Bar-Shalom R. Hybrid imaging (SPECT/CT and PET/CT)—Improving the diagnostic accuracy of functional/metabolic and anatomic imaging. Semin Nucl Med. 2009;39:264–275. [PubMed]

13. Patton JA, Townsend DW, Hutton BF. Hybrid imaging technology: From dreams and vision to clinical devices. Semin Nucl Med. 2009;39:247–263. [PubMed]

14. Spanu A, Solinas ME, Chessa F, Sanna D, Nuvoli S, Madeddu G. 131I SPECT/CT in the follow-up of differentiated thyroid carcinoma: Incremental value versus planar imaging. J Nucl Med. 2009;50:184–190. [PubMed]

15. Ciappuccini R, Morera J, Pascal P, Rame JP, Heutte N, Aide N, Babin E, Reznik Y, Bardet S. Dual-phase 99mTc sestamibi scintigraphy with neck and thorax SPECT/CT in primary hyperparathyroidism: a single-institution experience. Clin Nucl Med. 2012;37:223–228. [PubMed]

16. Prommegger R, Wimmer G, Profanter C, Sauper T, Sieb M, Kovacs P, Bale R, Putzer D, Gabriel M, Margreiter R. Virtual neck exploration: a new method for localizing abnormal parathyroid glands. Annals of Surgery. 2009;250:761–765. [PubMed]

17. Chen L, Luo Q, Shen Y, Yu Y, Yuan Z, Lu H, Zhu R. Incremental value of 131I SPECT/CT in the management of patients with differentiated thyroid carcinoma. J Nucl Med. 2008;49:1952–1957. [PubMed]

18. Kohlfuerst S, Igerc I, Lobnig M, Gallowitsch HJ, Gomez-Segovia I, Matschnig S, Mayr J, Mikosch P, Beheshti M, Lind P. Posttherapeutic 131I SPECT-CT offers high diagnostic accuracy when the findings on conventional planar imaging are inconclusive and allows a tailored patient treatment regimen. Eur J Nucl Med Mol Imaging. 2009;36:886–893. [PubMed]

19. Schmidt D, Szikszai A, Linke R, Bautz W, Kuwert T. Impact of 131I SPECT/spiral CT on nodal staging of differentiated thyroid carcinoma at the first radioablation. J Nucl Med. 2009;50:18–23. [PubMed]

20. Wong KK, Cahill JM, Frey KA, Avram AM. Incremental value of 111-in pentetreotide SPECT/CT fusion imaging of neuroendocrine tumors. Acad Radiol. 2010;17:291–297. [PubMed]

21. Krausz Y, Keidar Z, Kogan I, Even-Sapir E, Bar-Shalom R, Engel A, Rubinstein R, Sachs J, Bocher M, Agranovicz S, Chisin R, Israel O. SPECT/CT hybrid imaging with 111In-pentetreotide in assessment of neuroendocrine tumours. Clin Endocrinol (Oxf) 2003;59:565–573. [PubMed]

22. Garcia-Talavera P, Gonzalez ML, Olmos R, Ruiz MA, Sainz A, Gamazo C, Gomez A. Contribution of SPECT/CT to the Diagnosis of a Pancreatic Tail Tumor in a Case of Multiple Endocrine Neoplasia Type 1. Clin Nucl Med. 2012;37:301–303. [PubMed]

23. Minako N, Takashi M, Koji T, Rokuri I, Masahiko K, Akira K, Masao K, Yoko N. Adrenal gland. A case of subclinical pheochromocytoma diagnosed pathohistologically. Clin Endocrinol. 2001;49:88 –92.

24. Nielsen JT, Nielsen BV, Rehling M. Location of adrenal medullary pheochromocytoma by I-123 metaiodobenzylguanidine SPECT. Clin Nucl Med. 1996;21:695–699. [PubMed]

25. Mariani G, Flotats A., Israel O, Kim EE, Kuwert T. Clinical Applications of SPECT/CT: New Hybrid Nuclear Medicine Imaging Systems. International Atomic Energy Agency. ISBN 978-92-0-107108-8. Vienna: 2008. pp. 3–3.